

Geochemical Tracers of Surface Water and Ground Water Contamination from Road Salt

Author: Jacob Anderson

Persistent link: <http://hdl.handle.net/2345/3313>

This work is posted on [eScholarship@BC](#),
Boston College University Libraries.

Boston College Electronic Thesis or Dissertation, 2013

Copyright is held by the author, with all rights reserved, unless otherwise noted.

Boston College
The Graduate School of Arts and Sciences
Department of Earth and Environmental Sciences

**GEOCHEMICAL TRACERS OF SURFACE WATER AND
GROUND WATER CONTAMINATION FROM ROAD SALT**

a thesis

by

JACOB ANDERSON

submitted in partial fulfillment of the requirements

for the degree of

Master of Science

August 2013

© copyright by JACOB SPENCER ANDERSON
2013

Abstract

Title: Geochemical tracer of surface water and ground water contamination from road salt

Author: Jacob Anderson

Advisor: Rudolph Hon

The application of road de-icers has lead to increasing solute concentrations in surface and ground water across the northern US, Canada, and northern Europe. In a public water supply well field in southeastern Massachusetts, USA, chloride concentrations in ground water from an unconfined aquifer have steadily risen for the past twenty years. The objectives of this study are to understand spatial and temporal trends in road salt concentrations in order to identify contamination sources and fate.

To this end, the methods of this project include field and lab work. Water samples were collected from surface, near-surface, and ground water from March 2012 to March 2013. The other major field data are specific conductance measurements from probes located in three piezometers. In the lab, all samples were analyzed for major ions with ion chromatography analysis. Additionally, trace elements were measured by inductively coupled plasma analysis on a subset of samples.

The results of these hydrogeochemical procedures showed several important trends. First, the highest concentrations of sodium and chloride from

near-surface samples were located near to roadways. Second, ground water samples taken from glacial sediments contained relatively high concentrations throughout the water column, whereas ground water samples from wetlands had high concentrations only near the surface. Third, there was no clear relationship between pH and cation concentrations. Finally, specific conductance data showed strong seasonal trends near to the surface, whereas values taken from deeper in the aquifer were steadily increasing.

Based on these results, it is highly probable that road salt application is the dominant contamination source. The pathways of road salt in the watershed include runoff into surface water and infiltration into the vadose zone and ground water. Road salt appears to preferentially travel through glacial features rather than floodplain features. It is possible that sodium from road salt is sorbed to aquifer sediment and displaces other cations. However, the low values of trace metals suggest that cation exchange is not mobilizing heavy metals. Finally, the increasing specific conductance values deep in the aquifer suggest that road salt is retained within the aquifer and concentrations will likely increase in the future if the current road salt application procedures are continued.

Acknowledgements

I would like to thank my thesis committee, Dr. Rudolph Hon and Dr. Martha Carlson Mazur for their support of this project. Without their time and guidance, this project could not have been possible.

Second, the Norwell Water Department provided the technical and financial resources necessary to complete much of this work. Peter Dillon and Jack McInnis were especially generous with their technical expertise, insight, and funding.

Third, Dr. James Besancon selflessly provided technical resources and advice over the past year. His experience with ICP and IC instrumentation was invaluable for completing lab procedures and verifying data quality. Thanks to Wellesley College for granting access to their ICP equipment. Jim also went above and beyond by going out in field during to winter 2012-12 to help oversee the geoprobe sample collection. His help is much appreciated.

Additionally, the Water Resources Research Center at the University of Massachusetts Amherst generously contributed funding to this project. Their commitment to water quality research made it possible to complete some of the lab work by defraying costs.

Finally, I'd like to thank Keegan Dougherty for his unfailing positive attitude. His presence in the computer lab lifted the spirits of everyone around him. Thanks!

Table of Contents

Acknowledgements	i
List of Figures	iii
List of Tables	v
Section 1. Introduction	1
1.1 Overview	1
1.2 Road Salt Definition	2
1.3 Environmental Concerns.....	3
Section 2. Site Background	5
2.1 Physiographic Features, Land Use, and Climate	5
2.2 History of Public Water Supply Operations	12
2.3 Road Salt Application and Use	15
Section 3. Purpose and Scope	18
3.1 Objectives.....	18
3.2 Data Collection Plan	19
Section 4. Methods	19
4.1 Sample Collection	19
4.1.a Pushpoint Sampling.....	19
4.1.b Well and Surface Water Sampling	20
4.1.c Geoprobe Sampling	20
4.1.d Sample Preparation	21
4.2 Ion Chromatography	21
4.3 Inductively Coupled Plasma Emission Spectroscopy (ICP)	22
4.4 Temporal Data	23
4.5 Geospatial Analysis	24
4.6 Sampling Sites	25
4.6.a - Surface Elevation Map	25
4.6.b Vertical Sampling within the OPM Aquifer	28
4.6.c Cross-sections near NOR-1	30
4.7 Grain Size Analysis	33
Section 5. Results	34
5.1 – GIS Aquifer Characterization	34
5.1.a -Surface Elevation Map	34

	iii
5.1.b - Aquifer Thickness Map.....	36
5.1.c - Bedrock Elevation Map	37
5.2 Water Sample Laboratory Analysis	38
5.2.a Ion Chromatography (IC) Analysis.....	38
5.2.b Inductively Coupled Plasma (ICP) Analysis	52
5.3 Temporal Trends in Chloride Concentration	57
5.4 Miscellaneous Data	59
5.4.a Relationships Among Cations.....	59
5.4.b - Grain Size Analysis	61
5.5 Overview of Results	62
Section 6. Discussion	63
6.1 Aquifer Characteristics.....	63
6.2 High Concentrations Near Roads	63
6.3 Lateral Sampling.....	65
6.4 Cross-Sections Near NOR-1.....	65
6.5 Cation Transport and Retention	66
6.6 Seasonal Effects	68
Section 7. Conclusion.....	69
References	71

List of Figures

Figure 1: The amounts of salt consumption in the US vs. time. Total salt consumption is presented in blue, while de-icing salt consumption is in red. Source: USGS, 2005.	2
Figure 2: Phase diagrams of NaCl-H ₂ O and CaCl ₂ -H ₂ O. The eutetic points are the minimum temperatures that can still remain in the liquid phase (Marion, 1995). http://www.crrel.usace.army.mil/library/specialreports/SR95_12.pdf Last accessed on Jul, 29, 2013. ...	3
Figure 3: Outline of the Old Pond Meadow (OPM) aquifer (red), South Street well field (blue) along with surrounding Massachusetts municipalities.	6
Figure 4: Old Pond Meadow aquifer including the Third Herring Brook (green), Wildcat Brook (blue), esker (light green), and the Old Pond Meadow wetland (pink).	7
Figure 5: Land use types within the OPM aquifer (MassGIS, 2005).	9
Figure 6: Percentages of land use types within the OPM aquifer (MassGIS, 2005).	10
Figure 7: Impervious surface and non-impervious surface within the OPM aquifer (MassGIS, 2005).	11

Figure 8: Temperature and precipitation from a NOAA weather station near Norwell, MA (NOAA, 2013). http://www.noaa.gov/pastweather.html Last Accessed April 26, 2013.	12
Figure 9: South Street Well Field. Wells NOR-1, NOR-6 and the South Street water treatment facility... 13	
Figure 10: Chloride concentrations in NOR-1 and NOR-6. Samples were collected by the Norwell Water Department and analyzed by Analytical Balance Corporation in February of 2013.	15
Figure 11: Salt storage facilities and lengths of state and municipal roads within the OPM aquifer (MassGIS, 2005).	16
Figure 12: Aerial photos of salt storage facilities for the Town of Norwell and the MHD.	18
Figure 13: Three piezometers near NOR-1. Within each piezometer is an In-Situ, Inc., AquaTroll 200 that records temperature, depth, and specific conductance.....	23
Figure 14: Locations of near-surface ground water samples taken in March and July 2012.	28
Figure 15: Cross-section of piezometers and wells sampled in July, 2012.	30
Figure 16: Transect sampling locations. Cross-section transects A-A' and B-B' are shown in Figs 32 and 33.	32
Figure 17: Transect sampling locations and lidar surface elevation. Transects A-A' and B-B' are arbitrarily assigned through sampling locations. Cross-sections of these transects are shown in Figs. 26 - 30.	33
Figure 18: Surface elevation (m) calculated from MassGIS digital terrain files.....	35
Figure 19: Aquifer thickness (m) calculated from well near Norwell that encountered bedrock.	36
Figure 20: Bedrock elevation calculated from surface elevation and aquifer thickness.	38
Figure 21: Graduated symbols and colors corresponding to chloride concentrations from near-surface ground water samples (mg/l) taken in March 2012.	43
Figure 22: Graduated symbols and colors corresponding to chloride concentrations from near-surface ground water samples (mg/l) taken in July 2012.....	44
Figure 23: Cross-section of THB surface elevation profile and major geological units. Near-surface ground water sampling locations from March 2012 are shown as orange circles, and the locations of roads crossing the stream are shown as red stars.....	45
Figure 24: Bar chart of sodium and chloride concentrations of sampling locations along THB.	46
Figure 25: Sodium and chloride concentrations (ppm) in piezometers and wells.	47
Figure 26: Modified Stiff diagram of sodium and chloride concentrations along transect A-A' in Fig. 16. Chloride concentrations are presented to the right of the well profile. Sodium concentrations are presented to the left. The scale bar relates to a concentr	48
Figure 27: Modified Stiff diagram of sodium and chloride concentrations along transect B-B' in Fig. 16. Chloride concentrations are presented to the right of the well profile. Sodium concentrations are presented to the left. The scale bar relates to a concentr	49

Figure 28: Dimensionless ratios of sodium (meq/l) to the summation of calcium, magnesium, and potassium (meq/l) are presented to the right of the well profile along transect A-A' in Fig. 16. Sodium concentrations (mg/l) are shown to the left of the well profile.	50
Figure 29: Dimensionless ratios of sodium (meq/l) to the summation of calcium, magnesium, and potassium (meq/l) are presented to the right of the well profile along transect B-B' in Fig. 16. Sodium concentrations (mg/l) are shown to the left of the well profile.	51
Figure 30: Dimensionless ratios of sodium (meq/l) to the summation of calcium, magnesium, and potassium (meq/l) are presented for historical wells shown in Fig. 15. Sodium concentrations (mg/l) are shown to the left of the well profile. The right and left scale	52
Figure 31: Concentrations of iron and manganese in piezometers and historical wells.	56
Figure 32: Estimated chloride concentrations in the shallow (blue), medium (red), and deep (green) piezometers from March 2011 to March 2013. Atmospheric temperature (purple) from a Norwell weather station is plotted on a secondary axis.	58
Figure 33: Extrapolation of chloride concentration in the deep piezometer to the EPA's secondary contaminant level for chloride. At the observed rate, chloride values will cross the EPA's allowable secondary contaminant threshold in the year 2020.....	59
Figure 34: Concentration of sodium (meq/l) vs. chloride (meq/l) for all samples analyzed with IC.	60
Figure 35: Summation of the concentrations of K ⁺ , Mg ⁺² , Ca ⁺² , and Na ⁺ (meq/l) vs. chloride (meq/l) for all samples analyzed with IC.	61
Figure 36: Grain size analysis from soil samples near NOR-1 and NOR-6.....	62

List of Tables

Table 1: Near-surface groundwater sample locations - March 2012	25
Table 2: Near-surface groundwater sample locations - July 2012.....	27
Table 3: Locations of vertical sampling within the OPM aquifer	29
Table 4: Cross-section sample locations	31
Table 5: Ion Chromatography results from lateral sampling - March 2012 (mg/L)	38
Table 6: Ion Chromatography results from lateral sampling - July 2012 (mg/L)	40
Table 7: Ion Chromatography results from vertical sampling - July 2012 (mg/l)	40
Table 8: Ion Chromatography results from lateral transect samples	41
Table 9: Lateral sampling ICP results (mg/l).	53
Table 10: ICP results for transect samples.....	55

Section 1. Introduction

1.1 Overview

Each winter, highway departments in North America, Europe, and other parts of the world strive to maintain high levels of service when driving conditions are worsened by inclement weather. De-icer chemicals, primarily sodium chloride (NaCl), are applied to roadways in order to mitigate transportation hazards that are caused by snow and ice. The application of road salt after snow and ice storms has reduced accidents, improved mobility, and reduced travel costs (Shi et al., 2009). Consequently, the amount of road salt applied annually in the United States has increased steadily since the 1950s, to the current rate of several millions of tons per year (Fig. 1) (Kostick, 2007). While road salt is an important part of maintaining driver safety during winter storms, anthropogenic loading of NaCl and other chloride salts, such as calcium chloride (CaCl₂) and magnesium chloride (MgCl₂), degrades ground water and surface water quality (Godwin et al., 2003; Forman and Alexander, 1998; Hoffman et al., 1981; Panno et al., 1999; Wilcox, 1986).

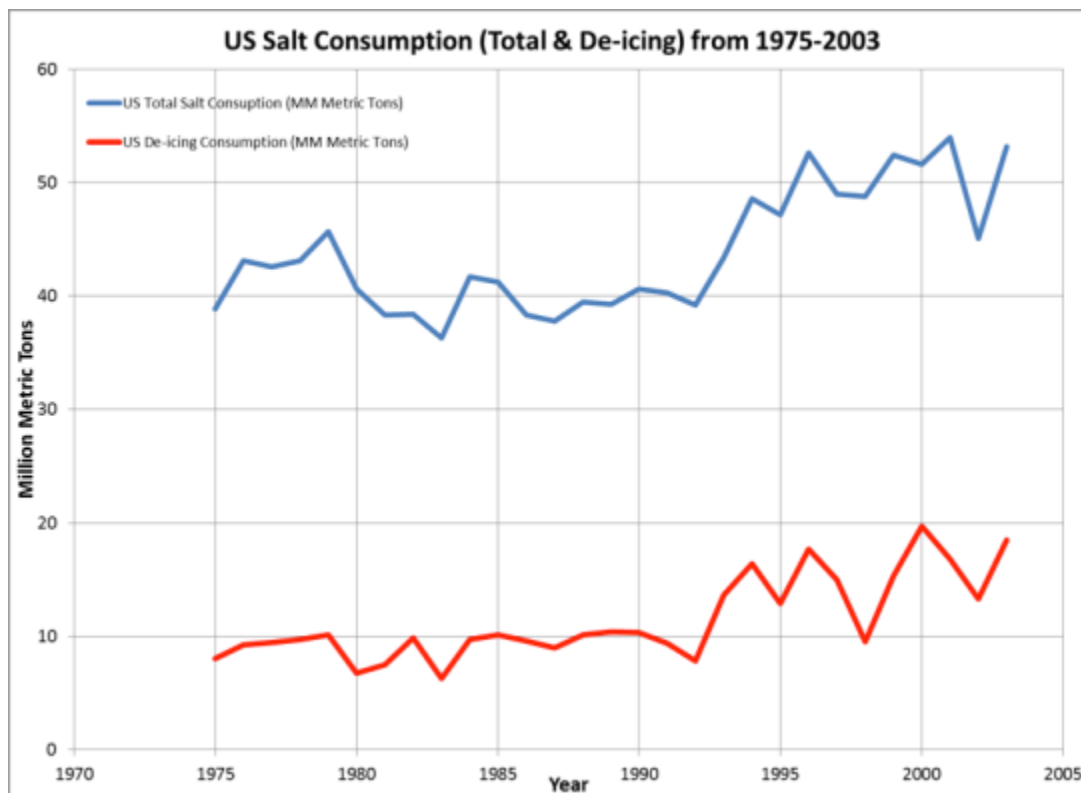


Figure 1: The amounts of salt consumption in the US vs. time. Total salt consumption is presented in blue, while de-icing salt consumption is in red. Source: Kostick, 2007.

1.2 Road Salt Definition

Road salt, or a deicing agent, is defined as any chemical that lowers the freezing temperature of water. The freezing point of water is proportional to the concentrations of ions in solution. Chloride salts are effective deicers because they are highly soluble and have a large number of ions per unit weight. The most common and economical form of road salt is impure halite (NaCl) that has been treated with an anti-caking agent (Fay and Shi, 2012). The effectiveness of deicing chemicals is described by the freezing point-concentration relationship on a phase diagram (Shi et al., 2009). The lowest possible freezing temperature on the phase diagram is called the eutectic point, which occurs when the liquid solution is in equilibrium with the solid phase. Once the ambient air temperature drops

below the eutectic point of NaCl (-21C), highway departments often apply other chemicals such CaCl₂ because the eutectic point of a CaCl₂ solution is -51C (Fig. 2) (Fay and Shi, 2012).

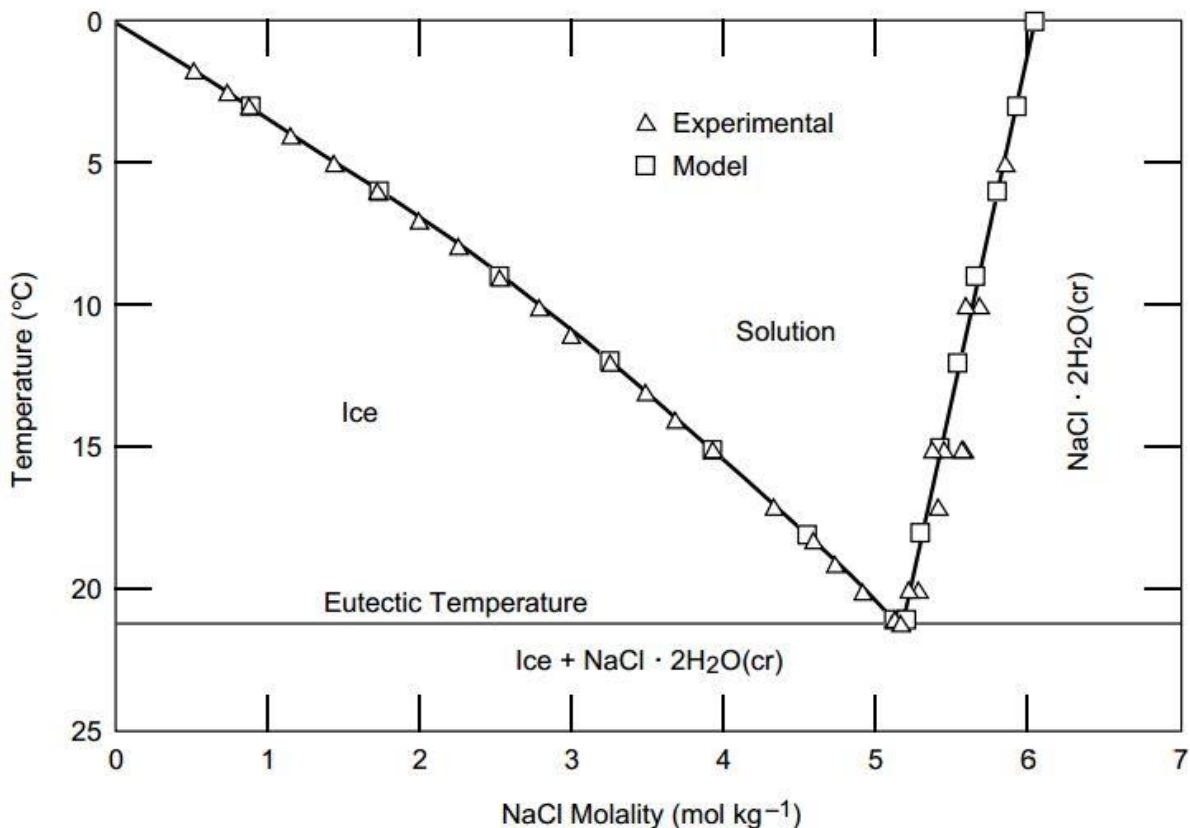


Figure 2: Phase diagrams of NaCl-H₂O and CaCl₂-H₂O. The eutectic points are the minimum temperatures that can still remain in the liquid phase (Marion, 1995). http://www.crrel.usace.army.mil/library/specialreports/SR95_12.pdf Last accessed on July, 29, 2013.

1.3 Environmental Concerns

Over the past ten years, there have been numerous documented cases of elevated chloride concentrations in urban watersheds (Lax and Peterson, 2009; Kelly et al., 2007; Bester et al., 2006) with some reaching as high as 9400 mg/l (Harte and Trowbridge, 2010). In general, groundwater chloride concentrations are relatively linearly related to watershed road density (Wegner and Yaggi, 2001). In one watershed in the Toronto area, 55% of de-icing salts applied each winter were retained in the

aquifer (Howard and Haynes, 1993). In the same metropolitan area, a numerical simulation of chloride transport suggested that it would take approximately 100 years for chloride concentrations to return to background levels, assuming that all salting was immediately stopped (Bester et al., 2006).

As a result of these individual cases, the use of road salt is becoming a growing environmental concern. In some urban areas, sodium (Na^+) and chloride (Cl^-) have been classified as major pollutants (Kelly et al., 2007). For example, water contaminated with road salt can corrode cars and infrastructure (Kelly et al., 2007); threaten fluvial, lacustrine, and riparian ecosystems (Sun et al., 2010); and have negative human health impacts (Jones et al., 1992).

Another water quality concern from road salt application is cation exchange. Increased cation concentrations can cause acidification and mobilize heavy metals (Lofgren, 2001). Aquifer sediments, such as clay particles and humus, have a measurable amount of sites that can sorb cations at a given pH (Ma and Eggleton, 1999). In addition to clays, organic matter colloids, called humus, have negatively charged oxygen molecular assemblages on their surfaces.

The amount of sites available in aquifer sediments is called cation exchange capacity (Bricker, 1999). When sodium from road salt becomes sorbed to clay or humus, it displaces another cation that previously occupied that cation exchange site. Pugh et al. (1996) indirectly measured cation exchange by observing the ratio of sodium to other major cations. Ion exchange from deicing salts is an environmental concern since it may deplete soil fertility through accelerated leaching of Ca^{+2} and Mg^{+2} (Shanley, 1994).

Road deicers can mobilize heavy metals directly through the processes of cation exchange, chloride complex formation, and colloid dispersion (Nelson et al., 2009) or indirectly by acidification and

mineral weathering (Granato et al., 1995). Put another way, cation exchange and mineral weathering are not independent. Hydrogen ions released from cation exchange can chemically weather minerals that may contain heavy metals (Mason et al., 1999).

The deleterious effects of road salt on water quality are particularly important in areas where groundwater is the principle water supply. Watershed managers must balance road-salting practices against the public demand for clean water. Consequently, research regarding road salt transport in urban watersheds provides the scientific basis for these decisions. Given that solute concentrations are increasing with each application, a comprehensive understanding of transport pathways is urgently needed.

Section 2. Site Background

2.1 Physiographic Features, Land Use, and Climate

The Old Pond Meadow (OPM) aquifer in southeastern Massachusetts is an area where road salt affects the public water supply (Figs. 3 and 4). This aquifer is unconfined, covers an area of approximately 28.9 km², and encompasses the towns of Norwell, MA (pop 10,506) and Hanover, MA (pop. 13,879). The OPM aquifer is particularly valuable because it provides the majority of the public water supply for these two towns. In recent years, urban watersheds similar to the OPM aquifer have been threatened by land use changes. For this reason, watershed managers of the OPM aquifer are concerned about its water quality.

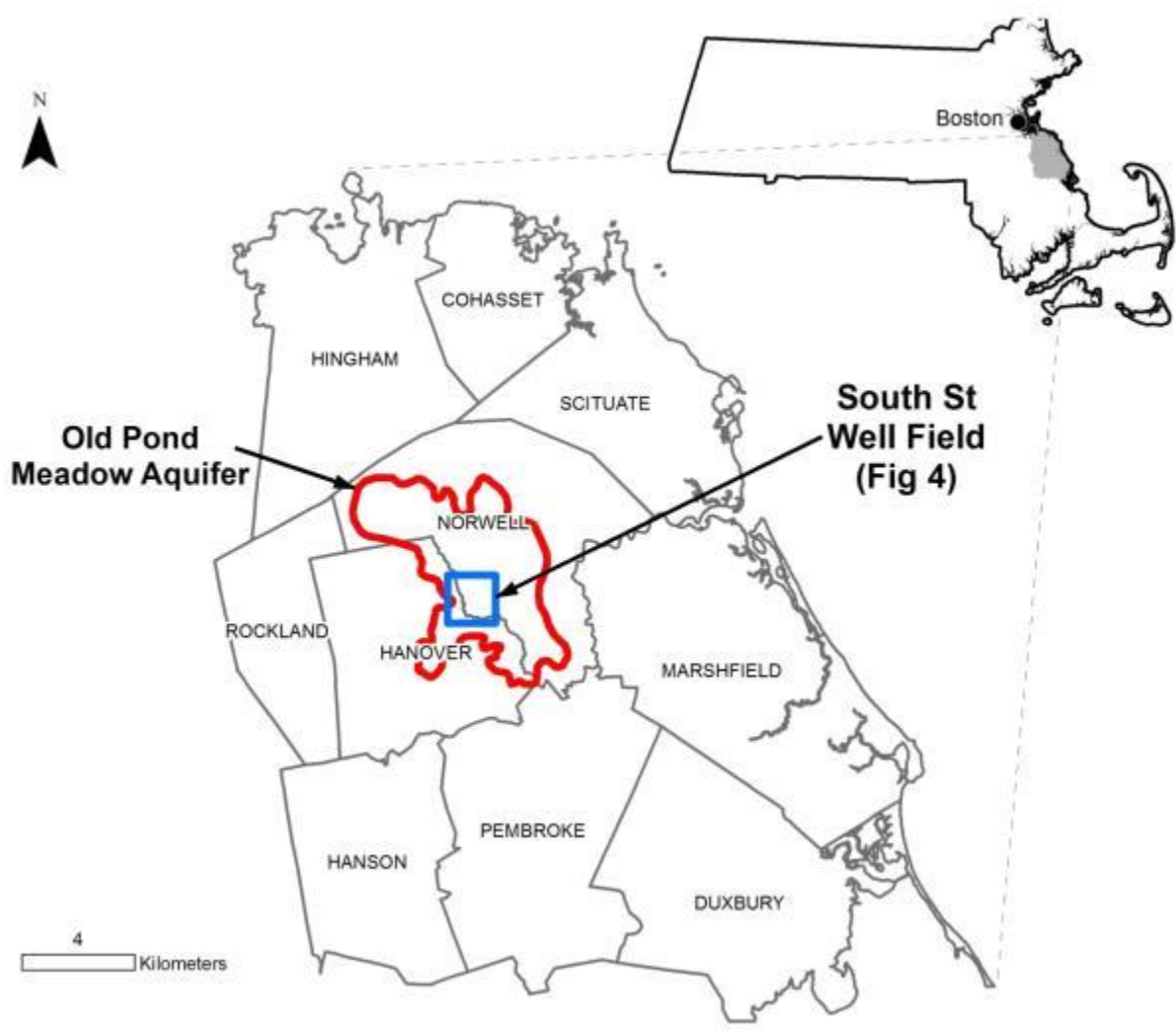


Figure 3: Outline of the Old Pond Meadow (OPM) aquifer (red), South Street well field (blue) along with surrounding Massachusetts municipalities.

Old Pond Meadow Aquifer, Southeastern Massachusetts

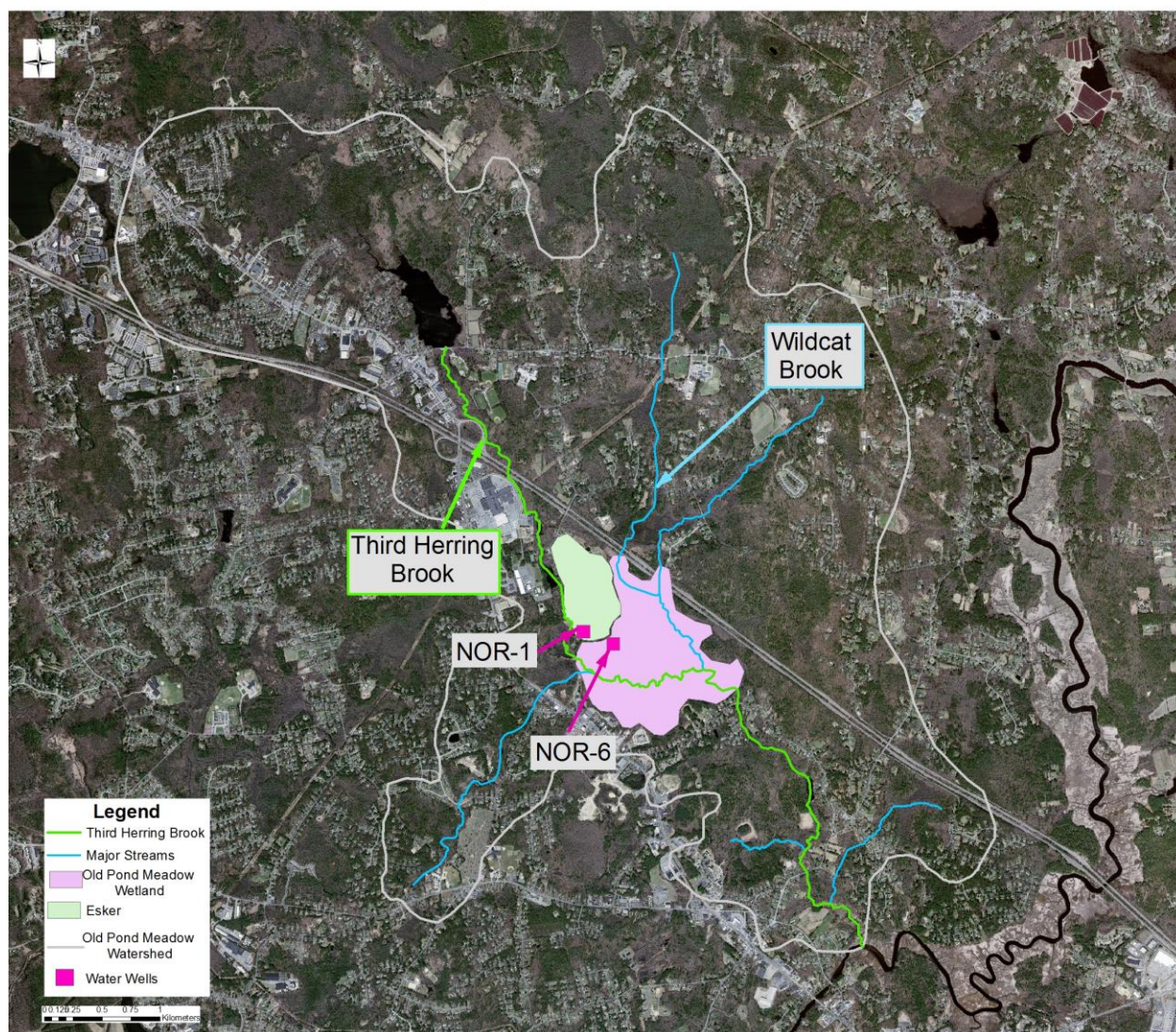


Figure 4: Old Pond Meadow aquifer including the Third Herring Brook (green), Wildcat Brook (blue), esker (light green), and the Old Pond Meadow wetland (pink).

The South Street well field lies in the center of the OPM aquifer, which was formed by the retreat of the last glaciation. The OPM aquifer soil primarily consists of glacial sediments in which the finest sediments overlay bedrock. In a general sense, the grain size increases upward, away from the bedrock to coarse sand in surface soils (Reed, 1999). Within glacial features such as moraines and

drumlins, the grain size is characterized as unsorted glacial till (Reed, 1999). In addition to grain size, these glacial features influence surface topography.

Surface elevation features that were originally deposited by glaciers impact surface water bodies and surface geology. A shallow basin in the northwest area of the OPM aquifer has been dammed to form Jacob's Pond. Downstream of the dam, the head waters of the Third Herring Brook flow along lowlands between glacial features. There is approximately 150 feet change in elevation relief along the Third Herring Brook. Within the Third Herring Brook floodplain, in addition to the Wildcat Brook floodplain, thick layers of peat overlay glacial sediments. Consequently, wetlands are a significant type of land use within the OPM aquifer.

The major land cover types within the OPM aquifer are forested wetland (25.0%), forest (17.4%), very low density residential (13.6%), non-forested wetland (11.0%), and low density residential (6.7%) (Figs. 5 and 6) (MassGIS, 2012). Other individual land use types are less than 3.5% each. Even though transportation land use comprises 1% of total land use, it is relevant as a potential source of road salt contamination.

Land Use Types, Old Pond Meadow Aquifer - Norwell, MA

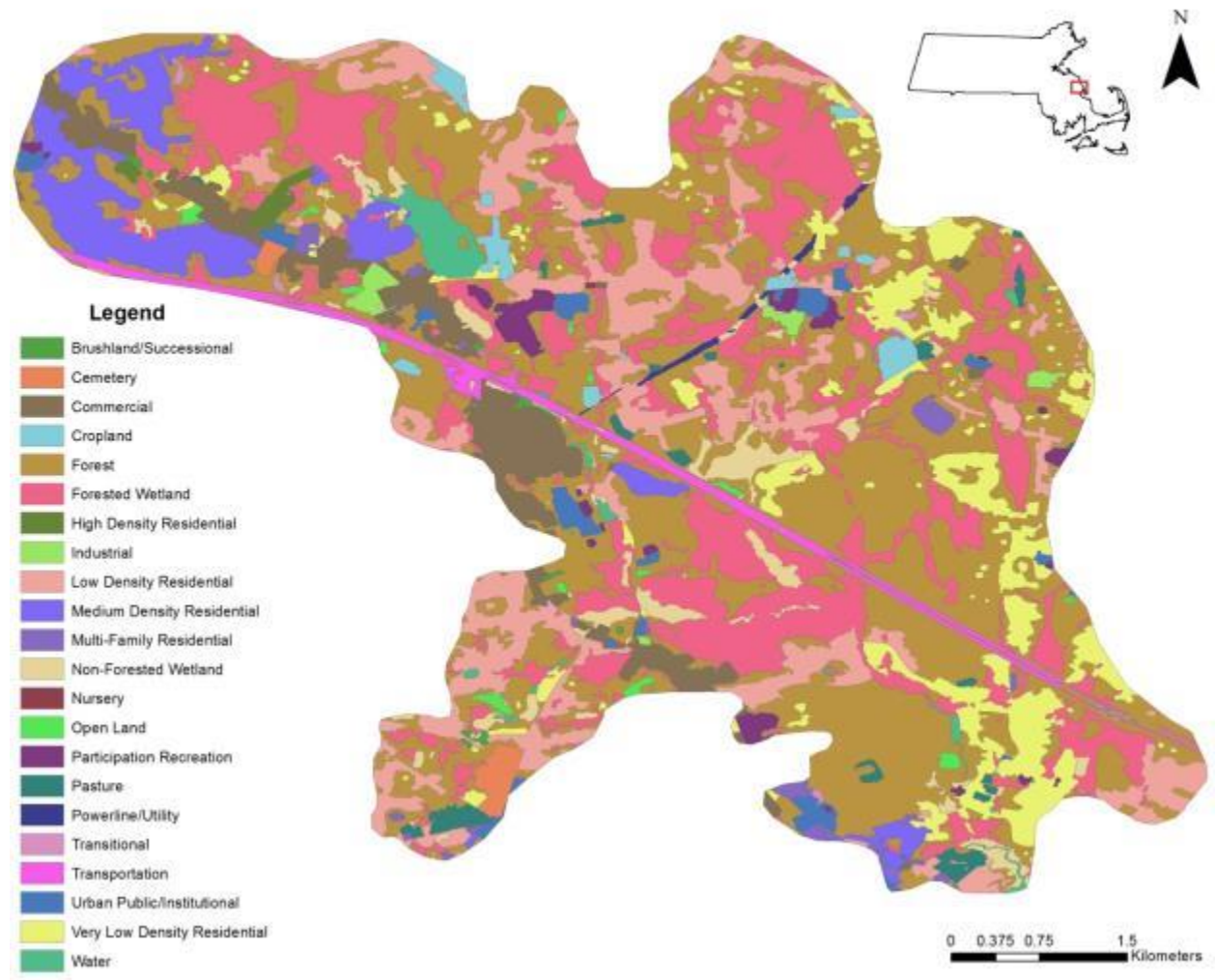


Figure 5: Land use types within the OPM aquifer. Source: MassGIS, 2005. <http://www.mass.gov/anf/research-and-tech/it-serv-and-support/application-serv/office-of-geographic-information-massgis/datalayers/layerlist.html>. Last accessed July 29, 2013.

Land Use Types - Old Pond Meadow Aquifer

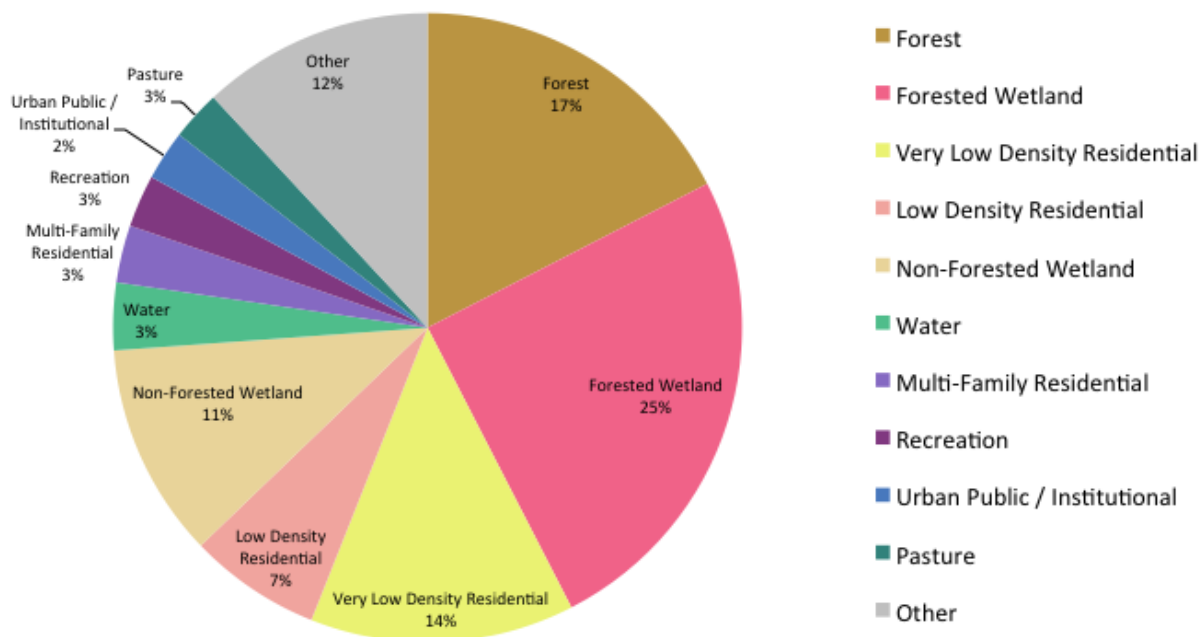


Figure 6: Percentages of land use types within the OPM aquifer. Source: MassGIS, 2005. <http://www.mass.gov/anf/research-and-tech/it-serv-and-support/application-serv/office-of-geographic-information-massgis/datalayers/layerlist.html>. Last accessed July 29, 2013.

Several types of land use, such as commercial and residential, prevent infiltration of water into soil. MassGIS defines impervious surface as buildings, roads, parking lots, brick, asphalt, concrete, and other man-made areas (MassGIS, 2012). This layer was created from orthophoto images and semi-automated techniques. Within the OPM aquifer, impervious surfaces represent 36% of land cover (Fig. 7). The majority of impervious surfaces correspond to commercial development along Washington Street.

Impervious Surface, Old Pond Meadow Aquifer - Norwell, MA

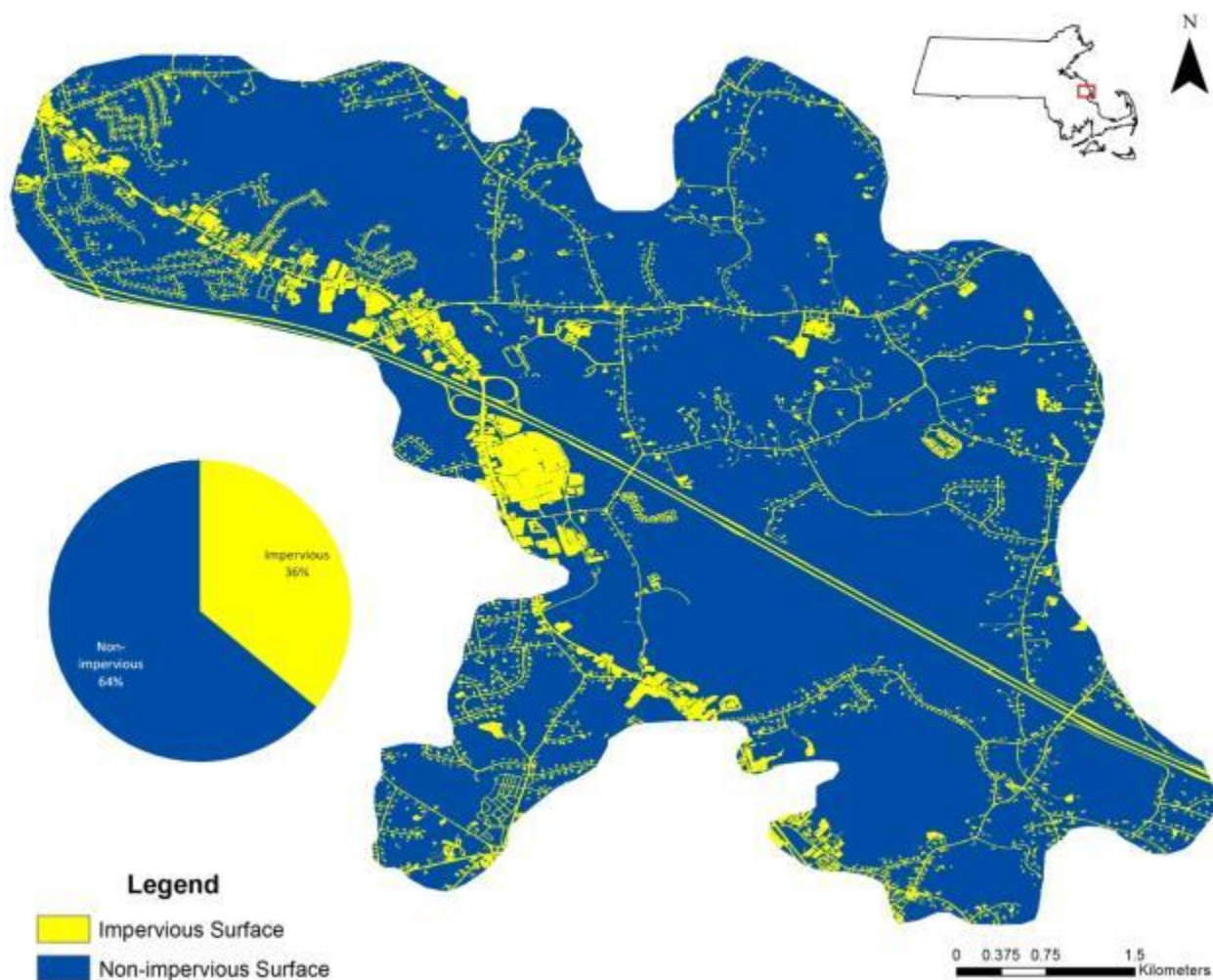


Figure 7: Impervious surface and non-impervious surface within the OPM aquifer. Source: MassGIS, 2005. <http://www.mass.gov/anf/research-and-tech/it-serv-and-support/application-serv/office-of-geographic-information-massgis/datalayers/layerlist.html>. Last accessed July 29, 2013.

The climate in Norwell is humid with an average annual precipitation of 48.0in (NOAA, 2013). Of the total precipitation, 36 in. is in the form of snow and ice. The average monthly temperatures range from 30.9 °F to 73.25 °F (Fig. 8) (NOAA, 2013).

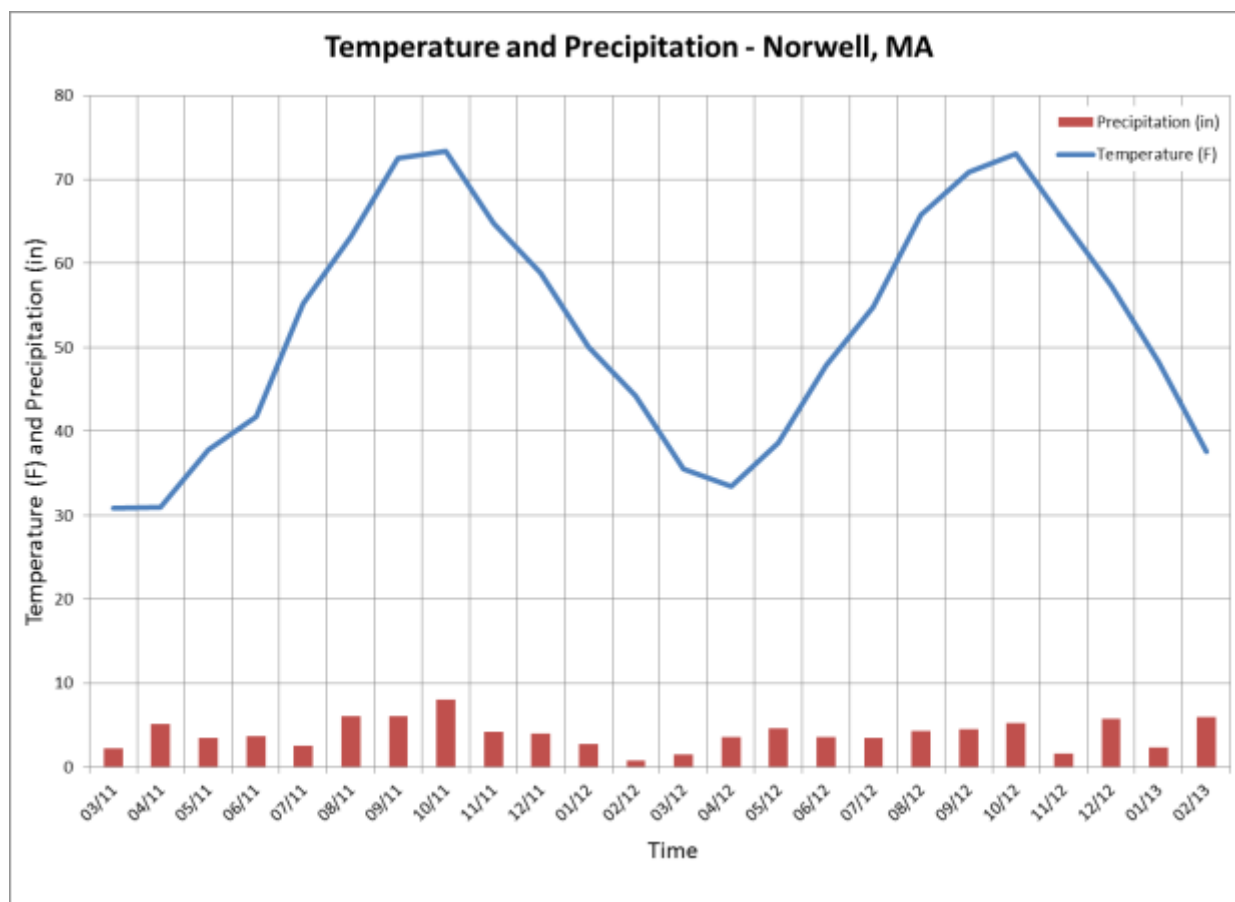


Figure 8: Temperature and precipitation from a NOAA weather station near Norwell, MA Source: NOAA, 2013. <http://www.noaa.gov/pastweather.html> Last Accessed April 26, 2013.

2.2 History of Public Water Supply Operations

In 1994, the Norwell Water Department completed the South Street Treatment Plant (Norwell Water Department, 2013). While there are other treatment plants and well fields at Grove Street and Washington Street, the South Street well field and treatment plant supplies the majority of Norwell's public water. The well field consists of two pumping wells: NOR-1 and NOR-6. The typical production volumes for the entire Norwell Water Department system are approximately one million gallons per day during the winter and two million gallons per day during the summer (Dillon, 2012). At the South Street

treatment plant, mixed water from NOR-1 and NOR-6 is treated for iron, manganese, and organics (Norwell Water Department, 2012). Treated water is pumped into storage tanks from where it enters the water distribution system and ultimately reaches homes and businesses.



Figure 9: South Street Well Field. Wells NOR-1, NOR-6 and the South Street water treatment facility.

Since the 1980s, the Norwell Water Department has monitored water quality at NOR-1 and NOR-6 (Dillon, 2012). Samples were collected from raw well water and analyzed at an off-site lab. NOR-6 appears to be influenced by a reducing environment (Krammer, 2005). Water from this well has low oxidation-reduction potential, low concentrations of dissolved oxygen, and high concentrations of iron

and manganese. In contrast to NOR-6, water from NOR-1 is not as reducing but has higher solute concentrations (Krammer, 2005).

During the past 20 years, the chloride concentrations in NOR-1 water have more than doubled (Fig. 10). Possible sources of chloride include a nearby salt storage facility and local salt application for deicing purposes (Dillon, 2012). Given that chloride concentrations are increasing at NOR-1, the Norwell Water Department is interested in identifying contamination sources and pathways. Understanding the transport of road salt in the OPM aquifer is an important part of fulfilling the current and future demands for high quality drinking water.

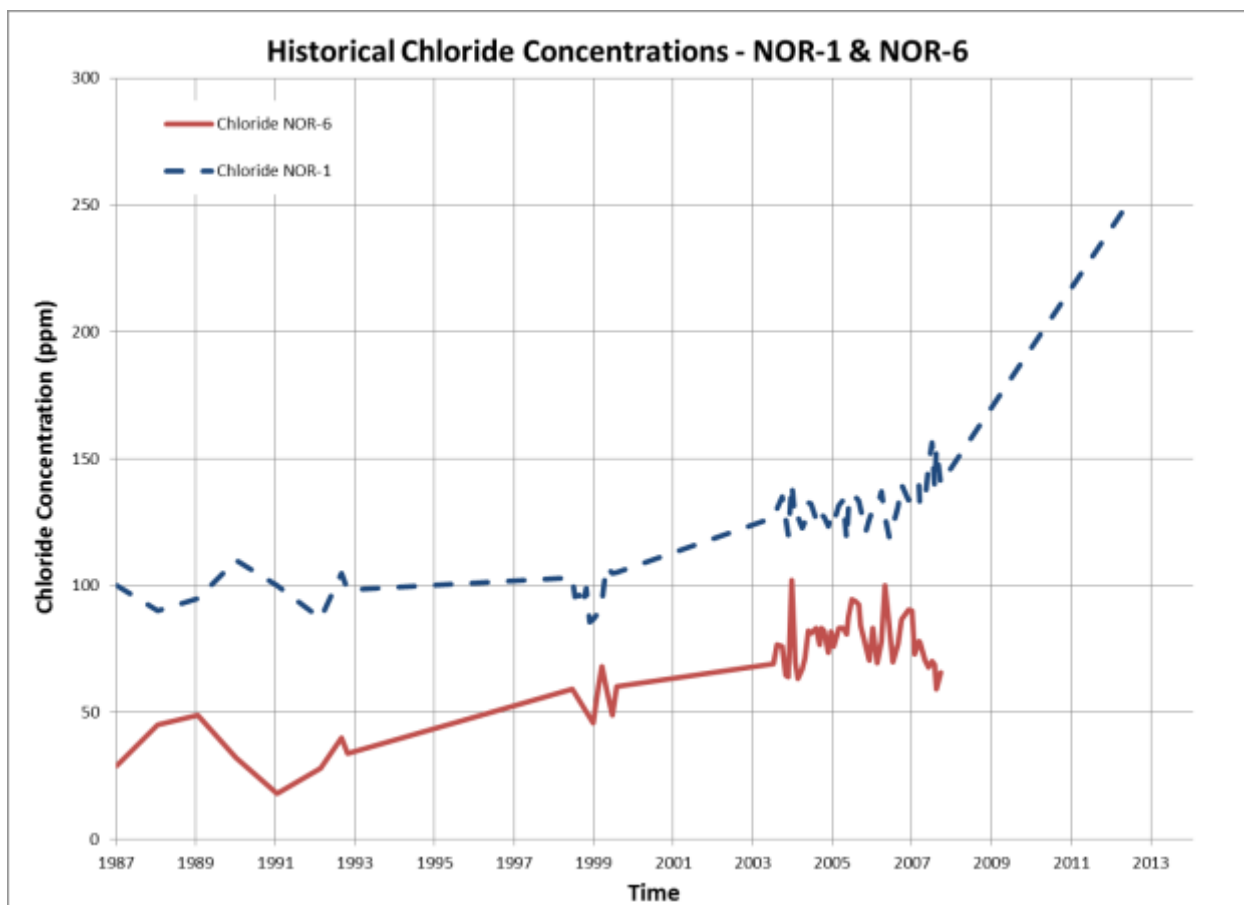


Figure 10: Chloride concentrations in NOR-1 and NOR-6. Samples were collected by the Norwell Water Department and analyzed by Analytical Balance Corporation in February of 2013.

2.3 Road Salt Application and Use

It is difficult to quantify the actual amount of salt released into the environment. Local application procedures and rates depend on the individual highway department but generally range from 100 to 500 pounds per lane-mile (lb/ln-mi) (Shi et al., 2009). For state highways within Massachusetts, the suggested application rate is 240 lb/ln-mi (MHD, 2008). The length of state roads within the OPM aquifer is 29.3 km or 18.2 mi (Fig. 11). Since there are two lanes for each road, the approximate amount of road salt applied by the state during each application is $18.2\text{mi} * 2 \text{ ln} * 240 \text{ lb/ln-mi} = 8736 \text{ lb}$.

Over the course of the winter, the total number of application events depends on the severity of local weather conditions. The MHD does not report the number of application events thereby making it difficult to upscale the value of 8736 lb/app to an aggregate value for each winter. In addition to NaCl, the Massachusetts Highway Department (MHD) may also apply liquid CaCl_2 , solid CaCl_2 , liquid MgCl_2 , and sand (MHD, 2008).

State and Town Roads, Old Pond Meadow Aquifer - Norwell, MA

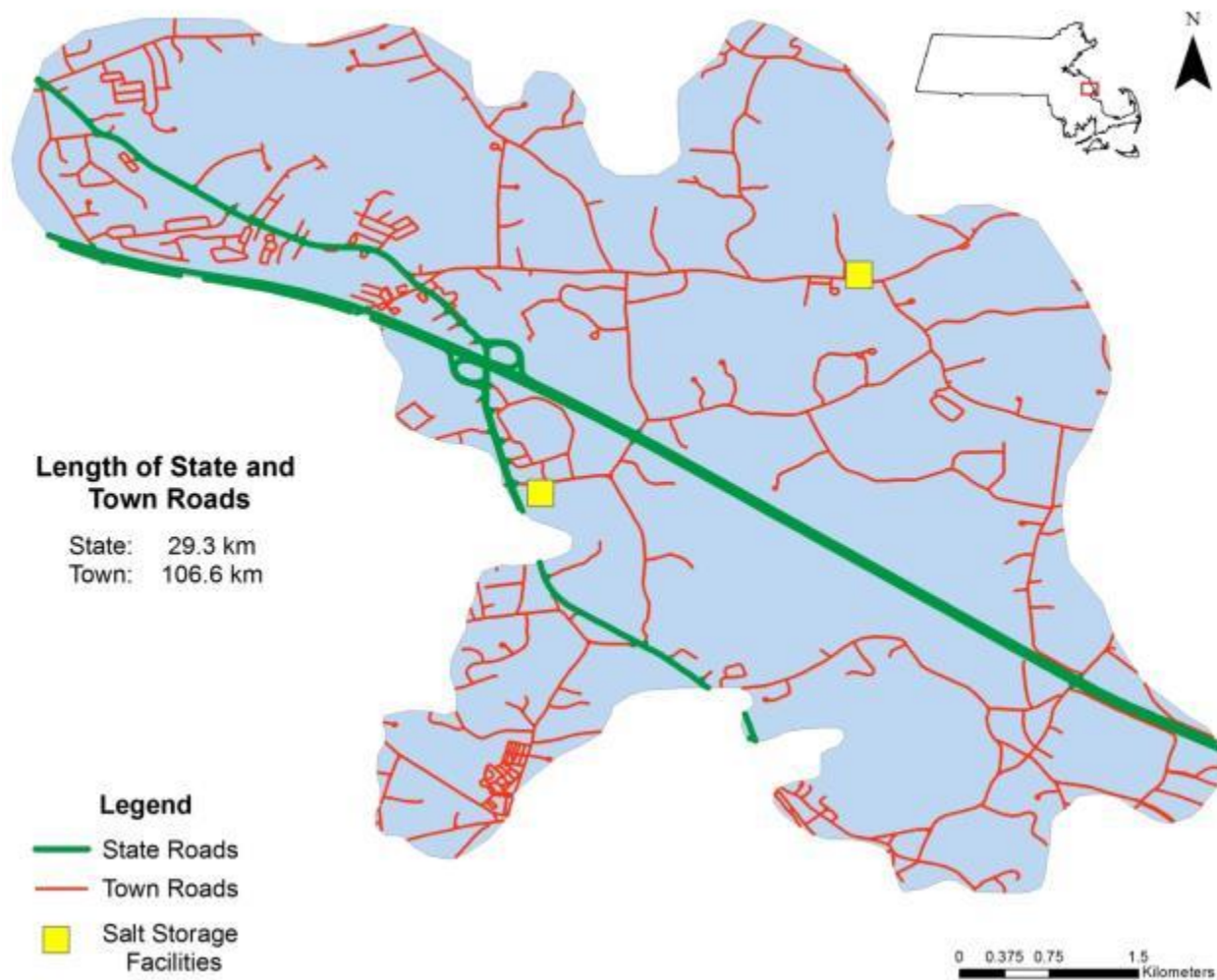


Figure 11: Salt storage facilities and lengths of state and municipal roads within the OPM aquifer. Source: MassGIS, 2005. <http://www.mass.gov/anf/research-and-tech/it-serv-and-support/application-serv/office-of-geographic-information-massgis/datalayers/layerlist.html>. Last accessed July 29, 2013.

However, MHD reports averages of annual salt use within six Massachusetts districts. Within the district that includes Norwell, Hanover, and 79 other towns, the average amount of road salt applied ranged from 16 tons per lane/mi/yr to 49 tons per lane/mi/yr during 2002 to 2011 (MHD, 2012).

Considering that there are 18.2mi of roads and 2 lanes per road in the OPM aquifer, the range of annual road salt application is $16 \text{ tons / ln / mi} * 2 \text{ ln} * 18.2 \text{ mi} = 582 \text{ tons}$ to $49 \text{ tones / ln / mi} * 2 \text{ ln} * 18.2\text{mi} = 1784 \text{ tons}$. These estimates only account for state road salt application and do not include salt application by the Town of Norwell, businesses, and residents. Therefore, the actual amount of road salt application may be much higher.

In addition to road salt application, leakage from salt storage facilities is the other major source of road salt contamination. Chloride concentrations as high as 13,500 mg/l were measured in ground water adjacent to an uncovered salt storage lot (Ohon, 1990). Ostendorf et al. (2006) estimated that 4400 kg of salt per year were introduced into the environment from an uncovered salt storage facility in Maine. For these reasons, the EPA recommends that salt storage facilities be covered and located outside of 100-year floodplains in order to minimize groundwater quality problems in the surrounding area (USEPA, 2012).

There are two salt storage facilities within the OPM aquifer area (Fig. 12). The Town of Norwell operates a covered salt storage facility located in the northeast area of the OPM aquifer. Additionally, the state of Massachusetts stores salt in several elevated and covered buildings in the southwest area of the OPM aquifer. Because of the potential for groundwater contamination by road salt application and leakage from storage facilities, an in-depth study of salt transport and fate is needed.



Figure 12: Aerial photos of salt storage facilities for the Town of Norwell and the MHD. Source: MassGIS, 2005. <http://www.mass.gov/anf/research-and-tech/it-serv-and-support/application-serv/office-of-geographic-information-massgis/datalayers/layerlist.html>. Last accessed July 29, 2013.

Section 3. Purpose and Scope

3.1 Objectives

Elevated chloride and sodium concentrations have been measured at a site in Norwell for several years (Dillon, 2012), yet spatial and temporal trends in road salt are still poorly understood. In order to recognize these patterns, it is necessary to identify road salt pathways from their sources to their discharge points. To this end, the objective of this study is to characterize trends in road salt solute concentrations by focusing on selected cross-sections and In-Situ, Inc., AquaTroll 200 probe data.

The approach in this thesis is to analyze sodium and chloride in addition to other major ions and trace elements. By measuring a large set of field- and lab-based hydrogeochemical parameters, it will be possible to resolve the role of other chloride salts, interactions of earth materials and solutes, and ion

mobilization within the context of solute transport. Overall, these data provide useful metrics for understanding transport even though actual transport mechanics cannot be resolved.

3.2 Data Collection Plan

Specifically, the data collection for this study included sensor data and water sample collection and analysis. In March 2011, three Insitu sensors were installed in piezometers to measure specific conductance. Since the sensors collected data independently, the field work for this project primarily consisted of collecting water samples. The specific methods of collecting water samples were: grab sample, pushpoint, low-flow, and geoprobe. Once the samples were collected and prepared, they were brought to the Boston College Department of Earth and Environmental Sciences for laboratory analysis. The major types of laboratory procedures included ion chromatography (IC) and inductively coupled plasma (ICP) emission spectroscopy.

Section 4. Methods

4.1 Sample Collection

4.1.a Pushpoint Sampling

Pushpoint sampling is a quick way of measuring groundwater properties along a streambed. The sampler was a stainless steel tube 91 cm long and 6 mm in diameter with a pointed tip and slotted screen at one end (Zimmerman et al., 2005). The probe was inserted 10 to 60 cm below the streambed, and a syringe pump connected to tube allowed for sample collection at the surface. Zimmerman et al. 2005 showed that this sampling procedure produced very little contamination from surface water or the

sampling procedure itself. One disadvantage of Pushpoint sampling is that samples cannot be collected at the exact same location on subsequent visits.

4.1.b Well and Surface Water Sampling

The surface-water sampling protocol attempted to collect representative samples of streams, lakes, and wetlands with minimal contamination. Grab sampling refers to simply filling surface water into a bottle at one discrete point. In the case of streams, water was taken from the center where water is assumed to be sufficiently well mixed. Field parameters such as specific conductance and temperature were measured in the surface-water body at the time of sample collection.

The groundwater sampling procedure for this study followed the EPA's Low Stress Purging and Sampling Procedure (USEPA, 2010). The Low Stress Purging and Sampling Procedure aims to minimize variability from individual personnel, equipment, and ambient variability in the environmental conditions (USEPA, 2010). A peristaltic pump set to a flow rate of 0.2 to 0.5 L/min minimized the intrusion of water from well storage. Additionally, depth-to-water and other field parameters were measured every minute to determine when stabilization occurred. If field parameters and depth-to-water remained within the tolerance limits defined by the EPA after purging, it is probable that pump uptake water reflected in the in situ formation fluids (USEPA, 2010).

4.1.c Geoprobe Sampling

Geoprobe sampling was performed in order to obtain groundwater samples at at specific aquifer depths. A geoprobe machine inserted drillpipe from the surface until it reached bedrock or refusal. The bottom segment of drillpipe was perforated with slotted screens. At five-foot intervals, a tube was lowered to the perforated pipe, and a peristaltic pump pulled water through the screens.

The geoprobe machine was operated by Maher Drilling Services, and sampling was conducted in January 2013. The locations of sampling sites were chosen by Peter Dillon with the Norwell Water Department. While sampling was attempted at every interval, sometimes there was not enough water in the perforated pipe to take a sample.

4.1.d Sample Preparation

Regardless of whether samples were collected by grab sample, Pushpoint sampling, or Low Stress Purging and Sampling, water samples were prepared with the following procedures in order to maintain high quality assurance. Nalgene 250ml or 500ml polyethylene containers were filled completely to minimize the sample's exposure to air. Within twelve hours of sample collection, samples were refrigerated in a Boston College laboratory. In order to protect laboratory sampling equipment, IC and ICP samples were filtered with a 45 micron Millipore filters. For ICP samples only, concentrated nitric acid was added until 2% of the ICP sample solution consisted of nitric acid (Besancon, 2012).

4.2 Ion Chromatography

Ion chromatography (IC) is an analytical technique that measures major ions in aqueous solutions. IC separates ions and polar molecules based on their size and charge. The sample is carried by an aqueous buffer, retained on a stationary phase, and detected by electrical conductivity. IC can measure the concentrations of the cations calcium, potassium, sodium, and magnesium. Anions such as chloride, bromide, fluoride, sulfate, nitrates, and nitrites are also measured. Anions and cations are measured in separate columns in separate mobile phases.

During sampling, which took place at Boston College, the analyte and eluent entered a column, where interaction with fixed ions of opposite charge occurs. Then, the ions went through a suppressor

so that each type of ion was separated and arrived at distinct times. A detector then measured the electrolytic conductivity of the solution. This conductivity was related to a concentration through the Dionex Chromeleon 7.0 processing software.

4.3 Inductively Coupled Plasma Emission Spectroscopy (ICP)

A PerkinElmer Optima 7000 ICP-Optical Emission Spectrometer, located at Wellesley College, measures optical emissions of ionized sample atoms. The process begins by heating argon to 5000 to 8000 K with a torch so that the molecules break down into electrons and ions (Manning and Grow, 1997). A high-powered radio frequency generator creates an electromagnetic field within a coil. The argon plasma interacts with the electromagnetic field to flow in a rotational symmetrical pattern.

After the argon has been ignited into plasma, a peristaltic pump delivers an aqueous sample into a nebulizer (Sarojam, 2010). The sample is converted into a mist and introduced into the argon plasma flame. The collisions between the plasma and the sample caused the sample itself to be changed into ions and electrons. Eventually, sample ions and electrons recombine into neutral atoms and emitted radiation at characteristic wavelengths of the atoms involved (Manning & Grow, 1997).

Within the optical detection system, transfer lenses focus emitted light on a diffraction grating where it separates into component wavelengths. Photodetectors measure the intensity of the predefined wavelengths (Sarojam, 2010). The wavelength intensities of samples were compared to calibration standards with known concentrations of each element. The elements analyzed with ICP were Ag, Al, As, Ba, Ca, Cd, Co, Cr, Cu, Fe, K, Mg, Mn, Mo, Na, Ni, P, Pb, Sb, Sn, Sr, Ti, V, and Zn.

4.4 Temporal Data

In March 2011, three piezometers (25 ft., 40 ft., and 60 ft. below ground surface) were drilled near to NOR-1 (Fig. 13). In-situ Aqua Troll 200 probes were installed at the base of each piezometer near the well screens. These probes were calibrated for temperature, pressure, and specific conductance in a Boston College laboratory. They were programmed to record temperature, pressure, and specific conductance at 15-minute intervals using In-situ Aqua TROLL 5 software.

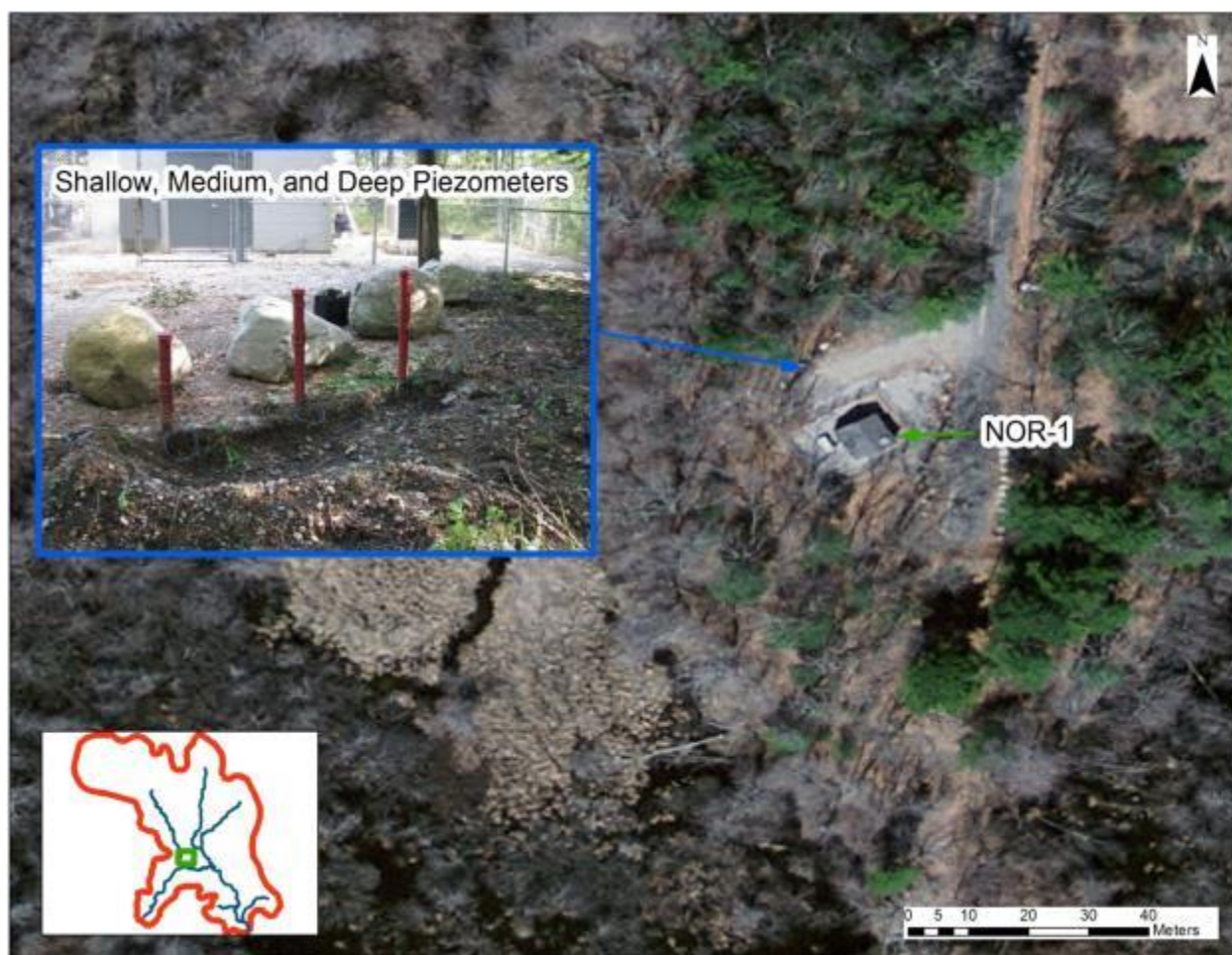


Figure 13: Three piezometers near NOR-1. Within each piezometer is an In-Situ, Inc., AquaTroll 200 that records temperature, depth, and specific conductance. Source: MassGIS, 2005. <http://www.mass.gov/anf/research-and-tech/it-serv-and-support/application-serv/office-of-geographic-information-massgis/datalayers/layerlist.html>. Last accessed July 29, 2013

4.5 Geospatial Analysis

A surface topography map of the study area was created showing elevation peaks, troughs, and changes in relief. The digital terrain model (DTM) represents the elevation of ground surface without objects such as trees or buildings. The Massachusetts Office of Geographic Information, also called MassGIS, provided DTM data points. The DTM data points were calculated from stereo 1:5,000 scaled digital orthophoto images (MassGIS, 2012). The number of data points per unit area was high enough to create elevation maps with an accuracy of +/- 1.5 m. Using DTM data points as an input, the inverse distance weighing (IDW) function in ArcGIS creates a raster image where the color of each cell relates to surface terrain elevation.

Aquifer thickness is defined as the distance from the surface terrain to refusal or bedrock. For example, a value of zero represents a bedrock outcrop, whereas a high aquifer thickness value signifies a deep soil column.

A raster image of aquifer thickness was calculated using data from well records near the study area. Both the Town of Norwell and the Massachusetts Department of Environmental Protection (DEP) keep records of domestic, public, irrigation, and other types of wells. Out of the well records available, 567 records contained information on the depth from the surface to bedrock.

A bedrock elevation map was developed using the surface elevation map and aquifer thickness map. The map algebra tool in ArcGIS performs mathematical functions on the values within various raster cells. In order to create a new bedrock elevation raster, the value of aquifer thickness was subtracted from surface elevation for every cell.

4.6 Sampling Sites

4.6.a - Surface Elevation Map

During the spring and summer of 2012, 68 near-surface ground water samples were taken using Pushpoint sampling (Tables 1 and 2). The most extensive sampling took place during the week of March 4, 2012. Approximately every 500 m along the THB and WCB, three samples were on the west bank, the center of the stream, and the east bank (Fig. 14). At certain sampling locations, such as three and four, rocky soil conditions made it impossible to take a sample. In July 2012, 13 samples were taken along the center of the THB upstream of NOR-1.

Table 1: Near-surface groundwater sample locations - March 2012

Sample ID	Collection Date	Sample Collection Method	Latitude	Longitude	Specific Conductance	
1	W	3/6/2012	Pushpoint	42.139400	-70.834953	N/A
1	C	3/6/2012	Pushpoint	42.139473	-70.835342	N/A
1	E	3/6/2012	Pushpoint	42.139744	-70.835464	N/A
2	W	3/6/2012	Pushpoint	42.139496	-70.836121	N/A
2	C	3/6/2012	Pushpoint	42.157246	-70.824547	N/A
2	E	3/6/2012	Pushpoint	42.157391	-70.824356	N/A
3	W	3/6/2012	Pushpoint	42.154297	-70.824944	N/A
3	C	3/6/2012	Pushpoint	42.154411	-70.825195	N/A
3	E	3/6/2012	Pushpoint	42.154446	-70.825607	N/A
4	C	3/6/2012	Pushpoint	42.150627	-70.824867	N/A
5	W	3/6/2012	Pushpoint	42.150471	-70.824722	N/A
5	C	3/6/2012	Pushpoint	42.150452	-70.824753	N/A
5	E	3/6/2012	Pushpoint	42.145271	-70.825729	N/A
6	W	3/9/2012	Pushpoint	42.145557	-70.825523	N/A
6	CW	3/9/2012	Pushpoint	42.147354	-70.824715	N/A
6	CE	3/9/2012	Pushpoint	42.147438	-70.824486	N/A
6	E	3/9/2012	Pushpoint	42.134731	-70.834198	N/A
7	W	3/6/2012	Pushpoint	42.134777	-70.833984	N/A

7	C	3/6/2012	Pushpoint	42.134750	-70.834404	N/A
7	E	3/7/2012	Pushpoint	42.136757	-70.833946	N/A
8	W	3/7/2012	Pushpoint	42.136211	-70.834007	N/A
8	C	3/7/2012	Pushpoint	42.136669	-70.834045	N/A
8	E	3/7/2012	Pushpoint	42.117401	-70.809486	N/A
9	W	3/6/2012	Pushpoint	42.117104	-70.809578	N/A
9	C	3/6/2012	Pushpoint	42.125694	-70.811096	N/A
9	E	3/6/2012	Pushpoint	42.125595	-70.811020	N/A
10	W	3/7/2012	Pushpoint	42.122597	-70.808853	N/A
10	C	3/7/2012	Pushpoint	42.125462	-70.811211	N/A
10	E	3/7/2012	Pushpoint	42.122734	-70.808594	N/A
11	W	3/7/2012	Pushpoint	42.126820	-70.813934	N/A
11	C	3/7/2012	Pushpoint	42.127045	-70.813721	N/A
11	E	3/7/2012	Pushpoint	42.127026	-70.813766	N/A
12	W	3/7/2012	Pushpoint	42.129238	-70.816345	N/A
12	C	3/7/2012	Pushpoint	42.129002	-70.816231	N/A
13	W	3/7/2012	Pushpoint	42.128944	-70.816261	N/A
13	C	3/7/2012	Pushpoint	42.131626	-70.817436	N/A
13	E	3/7/2012	Pushpoint	42.131470	-70.817360	N/A
14	C	3/7/2012	Pushpoint	42.131588	-70.817345	N/A
14	E	3/7/2012	Pushpoint	42.132355	-70.831459	N/A
15	W	3/7/2012	Pushpoint	42.132210	-70.831337	N/A
15	C	3/7/2012	Pushpoint	42.132721	-70.831062	N/A
15	E	3/7/2012	Pushpoint	42.143654	-70.837173	N/A
16	W	3/8/2012	Pushpoint	42.143490	-70.837273	N/A
16	C	3/8/2012	Pushpoint	42.143227	-70.837227	N/A
16	E	3/8/2012	Pushpoint	42.147160	-70.839211	N/A
17	W	3/8/2012	Pushpoint	42.147144	-70.839066	N/A
17	C	3/8/2012	Pushpoint	42.156124	-70.846565	N/A
17	E	3/8/2012	Pushpoint	42.156128	-70.846375	N/A
18	W	3/8/2012	Pushpoint	42.156109	-70.846481	N/A
18	C	3/8/2012	Pushpoint	42.153000	-70.844650	N/A
18	E	3/8/2012	Pushpoint	42.158218	-70.846886	N/A
19	W	3/8/2012	Pushpoint	42.158218	-70.846863	N/A
19	C	3/8/2012	Pushpoint	42.158062	-70.846832	N/A
19	E	3/8/2012	Pushpoint	42.153351	-70.844734	N/A
20	W	3/8/2012	Pushpoint	42.147278	-70.824562	N/A
20	C	3/8/2012	Pushpoint	42.136662	-70.833900	N/A
20	E	3/8/2012	Pushpoint	42.134766	-70.834328	N/A

Table 2: Near-surface groundwater sample locations - July 2012

Sample ID	Collection Date	Sample Collection Method	Latitude	Longitude	Specific Conductance
1	7/2/2012	Pushpoint	42.143616	-70.837891	N/A
2	7/3/2012	Pushpoint	42.136604	-70.833977	N/A
3	7/2/2012	Pushpoint	42.137669	-70.834572	N/A
4	7/2/2012	Pushpoint	42.143448	-70.837029	N/A
5	7/2/2012	Pushpoint	42.137402	-70.834137	N/A
6	7/2/2012	Pushpoint	42.136082	-70.834091	N/A
7	7/2/2012	Pushpoint	42.141914	-70.836952	N/A
8	7/2/2012	Pushpoint	42.135014	-70.834450	N/A
9	7/2/2012	Pushpoint	42.135860	-70.834274	N/A
10	7/2/2012	Pushpoint	42.135349	-70.834976	N/A
11	7/2/2012	Pushpoint	42.134399	-70.833733	N/A
12	7/2/2012	Pushpoint	42.134991	-70.834579	N/A

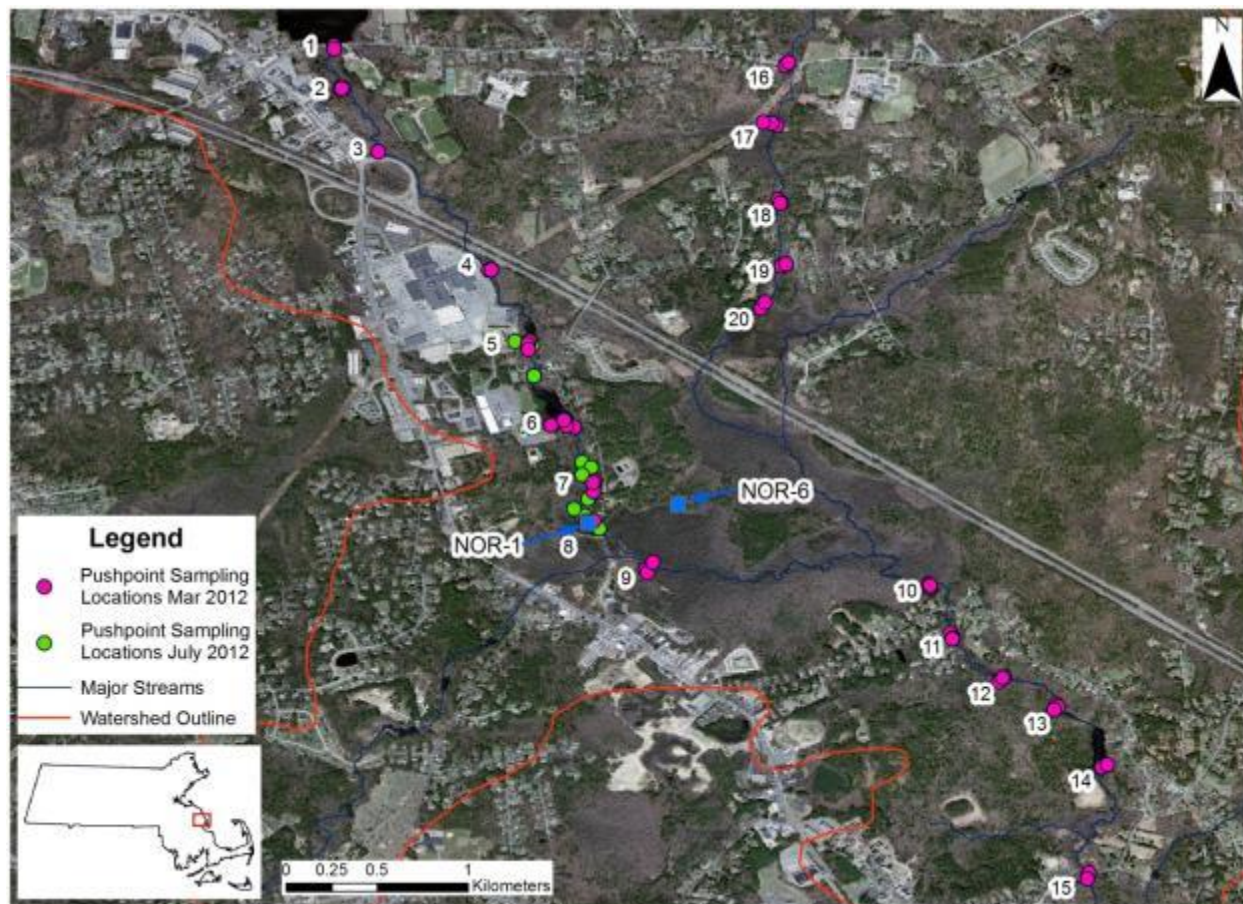


Figure 14: Locations of near-surface ground water samples taken in March and July 2012.

4.6.b Vertical Sampling within the OPM Aquifer

In July 2012, piezometers and historical wells were sampled along an east-west transect (Table 3, Fig. 14). The piezometers were located in an esker near NOR-1, whereas historical monitoring wells were located in an upland region surrounded by wetlands (Fig. 15). Historical well sampling was limited to wells with PVC rather than metal casings to avoid contamination from metal wellbores. Water

samples were taken with a peristaltic pump in accordance with the EPA's Low Stress Purging and Sampling Procedure (USEPA, 2010).

Table 3: Locations of vertical sampling within the OPM aquifer

Sample ID	Collection Date	Sample Collection Method	Latitude	Longitude	Specific Conductance
97-4	7/12/2012	Low-Flow	42.134623	-70.823163	N/A
97-5	7/12/2012	Low-Flow	42.135381	-70.822806	N/A
98-2 S,M,&D	7/12/2012	Low-Flow	42.134776	-70.823216	N/A
98-3 S,M,&D	7/12/2012	Low-Flow	42.135046	-70.821991	N/A
98-5	7/12/2012	Low-Flow	42.134721	-70.822768	N/A
98-4	7/12/2012	Low-Flow	42.13502	-70.822308	N/A

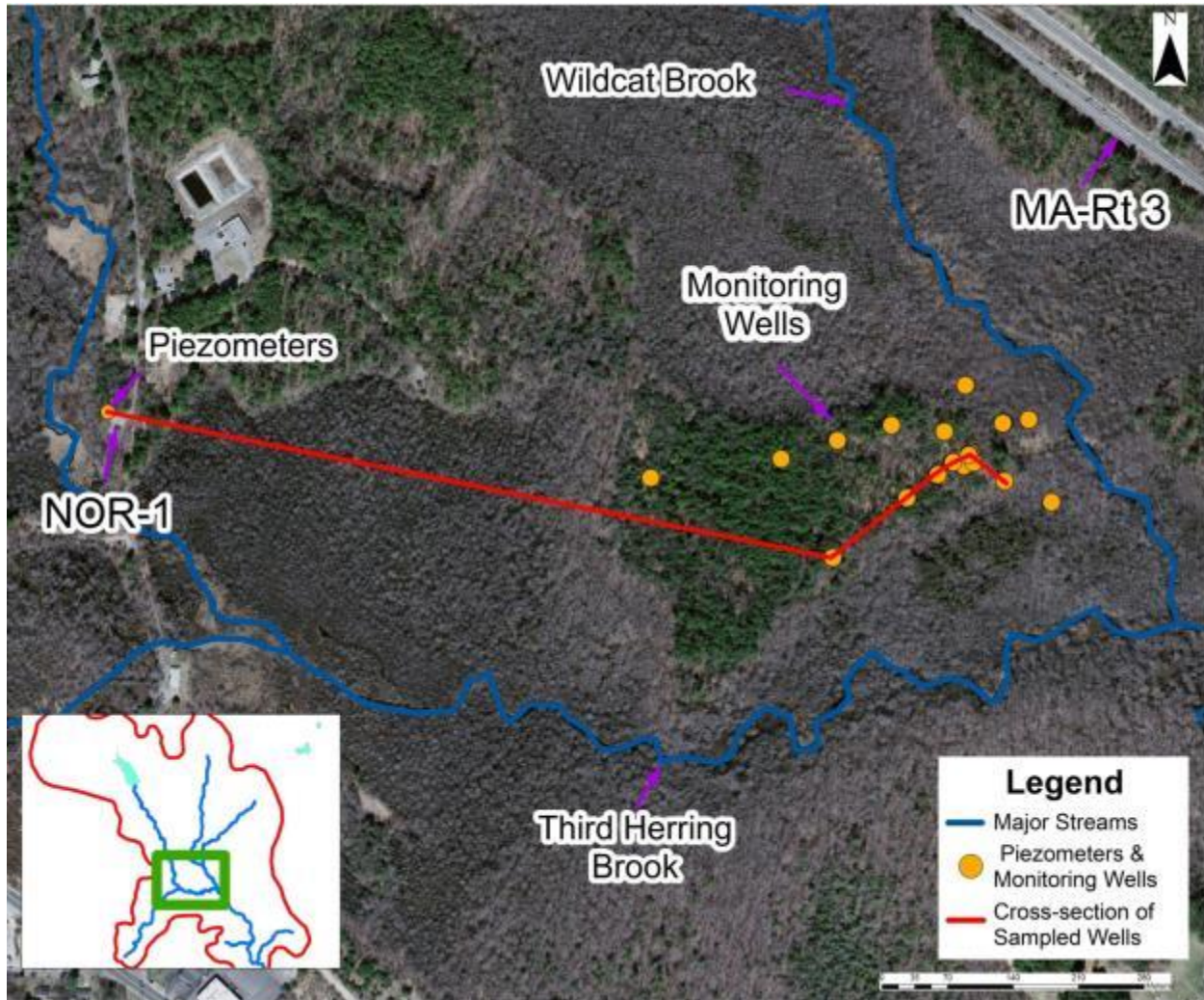


Figure 15: Cross-section of piezometers and wells sampled in July, 2012.

4.6.c Cross-sections near NOR-1

At seven locations near NOR-1, water samples were taken at five foot depth intervals using a geoprobe. These locations are listed in Table 4.

Table 4: Cross-section sample locations

Sample ID	Collection Date	Sample Collection Method	Latitude (deg)	Longitude (deg)	Specific Conductance
1	1/28/2013	Geoprobe	42.13462092	-70.83428982	N/A
2	1/28/2013	Geoprobe	42.13470960	-70.83425327	N/A
3	1/28/2013	Geoprobe	42.13490431	-70.83430826	N/A
4	1/28/2013	Geoprobe	42.13512962	-70.83427138	N/A
5	1/30/2013	Geoprobe	42.13527152	-70.83414766	N/A
6	1/31/2013	Geoprobe	42.13456987	-70.83367559	N/A
7	1/31/2013	Geoprobe	42.13504700	-70.83408700	N/A

Sampling locations one through six were located within the THB floodplain, whereas sampling location seven was situated in an esker and had a higher surface elevation (Fig. 16). The higher surface elevation of the esker compared to the floodplain is denoted by lidar surface elevation (Fig. 17).

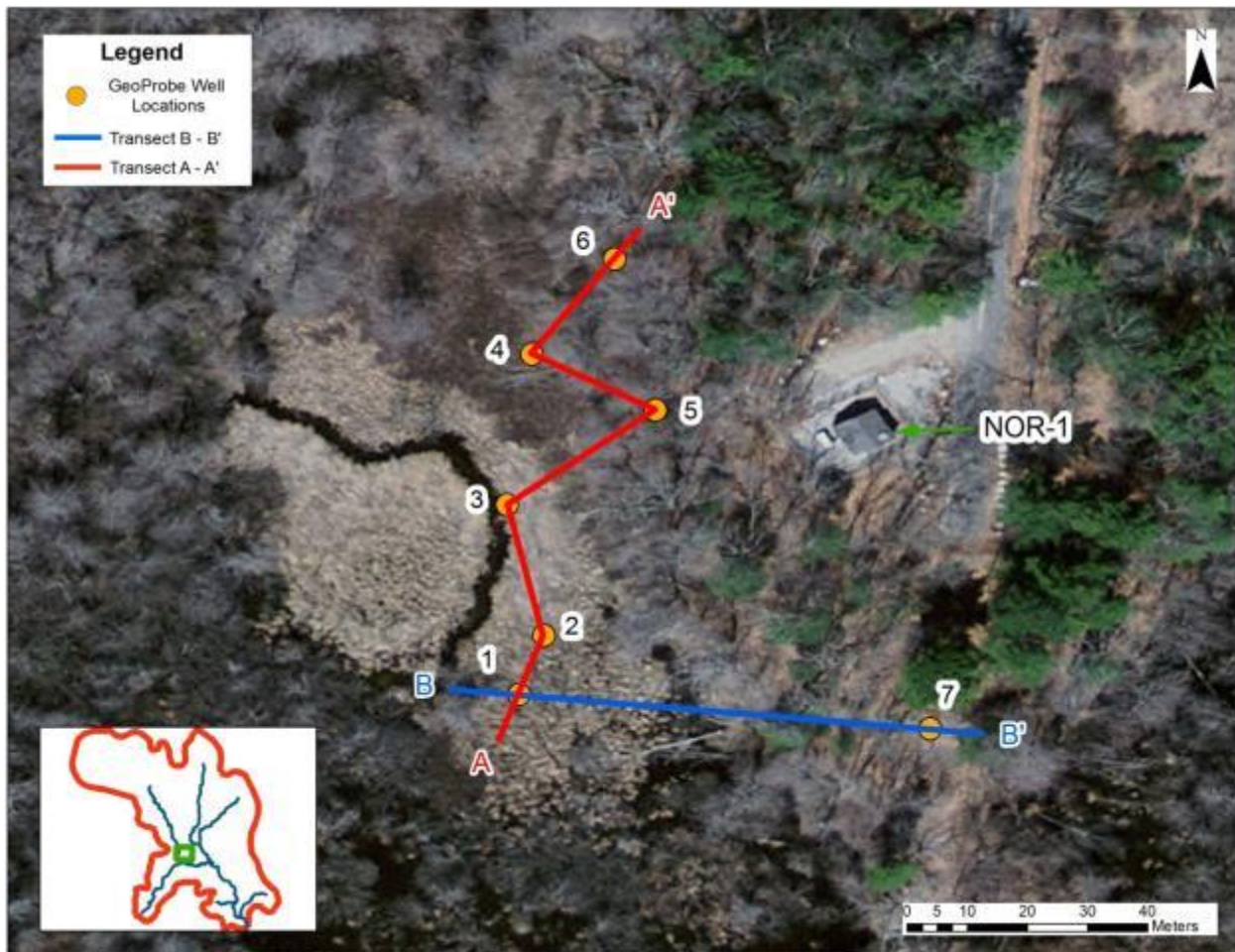


Figure 16: Location of direct-push drilling sits completed January – February 2013. Cross-section transects A-A' and B-B' are shown in Figs 32 and 33.

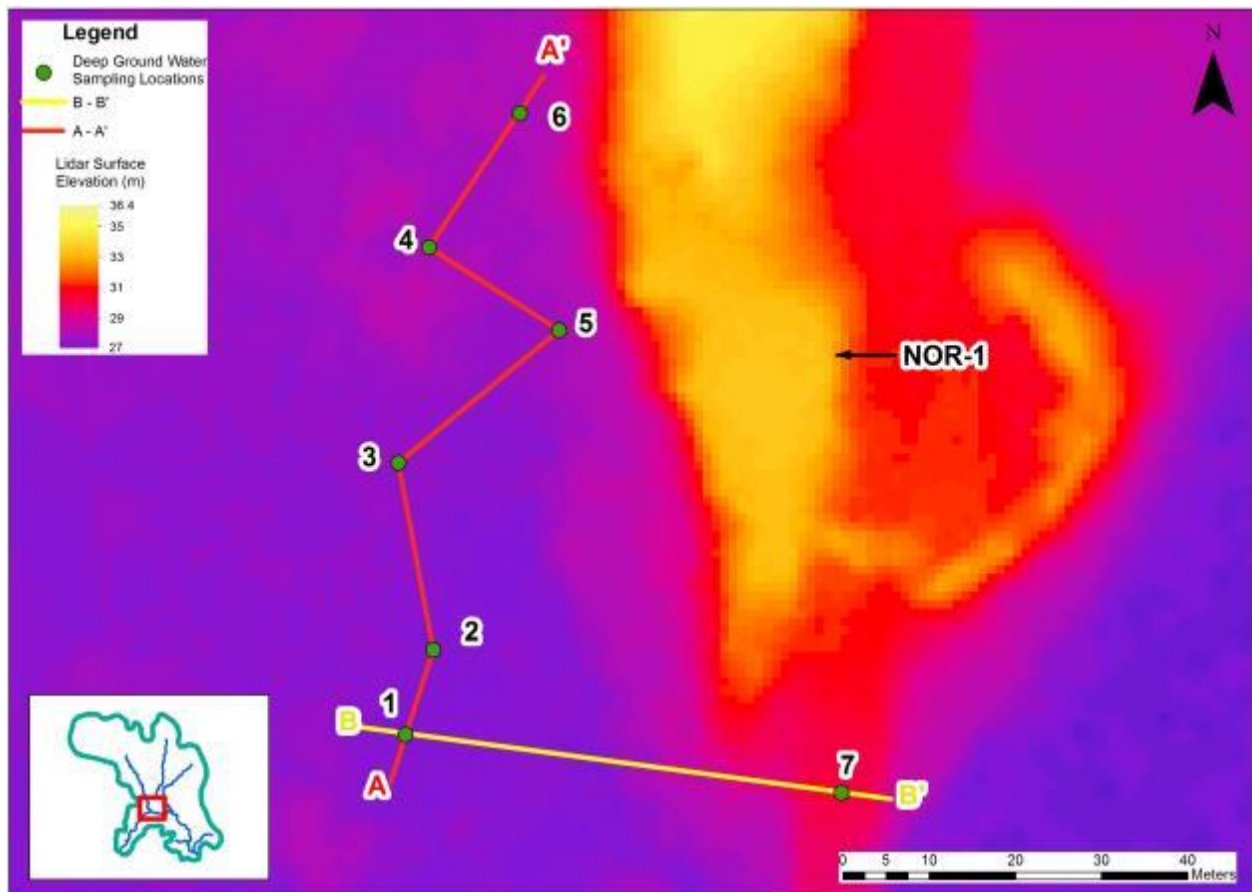


Figure 17: Transect sampling locations and lidar surface elevation. Transects A-A' and B-B' are arbitrarily assigned through sampling locations. Cross-sections of these transects are shown in Figs. 26 - 30.

4.7 Grain Size Analysis

Soil samples from the O soil horizon were taken near NOR-1 and NOR-6. Each sample was sieved and weighted to determine the distribution of grain sizes among certain ranges.

Section 5. Results

5.1 – GIS Aquifer Characterization

5.1.a -Surface Elevation Map

The DTM elevation raster shows several trends in surface elevation. The highest elevations are in the northern part of the study area and a summit in the southeastern corner. There are elevation troughs through the middle of the study area and along the coasts.

While there are several user-defined options for calculating IDW rasters, the density of DTM data points is so high that these options do not result in significant variation in the final raster. However, these options are relevant to the creation of the aquifer thickness raster and will be addressed in the following section.

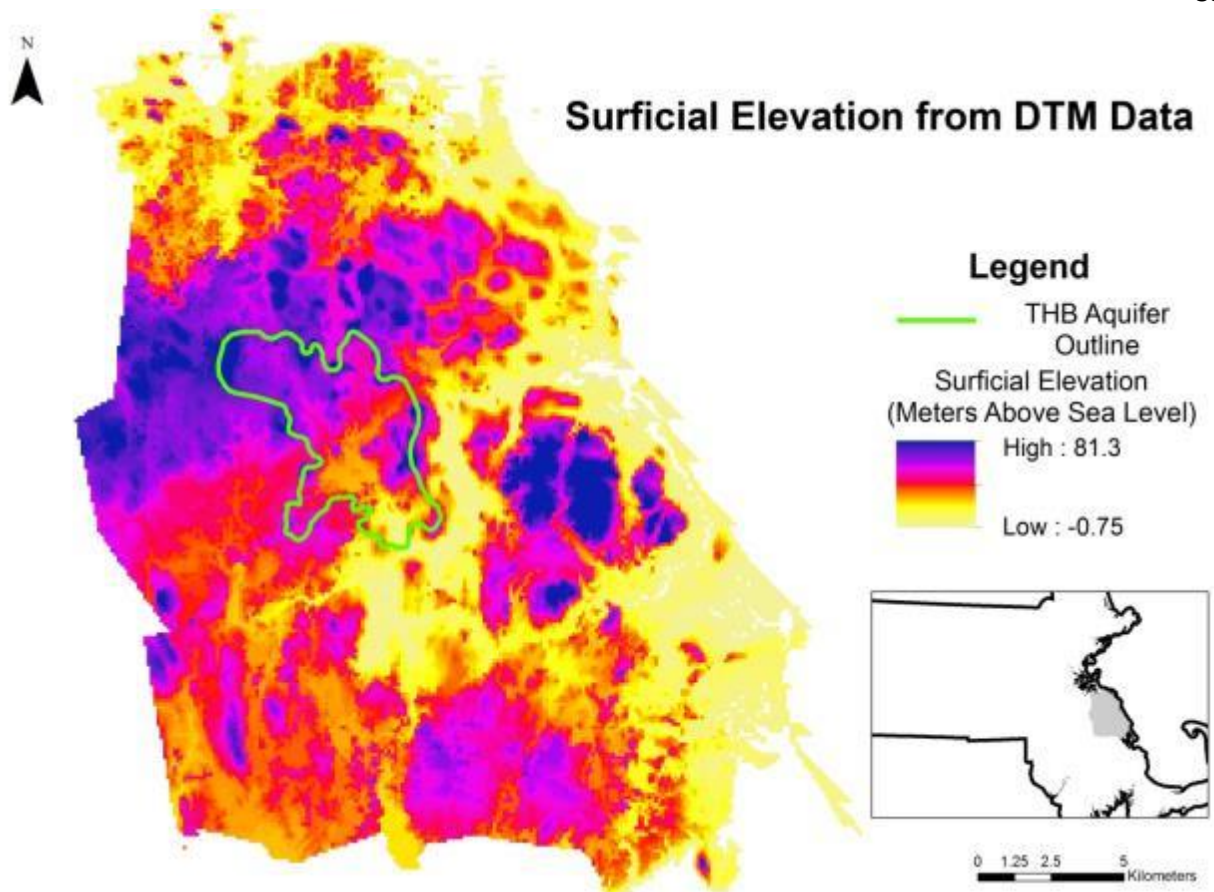


Figure 18: Surface elevation (m) calculated from MassGIS digital terrain files.

5.1.b - Aquifer Thickness Map

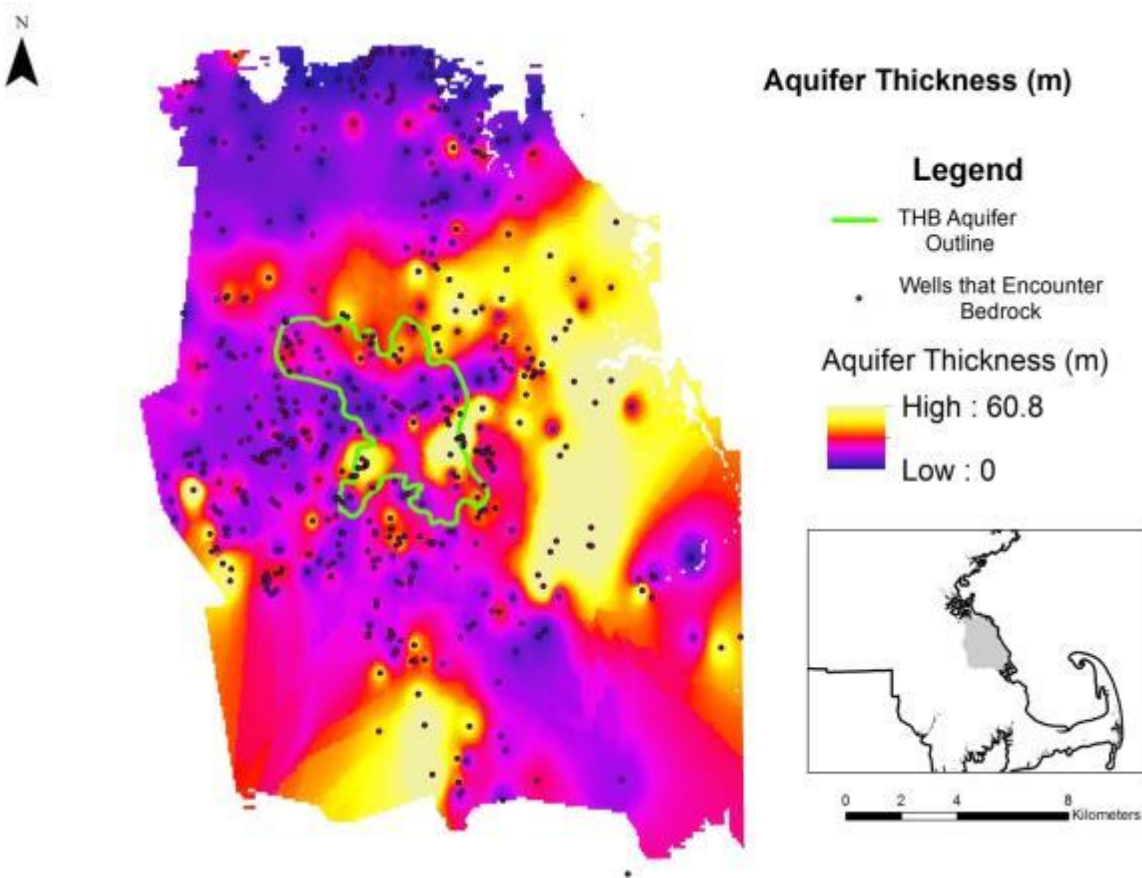


Figure 19: Aquifer thickness (m) calculated from well near Norwell that encountered bedrock.

The ArcGIS IDW tool estimated the aquifer thickness across the field area based on well location and aquifer thickness (Fig. 19). The weighting factor and neighborhood search options influenced the IDW algorithm. A weighting factor of two was chosen for the aquifer thickness map. This value indicates that the weight of a data point decreases with the inverse of the distance squared.

A relatively high weighting factor is necessary because surface elevation and depth-to-bedrock can change dramatically in a short distance. This relatively high weighting factor limited the influence of questionable data points, but caused the pock marks features in the output raster.

Several spatial trends in aquifer thickness were observed across the study area. Through the middle of the town of Norwell along an east/west line, the aquifer thickness was very low. This area has a bedrock outcrop near the Hanover Mall (Fig. 19). Conversely, in the southern part of Norwell, the aquifer thickness is much higher. These values have important implications for estimating bedrock elevation.

5.1.c - Bedrock Elevation Map

The bedrock elevation map shows that the bedrock generally slopes from north to south. The highest elevations are located in the northwest section of the study area while the lowest values are in the southeast section. The bedrock elevation map generally corresponds with surface elevation map.

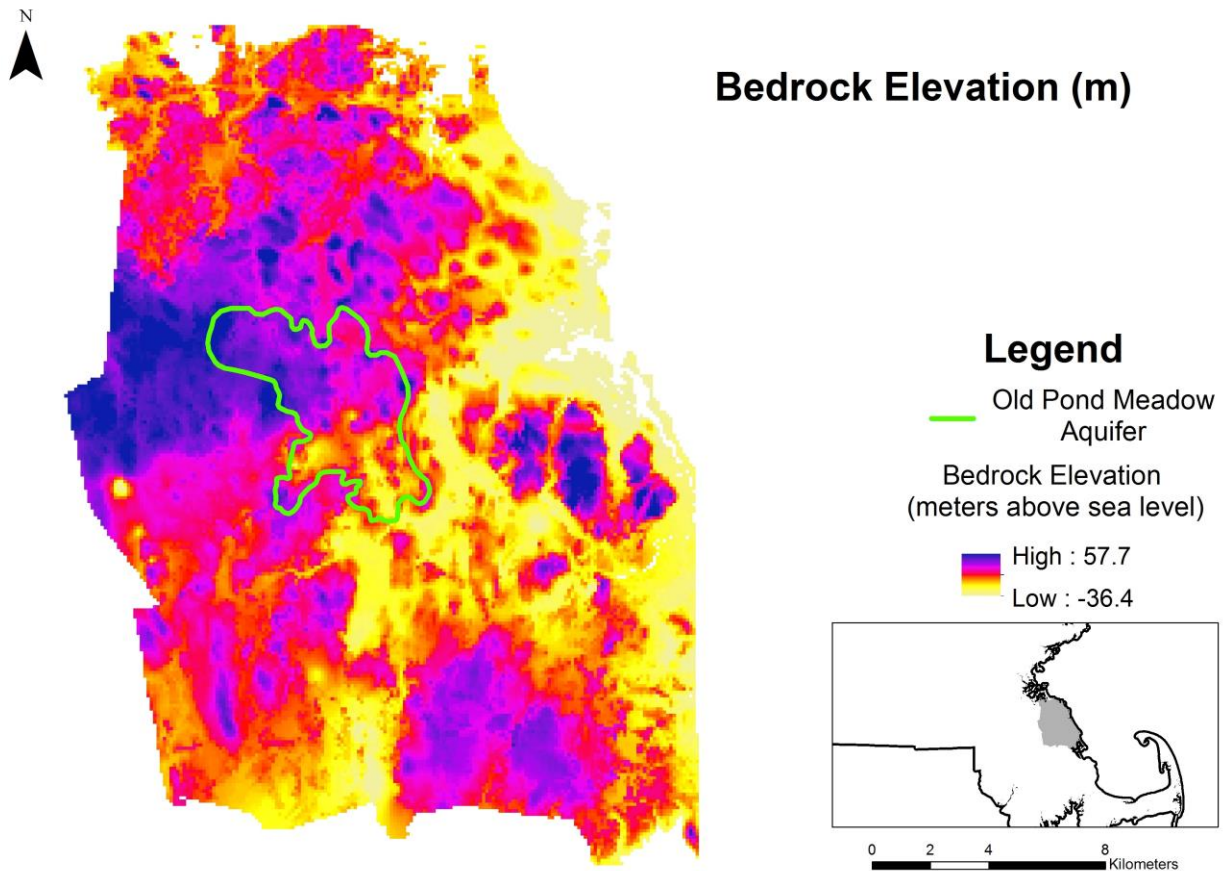


Figure 20: Bedrock elevation calculated from surface elevation and aquifer thickness.

5.2 Water Sample Laboratory Analysis

5.2.a Ion Chromatography (IC) Analysis

Ion Chromatography (IC) results for near-surface ground water samples are listed in Tables 5 and 6. The chloride concentrations along the center of the streams for lateral sampling are presented as graduated symbols on an aquifer map in Figs. 21 and 22. In both March and July data, the highest concentrations were often located near roads, whereas lower chloride values were far from roads and in wetlands. This trend is more evident in a cross-section schematic (Fig. 23) and bar chart (Fig. 24).

Table 5: Ion Chromatography results from lateral sampling - March 2012 (mg/L)

Sampling Location	Collection Date	Li	Na	K	Mg	Ca	F	Cl	NO ₂ ⁻	SO ₄ ⁻²	Br	NO ₃ ⁻
1 W	3/6/2012	0.00	114.00	3.36	3.33	9.53	0.09	276.00	2.12	19.20	0.18	11.60
1 C	3/6/2012	0.00	75.00	2.02	3.32	7.33	0.10	200.00	1.60	1.48	0.40	4.66
1 E	3/6/2012	0.00	91.00	2.02	7.19	12.10	0.05	270.00	1.22	2.75	0.61	1.75
2 W	3/6/2012	0.00	116.00	1.64	2.32	7.70	0.09	272.00	0.73	47.80	0.24	0.08
2 C	3/6/2012	0.00	58.40	4.78	6.80	19.50	0.05	132.00	2.47	87.60	0.21	12.70
2 E	3/6/2012	0.00	206.00	2.48	6.01	18.00	0.04	519.00	0.95	102.00	0.32	0.00
3 W	3/6/2012	0.00	63.30	1.06	4.67	12.60	0.04	186.00	1.51	14.10	0.32	0.02
3 C	3/6/2012	0.00	72.30	2.87	4.74	12.80	0.04	211.00	1.01	71.50	0.35	0.48
3 E	3/6/2012	0.00	73.60	2.94	3.86	10.50	0.10	208.00	1.43	9.87	0.21	2.52
4 C	3/6/2012	0.00	96.90	3.07	10.20	20.40	0.08	299.00	1.41	31.90	0.08	3.20
5 W	3/6/2012	0.00	55.20	2.11	4.54	12.20	0.05	117.00	3.35	33.80	0.21	16.00
5 C	3/6/2012	0.00	70.30	5.15	7.14	38.50	0.04	207.00	4.52	33.90	0.50	37.80
5 E	3/6/2012	0.00	47.40	1.68	2.73	6.43	0.04	130.00	0.90	7.71	0.14	0.02
6 W	3/9/2012	0.00	78.10	3.08	3.70	10.30	0.05	204.00	1.92	18.50	0.27	2.96
6 CW	3/9/2012	0.00	73.00	3.93	4.76	11.80	0.06	206.00	2.03	12.60	0.30	0.04
6 CE	3/9/2012	0.00	91.60	3.07	5.84	16.60	0.07	246.00	4.25	4.35	0.60	2.98
6 E	3/9/2012	0.00	92.70	2.91	4.58	11.90	0.05	251.00	2.51	4.73	0.40	0.42
7 W	3/6/2012	0.00	6.60	0.72	1.96	7.60	0.20	12.40	2.66	12.50	0.21	0.02
7 C	3/6/2012	0.00	37.20	2.42	3.12	11.10	0.07	82.10	2.94	19.50	0.28	11.90
7 E	3/7/2012	0.00	70.70	2.44	0.00	11.40	0.04	135.00	0.65	12.40	0.14	0.00

8	W	3/7/2012	0.00	99.00	2.31	5.85	14.30	0.05	270.00	2.04	14.70	0.44	0.71
8	C	3/7/2012	0.00	34.70	1.44	4.36	2.27	0.00	96.10	0.51	14.50	0.34	1.31
8	E	3/7/2012	0.00	89.40	2.41	4.96	12.40	0.05	240.00	2.15	13.00	0.42	0.19
9	W	3/6/2012	0.00	84.50	3.70	5.23	12.50	0.04	221.00	1.77	22.30	0.34	11.80
9	C	3/6/2012	0.00	79.70	2.68	4.93	12.60	0.08	216.00	2.50	1.67	0.42	10.80
9	E	3/6/2012	0.00	49.60	6.55	5.55	24.40	0.08	142.00	0.89	110.00	0.25	0.07
10	W	3/7/2012	0.00	89.30	2.44	4.97	12.40	0.05	240.00	2.12	13.00	0.42	0.19
10	C	3/7/2012	0.00	49.50	5.80	0.00	30.30	0.07	133.00	3.00	20.60	0.37	1.38
10	E	3/7/2012	0.00	37.30	1.58	4.49	1.78	0.00	101.00	0.59	15.20	0.35	1.67
11	W	3/7/2012	0.00	96.70	1.90	2.77	5.66	0.06	239.00	1.17	9.29	0.03	0.01
11	C	3/7/2012	0.00	49.20	1.85	2.44	6.13	0.06	126.00	1.35	9.80	0.10	0.07
11	E	3/7/2012	0.00	2460.00	1370.00	13.20	51.50	0.00	8660.00	34.30	122.00	8.66	0.00
12	W	3/7/2012	0.00	56.70	2.55	0.00	8.08	0.03	94.60	1.10	6.67	0.16	0.00
12	C	3/7/2012	0.00	64.10	4.80	0.00	19.80	0.03	98.80	1.41	65.00	0.26	9.27
13	W	3/7/2012	0.00	44.10	1.02	0.00	11.00	0.06	62.60	0.49	111.00	0.79	0.86
13	C	3/7/2012	0.00	109.00	2.09	0.00	6.90	0.04	179.00	0.64	9.35	0.09	0.00
13	E	3/7/2012	0.00	98.00	2.81	0.00	16.20	0.04	172.00	2.76	2.88	0.35	2.06
14	C	3/7/2012	0.00	105.00	1.97	0.00	7.33	0.03	178.00	0.59	9.24	0.10	0.00
14	E	3/7/2012	0.00	101.00	3.44	0.00	17.00	0.02	189.00	1.62	10.20	0.27	0.00
15	W	3/7/2012	0.00	26.50	1.07	2.95	1.44	33.00	67.80	0.64	9.63	0.22	0.01
15	C	3/7/2012	0.00	54.40	2.11	2.44	6.06	0.06	128.00	1.50	9.65	0.07	0.08
15	E	3/7/2012	0.00	51.80	2.62	3.41	8.69	0.05	136.00	1.80	12.00	0.15	0.01
16	W	3/8/2012	0.00	187.00	2.75	5.28	14.00	0.05	482.00	2.10	12.70	0.38	7.12
16	C	3/8/2012	0.00	20.30	0.88	1.44	3.48	0.07	35.60	0.92	18.20	0.07	0.00
16	E	3/8/2012	0.00	167.00	2.53	0.00	12.50	0.04	255.00	4.04	11.20	0.51	0.36
17	W	3/8/2012	0.00	49.70	1.90	0.00	5.53	0.05	90.20	1.12	2.89	0.12	1.00
17	C	3/8/2012	0.00	43.20	1.96	2.17	5.07	0.05	108.00	1.88	2.96	0.17	1.93
17	E	3/8/2012	0.00	80.60	2.70	3.07	6.78	0.07	196.00	1.91	13.50	0.18	0.03
18	W	3/8/2012	0.00	115.00	2.52	3.22	9.08	0.06	239.00	1.53	16.60	0.21	9.59
18	C	3/8/2012	0.00	6.48	0.65	1.90	7.14	0.15	10.50	2.24	10.80	0.00	0.00
18	E	3/8/2012	0.00	160.00	1.18	1.84	6.85	0.05	300.00	1.61	64.20	0.42	0.00
19	W	3/8/2012	0.00	85.90	2.18	4.80	11.70	0.03	168.00	1.62	9.17	0.32	0.19
19	C	3/8/2012	0.00	56.80	2.05	3.26	8.24	0.03	109.00	1.43	9.87	0.16	0.00
19	E	3/8/2012	0.00	33.50	1.27	4.03	1.89	0.00	66.60	0.55	10.20	0.26	0.93
20	W	3/8/2012	0.00	66.40	1.81	5.00	14.60	0.02	129.00	0.89	115.00	0.39	0.13
20	C	3/8/2012	0.00	93.00	1.39	2.59	5.13	0.04	169.00	0.99	6.72	0.17	0.00
20	E	3/8/2012	0.00	47.00	1.45	2.27	5.46	0.04	88.90	1.16	6.96	0.21	0.10

Table 6: Ion Chromatography results from lateral sampling - July 2012 (mg/L)

Sampling Location	Collection Date	Li	Na	K	Mg	Ca	F	Cl	NO ₂ ⁻	SO ₄ ⁻²	Br	NO ₃ ⁻
1	7/2/2012	0.00	75.60	3.28	12.90	30.20	0.06	340.00	3.21	9.76	2.13	8.37
2	7/3/2012	0.00	86.40	3.33	0.00	15.00	0.06	165.00	2.19	7.41	0.36	1.88
3	7/2/2012	0.00	69.20	3.37	4.70	16.60	0.04	186.00	2.34	0.00	0.23	0.09
4	7/2/2012	0.00	70.00	3.27	3.28	8.36	0.11	185.00	2.99	6.11	0.19	2.75
5	7/2/2012	0.00	165.00	4.32	5.02	19.90	0.08	436.00	4.89	21.40	0.75	4.42
6	7/2/2012	0.00	86.80	3.40	4.40	13.40	0.09	239.00	4.79	8.81	0.67	9.03
7	7/2/2012	0.00	79.90	3.89	4.58	14.10	0.09	218.00	3.46	17.90	0.55	2.08
8	7/2/2012	0.00	71.20	3.25	3.53	11.10	0.07	180.00	4.84	3.25	0.29	1.98
9	7/2/2012	0.00	75.60	4.07	4.89	15.10	0.11	206.00	4.17	10.20	0.39	1.12
10	7/2/2012	0.00	74.10	3.74	3.65	11.20	0.07	189.00	4.41	9.70	0.34	4.57
11	7/2/2012	0.00	81.30	3.60	5.75	15.40	0.07	215.00	0.00	27.40	0.78	8.71
12	7/2/2012	0.00	82.80	4.12	4.75	16.70	0.10	208.00	0.00	10.20	0.90	7.97
13	7/2/2012	0.00	71.20	3.25	3.53	11.10	0.07	180.00	4.84	3.25	0.29	1.98

Table 7: Ion Chromatography results from vertical sampling - July 2012 (mg/l)

Well Name	Na	K	Mg	Ca	F	Cl	NO ₂	SO ₄	Br	NO ₃
Piezometer S	172.00	3.26	8.01	23.60	0.05	404.00	0.00	22.20	0.68	9.83
Piezometer M	167.00	3.63	8.76	25.70	0.04	392.00	0.00	22.30	0.77	11.00
Piezometer D	105.00	6.81	7.52	24.20	0.06	233.00	0.00	29.80	0.81	15.80
97-5	14.50	1.79	3.03	12.00	0.25	11.40	0.00	9.60	0.37	0.18
98-4	29.00	1.24	4.57	13.90	0.10	81.40	2.95	22.00	0.20	0.21
98-3S	5.02	0.14	0.67	1.04	0.22	10.80	0.65	12.90	0.04	0.11
98-3M	6.07	0.41	1.12	3.48	0.06	12.00	0.80	16.10	0.14	1.46
98-3D	23.20	1.17	4.60	13.40	0.12	64.00	3.01	24.70	0.22	0.17
98-2S	5.02	0.32	0.69	0.91	0.15	13.00	0.49	9.90	0.06	1.24
98-2M	7.21	0.52	1.30	3.26	0.14	14.90	1.08	13.00	0.04	0.29
98-2D	20.30	1.04	4.44	11.90	0.10	60.20	3.87	22.10	0.28	0.29
97-4 (17-14')	5.32	0.51	1.22	1.88	0.17	13.70	1.25	8.65	0.05	0.56
97-4 (27-24')	6.02	0.49	1.47	3.24	0.14	16.00	1.02	9.34	0.05	0.30
97-4 (37-34')	15.60	0.94	4.17	10.90	0.15	44.70	2.60	19.40	0.15	1.04
97-4 (47-44')	17.10	0.97	4.59	12.70	0.09	50.60	2.93	20.60	0.31	0.55
97-4 (57-54')	18.00	1.19	4.28	11.70	0.11	50.40	3.68	21.40	0.27	0.59
97-4 (67-64')	20.10	1.11	4.69	12.60	0.11	56.80	4.38	22.50	0.33	0.80
97-4 (77-74')	19.80	1.10	4.68	12.90	0.12	55.70	4.37	22.40	0.37	2.25

97-4 (87-84')	16.70	1.12	5.36	16.20	0.13	49.60	4.91	22.00	0.53	1.38
98-2S	5.02	0.32	0.69	0.91	0.15	13.00	0.49	9.90	0.06	1.24
98-2M	7.21	0.52	1.30	3.26	0.14	14.90	1.08	13.00	0.04	0.29
98-2D	20.30	1.04	4.44	11.90	0.10	60.20	3.87	22.10	0.28	0.29
98-3S	5.02	0.14	0.67	1.04	0.22	10.80	0.65	12.90	0.04	0.11
98-3M	6.07	0.41	1.12	3.48	0.06	12.00	0.80	16.10	0.14	1.46
98-3D	23.20	1.17	4.60	13.40	0.12	64.00	3.01	24.70	0.22	0.17
98-1S	4.66	0.95	1.52	3.24	0.07	12.50	1.11	9.94	0.04	0.20
98-1M	9.12	0.93	4.53	11.10	0.13	16.20	4.35	10.90	0.42	2.50
98-1D	20.30	1.17	5.17	14.30	0.11	59.90	3.29	22.80	0.14	0.16
98-5	5.15	0.25	0.33	0.99	0.09	10.40	1.19	14.80	0.17	0.33
97-5	14.50	1.79	3.03	12.00	0.25	11.40	0.00	9.60	0.37	0.18
98-4	29.00	1.24	4.57	13.90	0.10	81.40	2.95	22.00	0.20	0.21

Table 8: Ion Chromatography results from lateral transect samples

Geoprobe Location & Depth Interval	F	Cl	SO ₄	NO ₃	Na	K	Mg	Ca
1: 0' - 5'	0.06	127.00	1.61	0.60	71.20	1.82	2.89	9.87
1: 25' - 30'	0.20	45.70	19.20	0.59	24.10	1.87	6.58	14.50
1: 30' - 35'	0.13	43.90	22.80	0.58	20.20	1.77	7.56	16.60
1: 35' - 40'	0.11	34.00	18.60	0.34	16.20	1.90	6.07	13.80
1: 45' - 50'	0.18	32.20	25.20	0.33	17.60	2.49	6.47	16.20
2: 0' - 5'	0.03	156.00	4.79	0.27	76.00	1.99	3.92	11.80
2: 20' - 25'	0.18	42.90	1.48	0.35	19.90	1.23	6.79	17.10
2: 25' - 30'	0.17	74.00	7.50	0.30	39.60	1.90	5.87	14.00
2: 30' - 35'	0.12	67.60	12.80	0.25	36.30	3.36	5.68	12.50
2: 35' - 40'	0.22	43.80	34.20	1.06	18.00	1.99	7.17	16.50
2: 40' - 45'	0.28	51.70	27.30	3.02	31.90	4.67	6.75	15.60
3: 25' - 30'	0.14	116.00	10.80	0.11	49.00	3.20	5.10	12.30
3: 30' - 35'	0.10	117.00	18.70	0.18	45.10	2.51	7.81	18.40
3: 35' - 40'	0.13	92.30	30.40	0.24	39.40	5.09	8.45	17.90
3: 40' - 45'	0.15	76.90	39.40	0.35	32.30	2.91	9.74	19.80
4: 20' - 25'	0.05	117.00	21.60	0.25	48.90	2.53	6.88	15.80
4: 30' - 35'	0.05	126.00	23.20	0.10	54.70	4.47	6.76	15.00
4: 35' - 40'	0.12	100.00	27.30	0.13	45.00	2.74	7.49	17.40
4: 40' - 45'	0.07	44.40	21.30	4.65	21.30	1.94	5.34	12.50
4: 45' - 50'	0.22	62.00	42.60	3.26	30.00	3.24	6.52	17.20
4: 50' - 55'	0.49	61.80	35.70	0.32	34.70	9.93	7.44	17.10

5: 0' - 5'	0.10	122.00	6.66	1.81	51.30	0.86	5.77	13.90
5: 5' - 10'	0.37	126.00	3.90	0.21	66.30	6.47	5.94	13.30
5: 10' - 15'	0.09	119.00	16.40	1.43	61.20	4.37	2.39	5.34
5: 20' - 25'	0.12	115.00	20.60	7.90	63.90	5.52	1.99	4.36
5: 30' - 35'	0.28	149.00	15.30	2.41	72.10	5.08	5.61	14.60
5: 35' - 40'	0.42	85.00	20.60	4.27	45.70	5.30	7.08	16.00
5: 40' - 45'	0.37	48.20	20.10	4.27	27.60	5.17	6.36	15.30
5: 45' - 50'	0.26	44.70	19.10	4.76	24.30	3.88	5.41	14.70
6: 10' - 15'	0.04	151.00	14.70	0.32	72.10	3.72	3.36	8.08
6: 15' - 20'	0.21	147.00	12.80	0.77	76.90	6.76	3.35	7.77
6: 20' - 25'	0.30	144.00	15.00	0.32	75.20	4.99	3.22	8.87
6: 25' - 30'	0.52	156.00	17.40	0.51	88.00	8.19	5.36	13.00
7: 10' - 15'	0.03	142.00	15.20	1.50	69.90	3.66	3.12	0.35
7: 15' - 20'	0.04	141.00	11.00	0.47	67.70	2.18	3.35	0.27
7: 20' - 25'	0.11	69.30	15.10	1.91	40.00	2.37	1.64	4.29
7: 25' - 30'	0.11	145.00	14.00	0.64	76.40	3.75	3.14	0.32
7: 35' - 40'	0.45	171.00	14.50	0.11	92.90	9.91	4.58	12.10
7: 40' - 45'	0.21	164.00	13.30	0.12	83.30	6.42	4.43	13.60
7: 45' - 50'	0.24	154.00	14.10	0.00	81.40	6.66	4.40	0.47
7: 50' - 55'	0.15	139.00	12.80	0.07	69.80	3.66	4.02	10.80
7: 55' - 60'	0.46	141.00	14.80	0.06	71.90	4.94	6.09	14.70
7: 57' - 62'	0.51	126.00	18.00	0.08	65.90	5.41	6.38	14.80

Chloride Concentrations of Near-Surface Water, March 2012

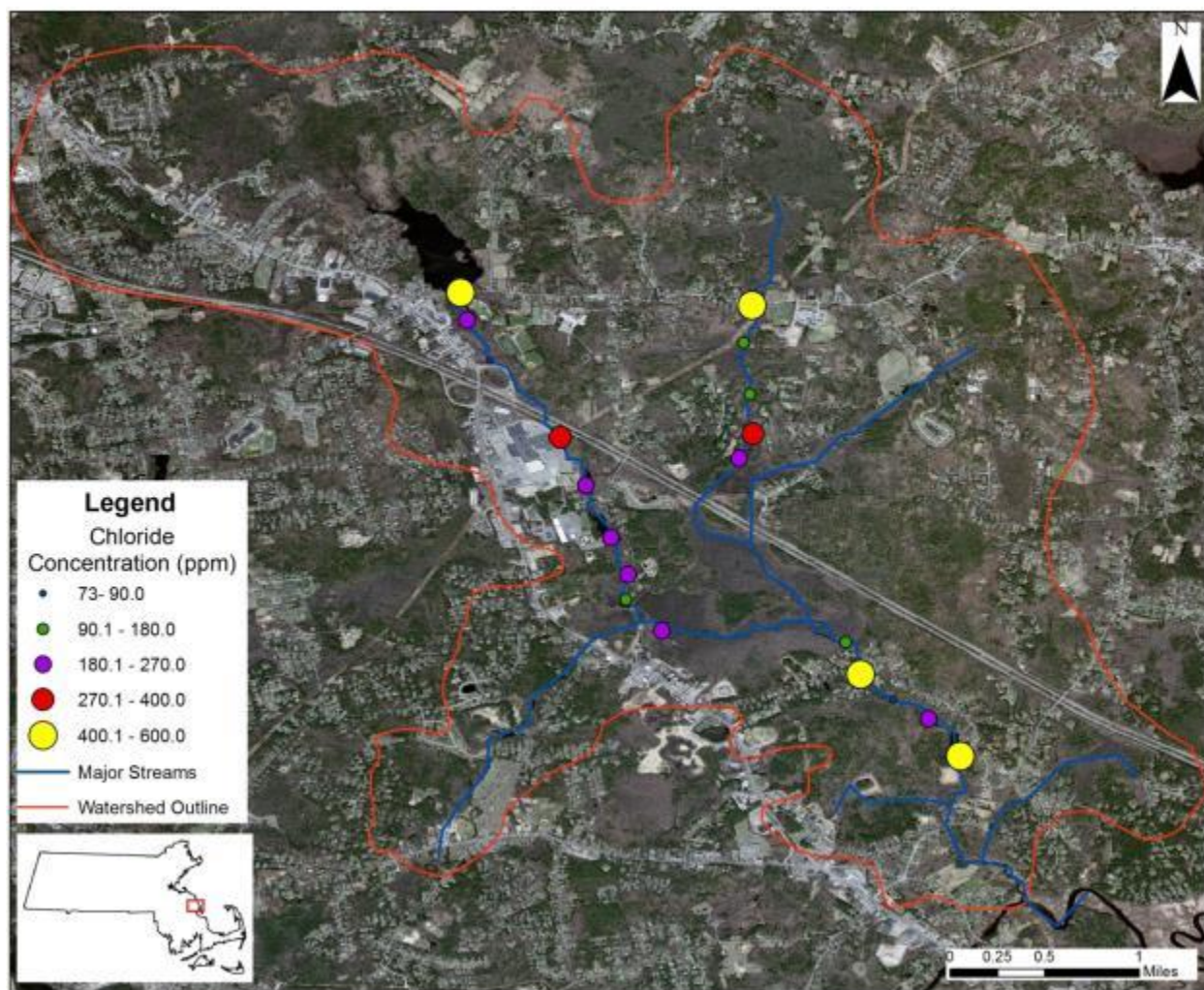


Figure 21: Graduated symbols and colors corresponding to chloride concentrations from near-surface ground water samples (mg/l) taken in March 2012.

Chloride Concentrations of Near-Surface Water, July 2012

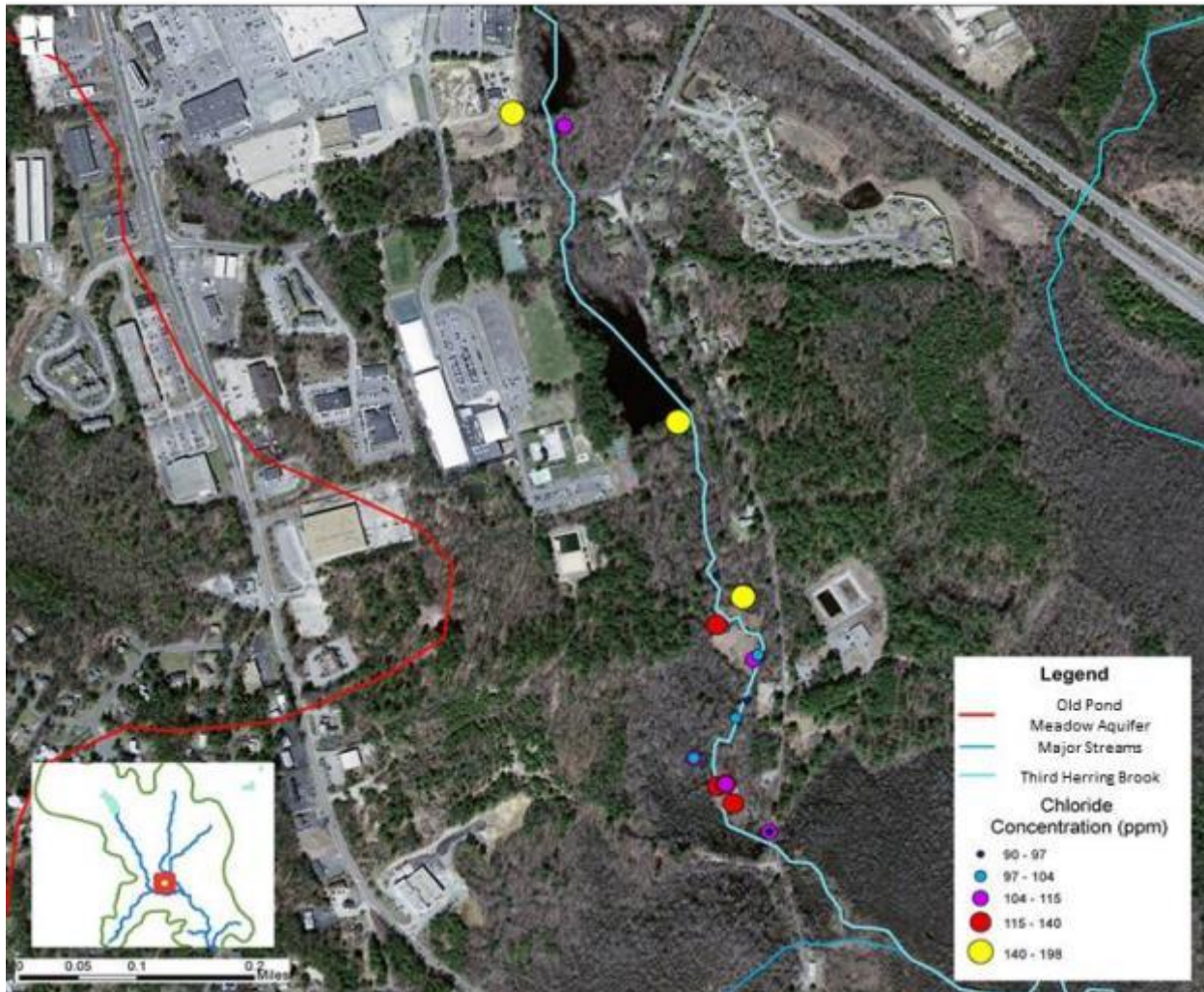


Figure 22: Graduated symbols and colors corresponding to chloride concentrations from near-surface ground water samples (mg/l) taken in July 2012.

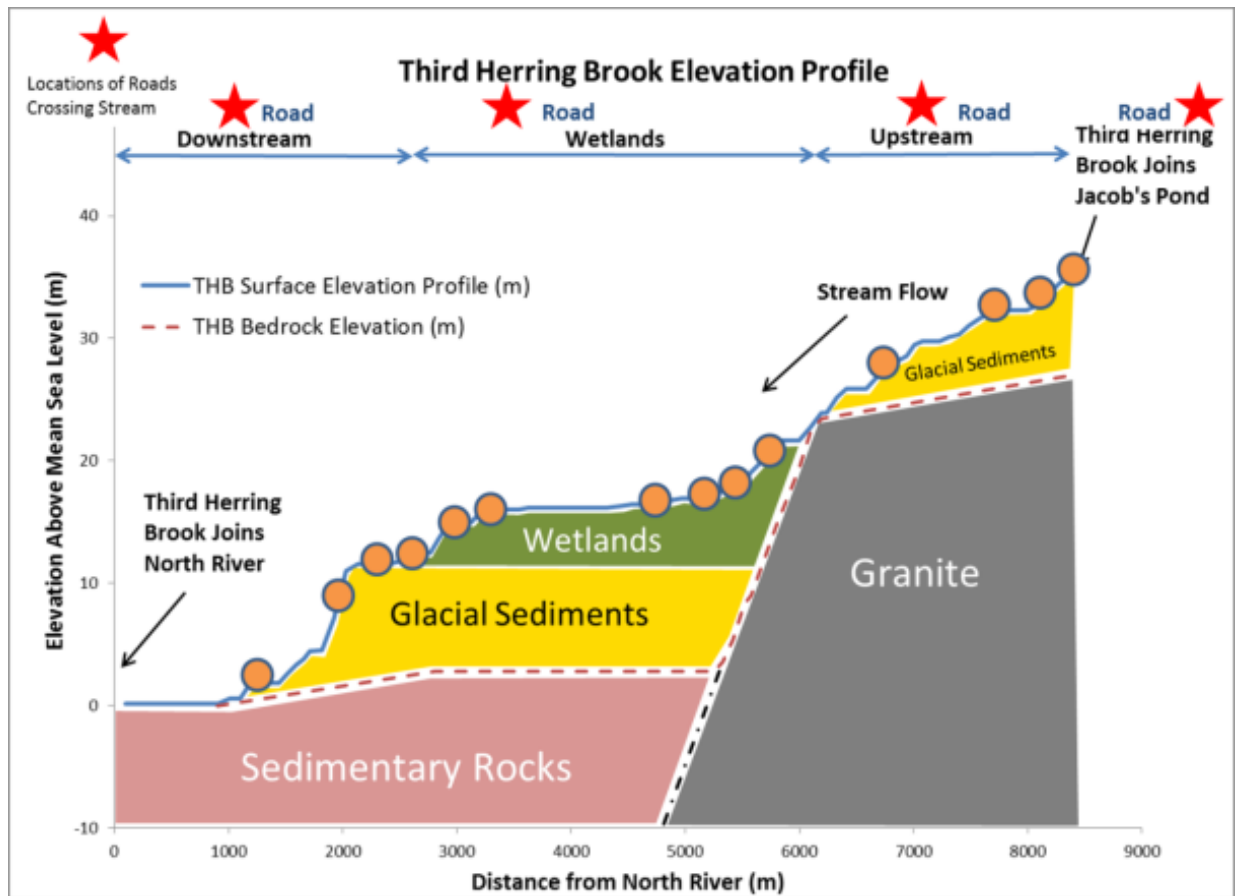


Figure 23: Cross-section of THB surface elevation profile and major geological units. Near-surface ground water sampling locations from March 2012 are shown as orange circles, and the locations of roads crossing the stream are shown as red stars.

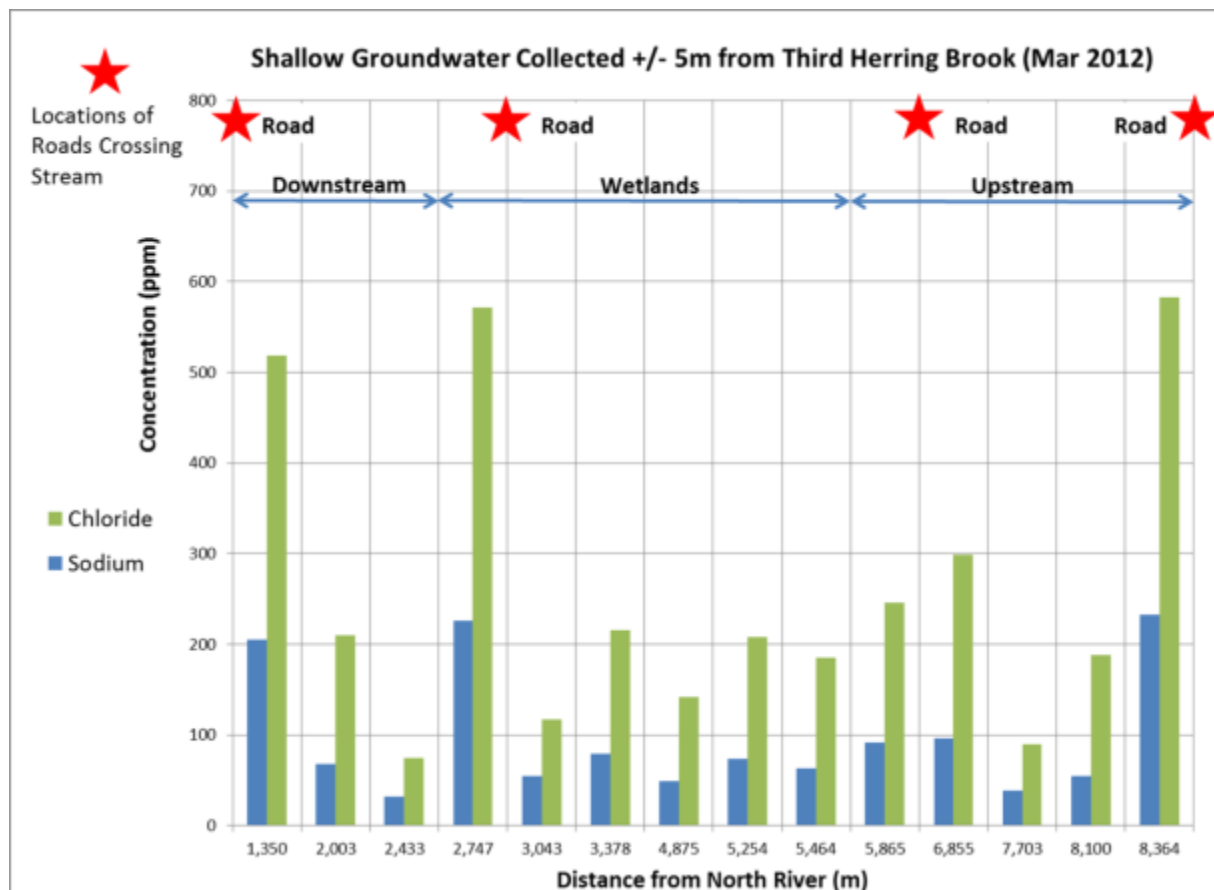


Figure 24: Bar chart of sodium and chloride concentrations of sampling locations along THB.

Well sample concentrations varied significantly based on sample location (Table 7). In the eastern part of the aquifer near the historical wells, sodium and chloride concentrations were relatively low (Fig. 25). When comparing triplet wells, such as 98-3 shallow, medium, and deep and 98-2 shallow, medium, and deep, Na⁺ and Cl⁻ concentrations were lower near the surface but higher near bedrock. In contrast, concentrations near the piezometers were an order of magnitude higher. In the western area of the cross-section, the highest concentrations were near the surface, and the deeper samples had lower concentrations.

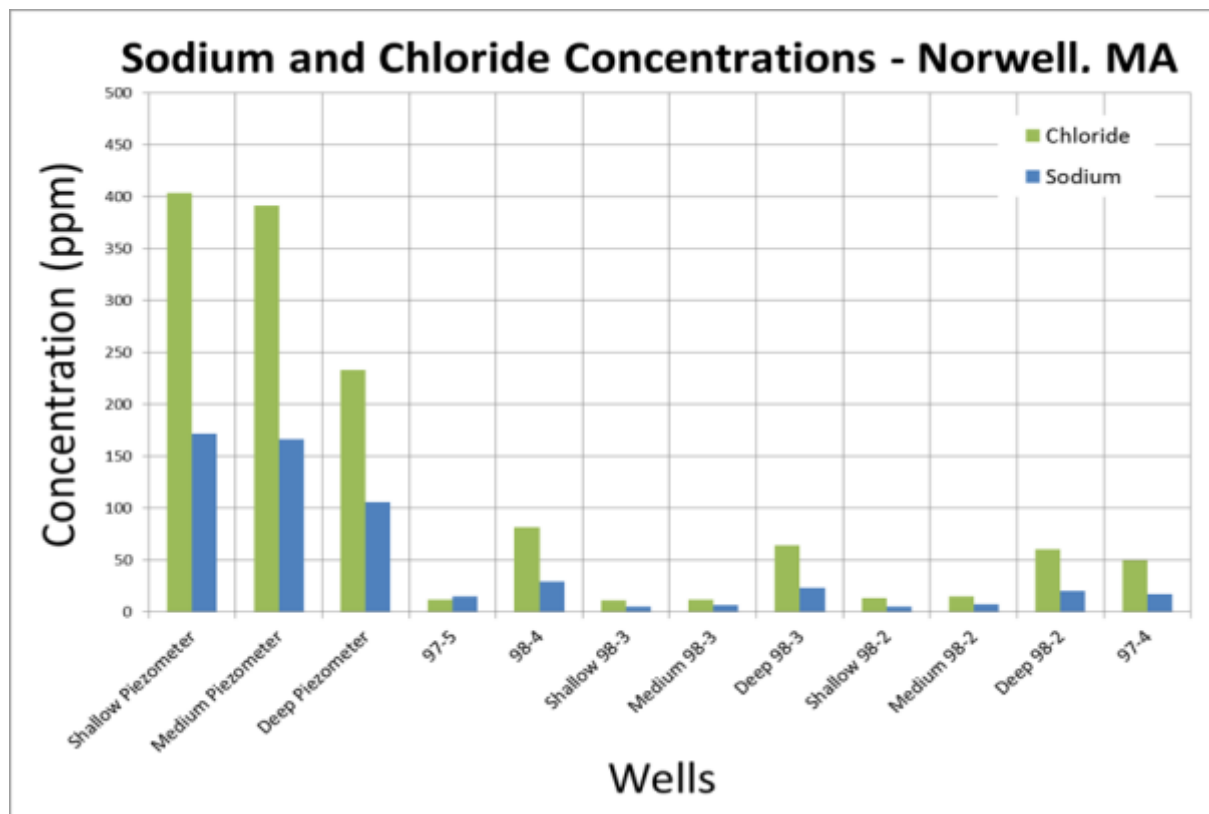


Figure 25: Sodium and chloride concentrations (ppm) in piezometers and wells.

There are several patterns that emerge by displaying transect data along approximate north-south transect A-A' and east-west transect B-B' (Fig. 16). In transect A-A', the highest concentrations were at the top of the soil profile. In some sampling sites, such as sites one and two in Fig. 26, the concentrations decreased with aquifer depth. At other locations, like sites five and six, concentrations were high at the shallow and medium aquifer depths. In contrast to sites one through six, site seven had high concentrations throughout the soil profile.

Several independent datasets suggest that there is a road salt contamination plume within the esker. The highest solute concentrations of the transect samples (Figs. 26 and 27) were observed at site seven that penetrates the esker. Sites six and five that are near the esker showed nearly as high values

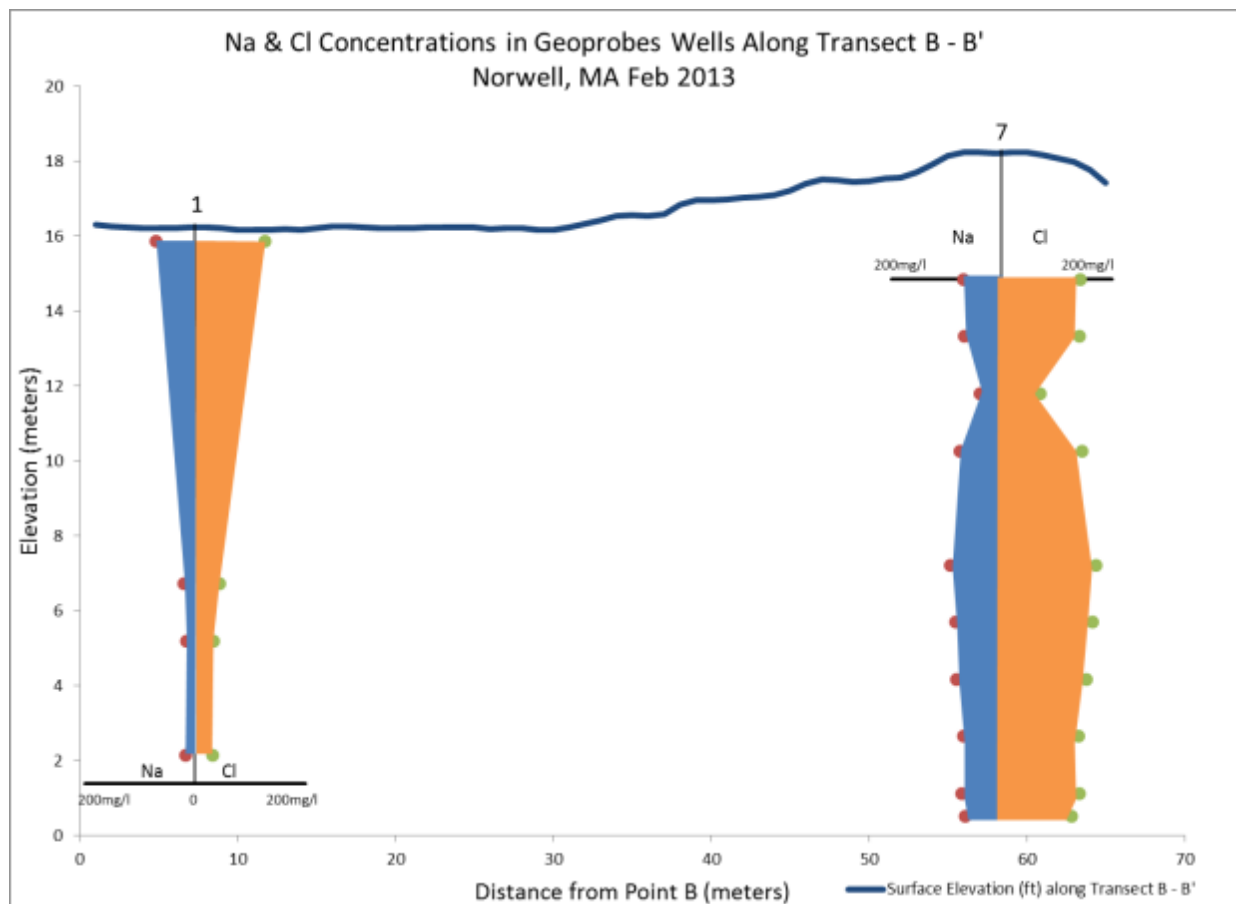


Figure 27: Modified Stiff diagram of sodium and chloride concentrations along transect B-B' in Fig. 16. Chloride concentrations are presented to the right of the well profile. Sodium concentrations are presented to the left. The scale bar relates to a concent

One general way to measure the occurrence of cation exchange is through the molar ratio of sodium to calcium, magnesium, and potassium (Kim and Yun, 2004). Since these four ions represent the major of cations in natural waters, it is likely that they also occupy the majority of cation exchange sites. Surface runoff contaminated with NaCl has a high Na/(Ca + Mg + K) ratio initially. If cation exchange is occurring, then this ratio decreases as sodium is exchanged for calcium, magnesium, and potassium.

Concentrations are converted from concentration by weight to milliequivalents per liter by dividing by the ion's molecular weight and charge. In transect locations one, two, three, four, and six,

the patterns of the $\text{Na}^+ / (\text{Ca}^{+2} + \text{Mg}^{+2} + \text{K}^+)$ ratios resembled sodium concentrations. The highest values were location near the surface while the lowest values were deeper in the aquifer. Locations five and seven, on the other hand, showed more variation in $\text{Na}^+ / (\text{Ca}^{+2} + \text{Mg}^{+2} + \text{K}^+)$ ratios (Figs. 28 and 29). The highest values for both sodium concentration and cation ratios were found in the middle part of the aquifer indicating at location 5. These data indicate that contaminated groundwater was transported through this area and that there was little cation exchange. The $\text{Na}^+ / (\text{Ca}^{+2} + \text{Mg}^{+2} + \text{K}^+)$ ratios for historical well samples had higher values than those deeper within the aquifer (Fig. 30).

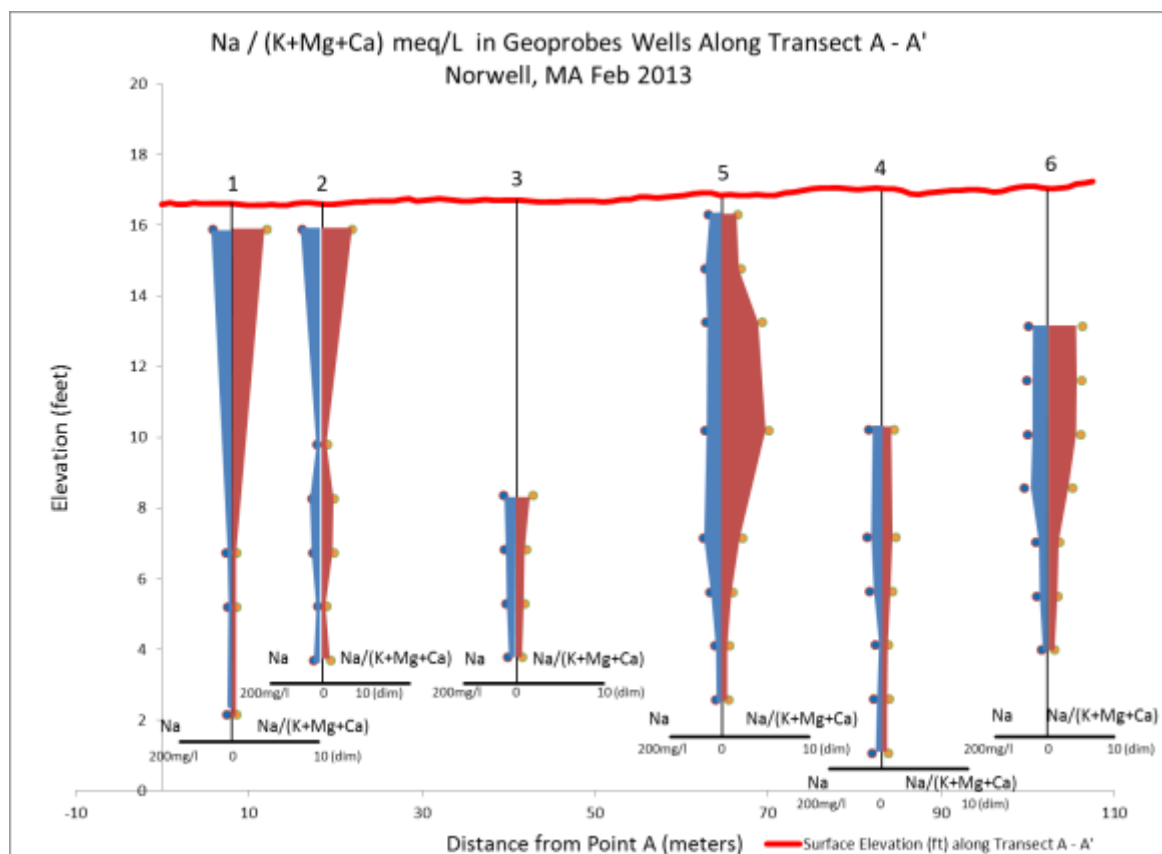


Figure 28: Dimensionless ratios of sodium (meq/l) to the summation of calcium, magnesium, and potassium (meq/l) are presented to the right of the well profile along transect A-A' in Fig. 16. Sodium concentrations (mg/l) are shown to the left of the well profile.

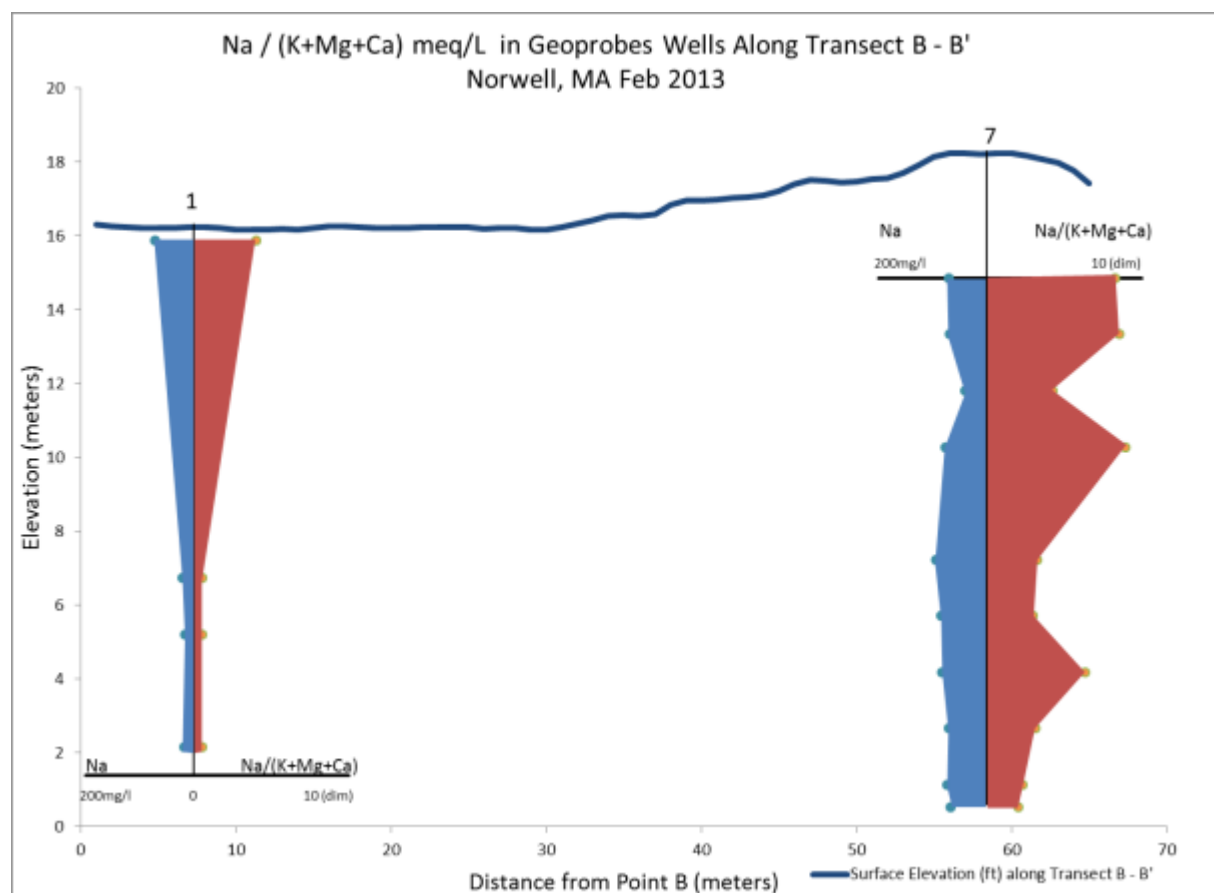


Figure 29: Dimensionless ratios of sodium (meq/l) to the summation of calcium, magnesium, and potassium (meq/l) are presented to the right of the well profile along transect B-B' in Fig. 16. Sodium concentrations (mg/l) are shown to the left of the well profile.

Table 9: Lateral sampling ICP results (mg/l).

Well	Ag	Al	As	Ba	Ca	Cd	Co	Cr	Cu	Fe	K	Mg
98-5	0.0025	0.755	0.0342	0.106	0.859	BDL	BDL	BDL	0.0186	BDL	0.375	0.35
98-3S	0.00263	0.553	0.0335	0.0464	0.914	BDL	BDL	BDL	0.0182	BDL	0.123	0.683
98-3M	0.00305	0.0478	0.0319	BDL	2.75	BDL	BDL	BDL	0.0155	BDL	0.437	1.08
98-3D	0.00259	0.0601	0.0343	0.0177	11.5	BDL	BDL	BDL	0.0184	17.9	1.22	4.67
98-2S	0.00259	0.595	0.034	0.0229	0.784	BDL	BDL	BDL	0.0181	BDL	0.32	0.692
98-2M	0.00279	0.105	0.0391	0.0159	9.67	BDL	BDL	0.00284	0.0226	12.3	1.24	4.42
98-2D	0.00267	0.0689	0.0353	0.0133	10.5	BDL	BDL	BDL	0.0186	13.8	1.04	4.75
98-1S	0.00264	0.0389	0.0343	0.00447	2.4	BDL	BDL	BDL	0.0182	BDL	1.08	1.34
98-1M	0.00256	0.138	0.0427	BDL	9.01	BDL	BDL	BDL	0.0193	0.0247	0.967	4.49
98-1D	0.00268	0.0559	0.0353	0.0172	12.5	BDL	BDL	BDL	0.0181	13	1.16	5.34
97-4 77-74'	0.00295	0.0554	0.0342	0.00103	10.7	BDL	BDL	BDL	0.0155	6.97	1.08	4.42
97-4 47-44'	0.00288	0.0579	0.0346	0.00618	11	BDL	BDL	BDL	0.0182	5.32	1.07	5.02
97-4 17-14'	0.00271	0.0352	0.0349	0.0226	1.93	BDL	BDL	BDL	0.0182	BDL	0.531	1.17
97-1	0.00294	0.0358	0.0375	BDL	8.44	BDL	BDL	BDL	0.0192	BDL	1.62	2.58
NOR-1	0.0025	0.0368	0.036	0.0233	14.2	BDL	BDL	BDL	0.119	BDL	3.07	6.07
Pie S	0.00275	0.0328	0.0365	0.115	20.5	BDL	BDL	BDL	0.0184	BDL	3.11	8.93
Pie M	0.00267	0.0247	0.0339	0.0843	22.7	BDL	BDL	BDL	0.0182	BDL	3.53	9.27
Pie D	0.00299	0.0237	0.0352	0.016	19.8	BDL	BDL	BDL	0.0157	BDL	6.45	7.43

Well	Mn	Mo	Na	Ni	P	Pb	Sb	Sn	Sr	Ti	V	Zn
98-5	0.000886	BDL	6.21	0.665	0.0439	BDL	BDL	BDL	0.00788	0.0578	0.0402	BDL
98-3S	0.00477	BDL	5.1	0.664	0.0326	BDL	BDL	BDL	0.0165	0.0574	0.0429	BDL

98-3M	BDL	BDL	5.74	0.635	BDL	BDL	BDL	BDL	0.0164	0.0577	0.0314	BDL
98-3D	0.641	BDL	23.2	0.664	0.0958	BDL	BDL	BDL	0.0695	0.0605	0.0471	BDL
98-2S	0.0165	BDL	5.24	0.665	0.0474	BDL	BDL	BDL	0.0104	0.0575	0.0428	BDL
98-2M	0.423	BDL	23.7	0.663	0.0671	BDL	BDL	BDL	0.059	0.0621	0.0509	BDL
98-2D	0.402	BDL	21.3	0.664	0.0806	BDL	BDL	BDL	0.0647	0.0611	0.0563	BDL
98-1S	BDL	BDL	4.49	0.664	0.0441	BDL	BDL	BDL	0.0241	0.0574	0.0428	BDL
98-1M	0.628	BDL	8.7	0.663	0.0491	BDL	BDL	BDL	0.0481	0.0622	0.0468	BDL
98-1D	0.698	BDL	19.9	0.664	0.084	BDL	BDL	BDL	0.0731	0.0601	0.0513	BDL
97-4 77-74'	BDL	BDL	18.6	0.633	BDL	BDL	BDL	BDL	0.0608	0.0593	0.0378	BDL
97-4 47-44'	BDL	BDL	18.9	0.663	0.0624	BDL	BDL	BDL	0.0643	0.0594	0.0488	BDL
97-4 17-14'	BDL	BDL	5.32	0.664	0.0509	BDL	BDL	BDL	0.0313	0.0574	0.0425	BDL
97-1	0.038	BDL	13.9	0.633	BDL	BDL	BDL	BDL	0.0416	0.0574	0.0286	BDL
NOR-1	0.312	BDL	99.7	0.666	0.00719	BDL	BDL	BDL	0.126	0.0575	0.0382	BDL
Pie S	0.0381	BDL	172	0.664	0.0449	BDL	BDL	BDL	0.2	0.0575	0.04	BDL
Pie M	0.0538	BDL	173	0.663	0.0342	BDL	BDL	BDL	0.212	0.0574	0.0391	BDL
Pie D	0.0262	BDL	106	0.637	BDL	BDL	BDL	BDL	0.163	0.0574	0.0306	BDL

Table 10: ICP results for transect samples

Location & Depth		As	Ba	Ca	Cd	Co	Cu	Fe	Mn	Na	Ni	Pb	Sr	Zn
1	0-5	0.0004	0.0458	8.6	0.0005	0.0007	0.0125	0.5160	1.2500	74.3	0.0059	BDL	0.0765	0.2000
1	25-30	BDL	0.0382	12.8	0.0004	0.0132	0.0024	0.0391	0.5990	24.6	0.0218	0.0011	0.0722	0.6760
1	30-35	BDL	0.0208	15.2	0.0006	0.0066	0.0016	0.0112	0.2440	21.7	0.0097	0.0007	0.0906	0.3730
1	35-40	BDL	0.0099	11.9	0.0005	0.0012	0.0006	BDL	0.6880	17.0	0.0104	BDL	0.0736	0.1720
1	40-45	BDL	0.0108	14.0	0.0004	0.0030	0.0006	0.0011	2.2500	17.2	0.0094	BDL	0.0778	0.2640
2	0-5	BDL	0.0854	10.5	0.0007	0.0006	0.0011	0.0113	0.6050	77.0	0.0106	BDL	0.0782	0.0707
2	20-25	0.0007	0.0353	15.1	0.0004	0.0010	0.0014	0.0425	1.2300	14.7	0.0032	BDL	0.0816	0.0064
2	25-30	BDL	0.0522	12.0	0.0005	0.0059	0.0020	0.0018	1.2500	36.5	0.0148	BDL	0.0705	0.1900
2	30-35	0.0004	0.0455	10.8	0.0007	0.0057	0.0012	0.0345	1.2300	34.2	0.0126	BDL	0.0702	0.2720
2	35-40	BDL	0.0164	14.2	0.0006	0.0062	0.0006	0.0442	1.0600	18.5	0.0038	BDL	0.0840	0.0109
2	40-45	BDL	0.0228	14.0	0.0004	0.0101	0.0012	0.1010	2.3000	32.8	0.0135	BDL	0.0825	0.2460
3	25-30	BDL	0.0580	10.7	0.0003	0.0052	BDL	0.0706	1.5000	47.1	0.0102	0.0020	0.0725	0.1550
3	30-35	BDL	0.0817	16.6	0.0016	0.0106	0.0031	0.0679	1.6900	44.4	0.0238	BDL	0.1120	0.4920
3	35-40	BDL	0.0479	15.9	0.0004	0.0054	0.0000	0.0284	1.1400	39.2	0.0216	BDL	0.1090	0.2550
3	40-45	BDL	0.0292	17.4	0.0006	0.0020	0.0006	0.0168	0.5670	33.7	0.0049	0.0006	0.1060	0.0368
4	20-25	BDL	0.0476	13.6	0.0004	0.0059	0.0001	0.0142	1.0900	47.8	0.0100	BDL	0.0907	0.3470
4	30-35	BDL	0.0365	13.0	0.0004	0.0036	0.0001	0.0984	2.4300	54.8	0.0080	BDL	0.0967	0.0196
4	35-40	BDL	0.0403	15.3	0.0006	0.0015	0.0008	0.0264	1.4600	46.4	0.0049	BDL	0.1090	0.0373
4	40-45	BDL	0.0169	10.8	0.0008	0.0030	0.0007	0.0035	2.9600	21.9	0.0098	BDL	0.0784	0.0682
4	45-50	BDL	0.0164	15.3	0.0006	0.0023	0.0008	0.0032	8.9800	31.1	0.0067	0.0001	0.1020	0.0400
4	50-55	0.0004	0.0258	14.8	0.0004	0.0016	0.0013	0.0119	4.9000	35.2	0.0033	BDL	0.0892	0.0092
5	0-5	BDL	0.0322	12.0	0.0004	0.0074	0.0009	0.1440	0.5130	52.3	0.0052	0.0001	0.0797	0.0521
5	5-10	0.0069	0.0232	11.2	0.0004	0.0011	0.0104	8.4700	0.4970	70.5	0.0047	0.0009	0.0814	0.0126
5	10-15	BDL	0.0196	4.3	0.0005	0.0022	0.0054	0.1860	0.2520	63.0	0.0092	BDL	0.0348	0.0190
5	20-25	BDL	0.0136	3.4	0.0009	0.0031	0.0118	0.5760	0.6610	62.3	0.0086	0.0004	0.0271	0.0044
5	25-30	BDL	0.0632	8.7	0.0006	0.0109	0.0148	0.1310	7.3100	71.9	0.0144	0.0010	0.0605	0.0539
5	30-35	BDL	0.0175	12.6	0.0004	0.0022	0.0021	0.0052	10.0	73.7	0.0077	BDL	0.0893	0.0047
5	35-40	0.0011	0.0066	13.8	0.0005	0.0013	0.0010	0.0043	4.4000	45.9	0.0022	BDL	0.0823	0.0012
5	40-45	0.0006	0.0073	13.1	0.0004	0.0020	0.0003	BDL	3.9800	27.9	0.0020	BDL	0.0844	0.0033
5	45-50	BDL	0.0095	12.5	0.0002	0.0029	0.0000	BDL	3.8200	24.9	0.0021	BDL	0.0789	0.0030
6	10-15	BDL	0.0412	6.8	0.0005	0.0067	0.0046	0.0269	0.4850	73.9	0.0140	BDL	0.0592	0.0572
6	15-20	BDL	0.0261	6.5	0.0002	0.0027	0.0040	0.0791	0.7220	80.1	0.0106	BDL	0.0537	0.0342
6	20-25	BDL	0.0251	7.3	0.0003	0.0045	0.0033	0.0486	1.4100	75.9	0.0066	BDL	0.0587	0.0115
6	30-35	BDL	0.0161	11.3	0.0004	0.0029	0.0061	0.0162	4.8800	41.2	0.0041	0.0004	0.0844	0.0151
6	35-40	BDL	0.0178	11.6	0.0003	0.0021	0.0031	0.0185	4.1300	37.5	0.0033	BDL	0.0865	0.0090

6	40-45	BDL	0.0108	10.4	0.0003	0.0060	0.0009	BDL	1.2500	20.8	0.0077	BDL	0.0787	0.0266
7	10-15	BDL	0.0370	6.3	0.0004	0.0032	0.0030	0.0046	0.5060	70.1	0.0143	0.0004	0.0527	0.0178
7	15-20	BDL	0.0251	6.9	0.0004	0.0051	0.0029	0.0005	0.3530	66.7	0.0161	BDL	0.0562	0.0567
7	20-25	BDL	0.0120	3.0	0.0003	0.0047	0.0029	0.0622	0.3070	38.6	0.0096	0.0006	0.0264	0.0235
7	25-30	BDL	0.0157	6.0	0.0003	0.0057	0.0009	BDL	0.4320	73.8	0.0263	0.0015	0.0454	0.1460
7	35-40	BDL	0.0227	9.8	0.0003	0.0008	0.0050	0.1520	0.3690	91.5	0.0035	BDL	0.0710	0.0068
7	40-45	BDL	0.0225	11.2	0.0003	0.0015	0.0020	0.0443	1.1000	81.0	0.0039	0.0001	0.0861	0.0092

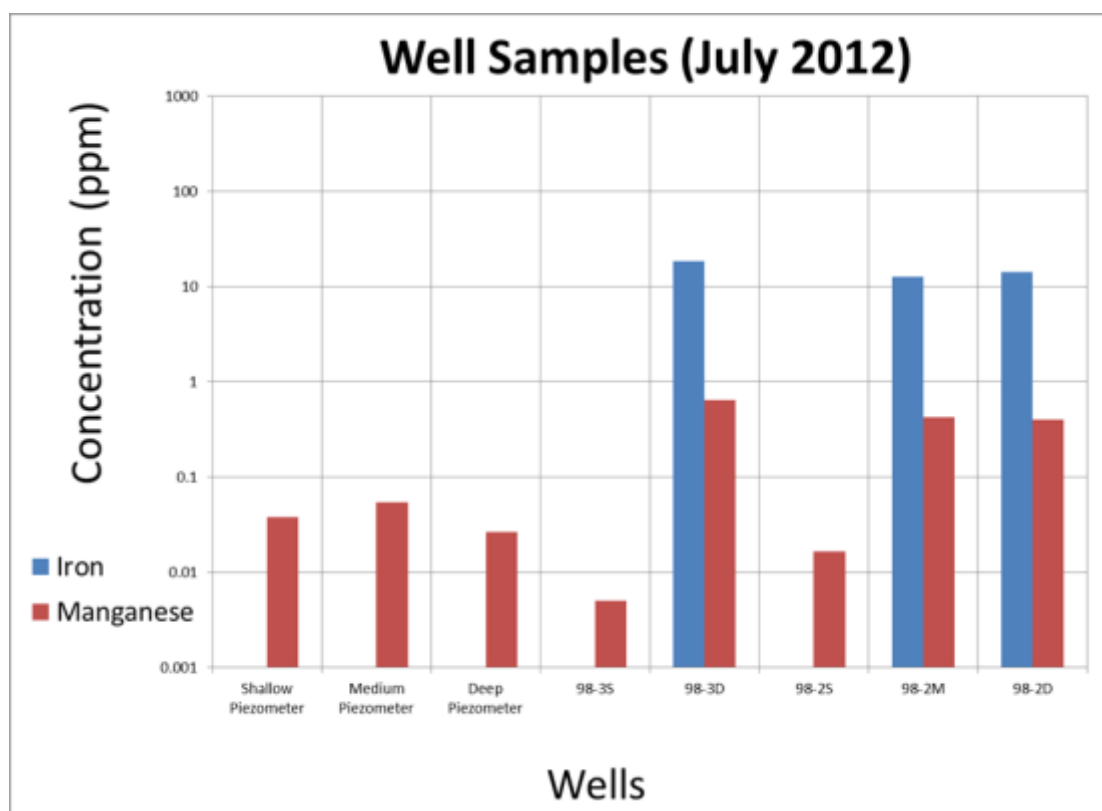


Figure 31: Concentrations of iron and manganese in piezometers and historical wells.

Ground water data collected along transects shown in Fig. 16 that were analyzed with ICP for 13 elements are shown in Table 10. The concentrations of As, Cd, Ni, and Pb were below 0.1 ppm for all samples. There was significant variation for redox-sensitive elements. In general, the largest concentrations of Mn and Fe related to deeper parts of the aquifer (Fig. 31).

5.3 Temporal Trends in Chloride Concentration

The chloride concentrations at shallow and medium aquifer depths had the highest concentrations and showed strong seasonal trends (Fig. 32). During the summer, concentrations at these locations exceeded the EPA's secondary contaminant level of 250 ppm. In the fall and winter, the concentrations decreased below the EPA threshold. This pattern resembled the atmospheric temperature collected at a Norwell weather station from Jan 2011 to Oct 2011 (Fig. 8).

In contrast to shallow and medium depth aquifer data, the chloride concentration in the deep piezometer was steadily increasing. The deep piezometer is located at the same depth interval as the screened interval of NOR-1. If the increasing trend in chloride concentration is extrapolated into the future, it will exceed the EPA secondary contaminant level in 2020 (Fig. 33). Data from this piezometer were unavailable from August 2012 to March 2013 due to a technical problem.

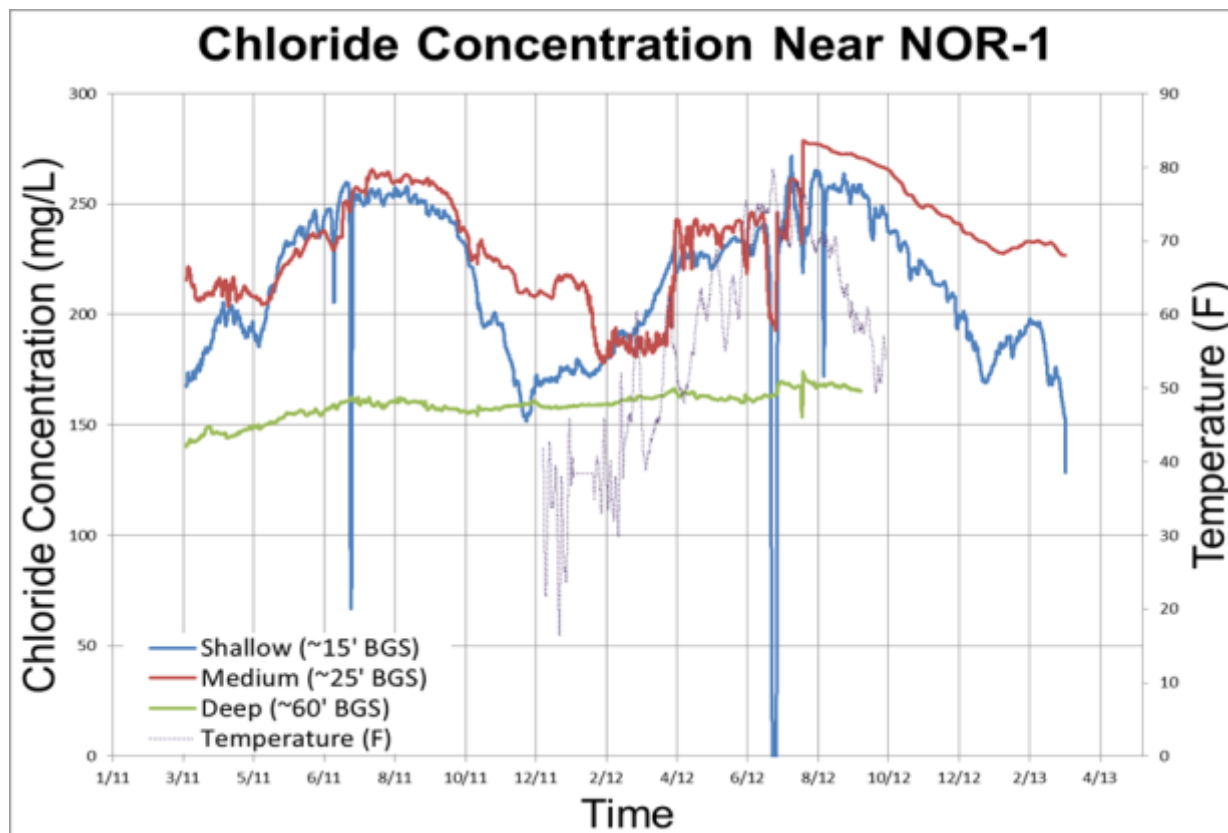


Figure 32: Estimated chloride concentrations in the shallow (blue), medium (red), and deep (green) piezometers from March 2011 to March 2013. Atmospheric temperature (purple) from a Norwell weather station is plotted on a secondary axis.

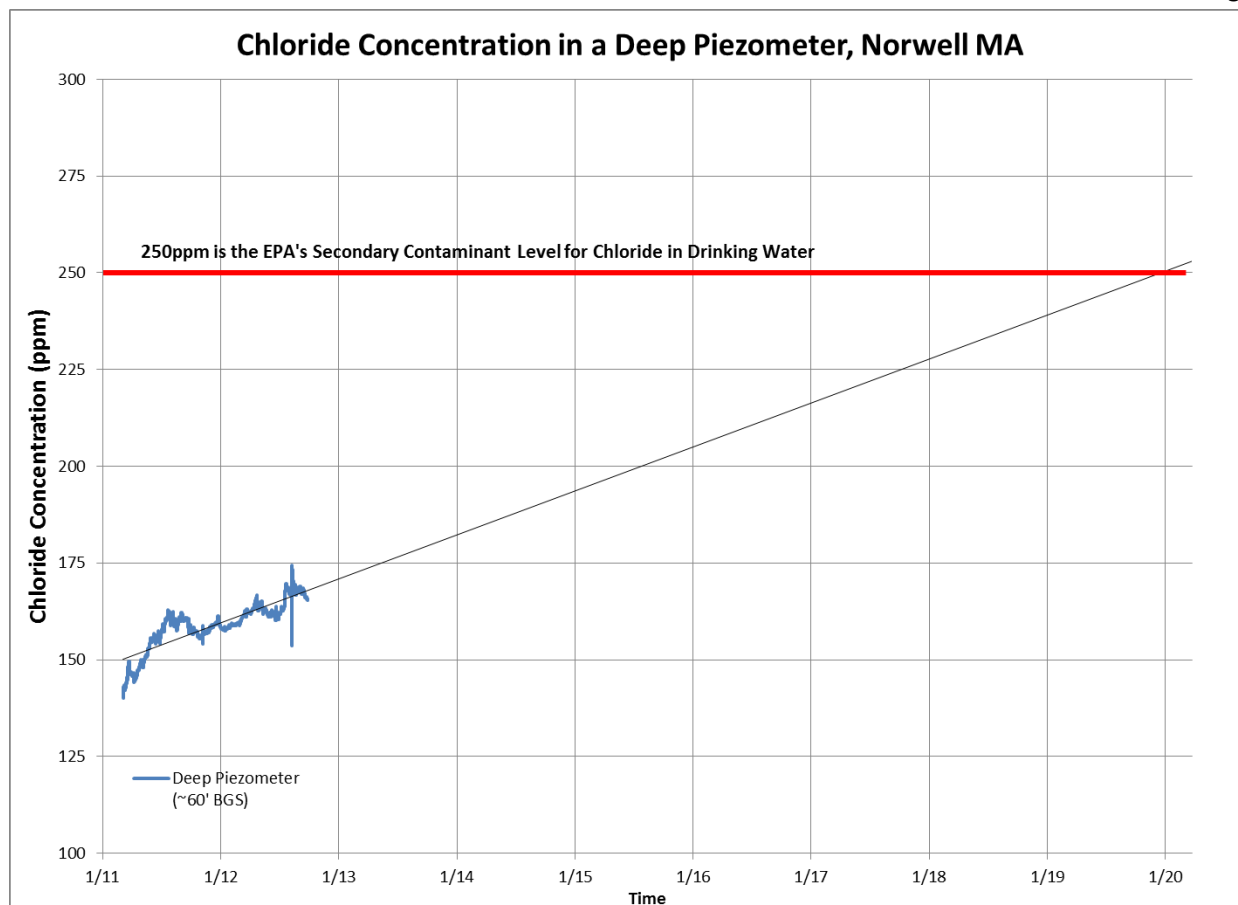


Figure 33: Extrapolation of chloride concentration in the deep piezometer to the EPA's secondary contaminant level for chloride. At the observed rate, chloride values will cross the EPA's allowable secondary contaminant threshold in the year 2020.

5.4 Miscellaneous Data

5.4.a Relationships Among Cations

The plot of sodium (meq/L) and chloride (meq/L) showed one group of samples near the unity line and another group of samples with a chloride to sodium ratio greater than one (Fig. 34), indicating that there are two separate clusters of sodium / chloride ratios. Since pure sodium chloride has a Cl/Na ratio of 1, samples with values near the unity line may only include sodium chloride. The second group

with a Cl/Na ratio less than 1 indicates that other de-icers besides NaCl have been applied or that some of the sodium ions were exchanged for other cations.

The plots showing the summation of potassium, magnesium, calcium, and sodium (meq/L) versus chloride (meq/L) indicated that the summation of total cations correlates well with chloride concentrations (Fig. 35). The slope of the trendline through these data is 1.0315 with an R^2 of 0.887, suggesting a high degree of correlation that indicates the negative charges of chloride are balanced by the positive charges of potassium, sodium, calcium, and magnesium.

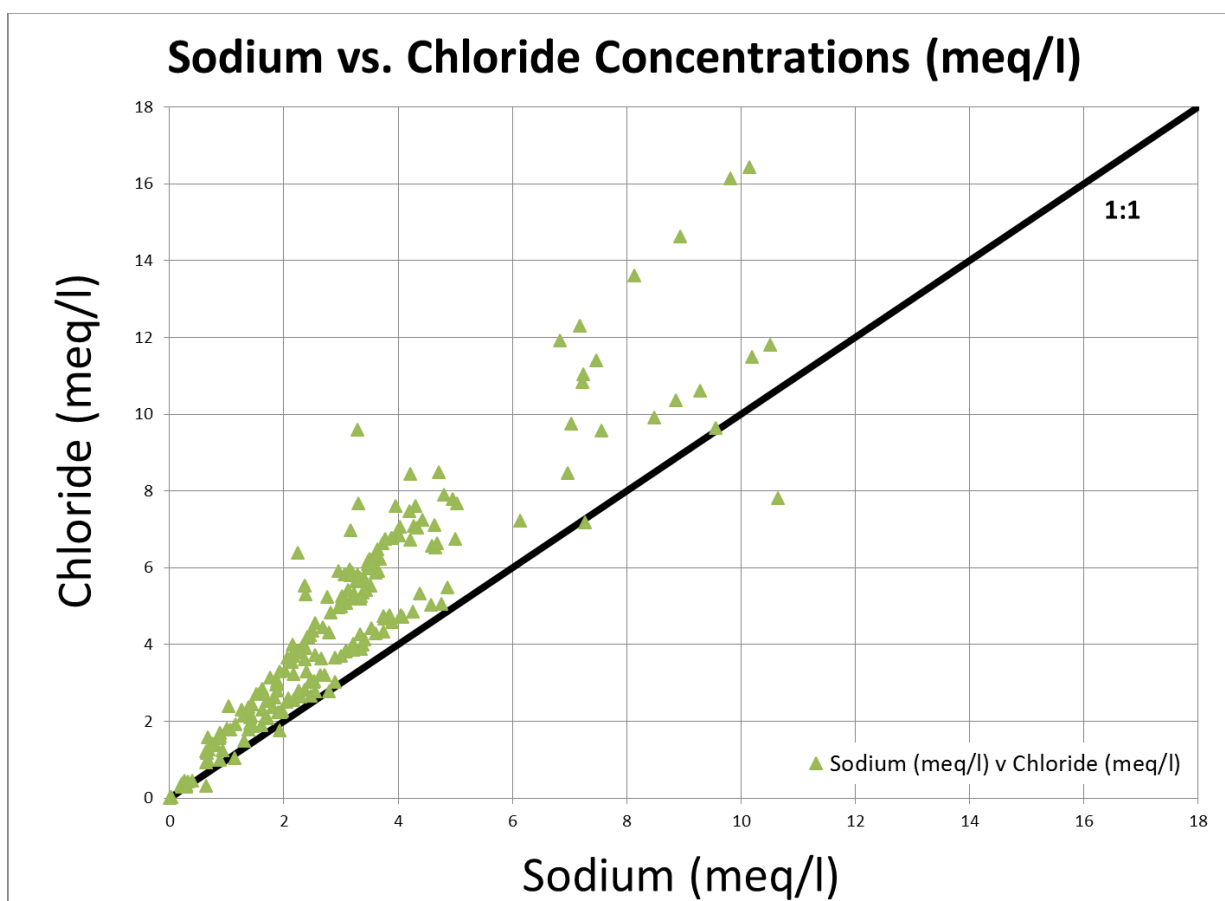


Figure 34: Concentration of sodium (meq/l) vs. chloride (meq/l) for all samples analyzed with IC.

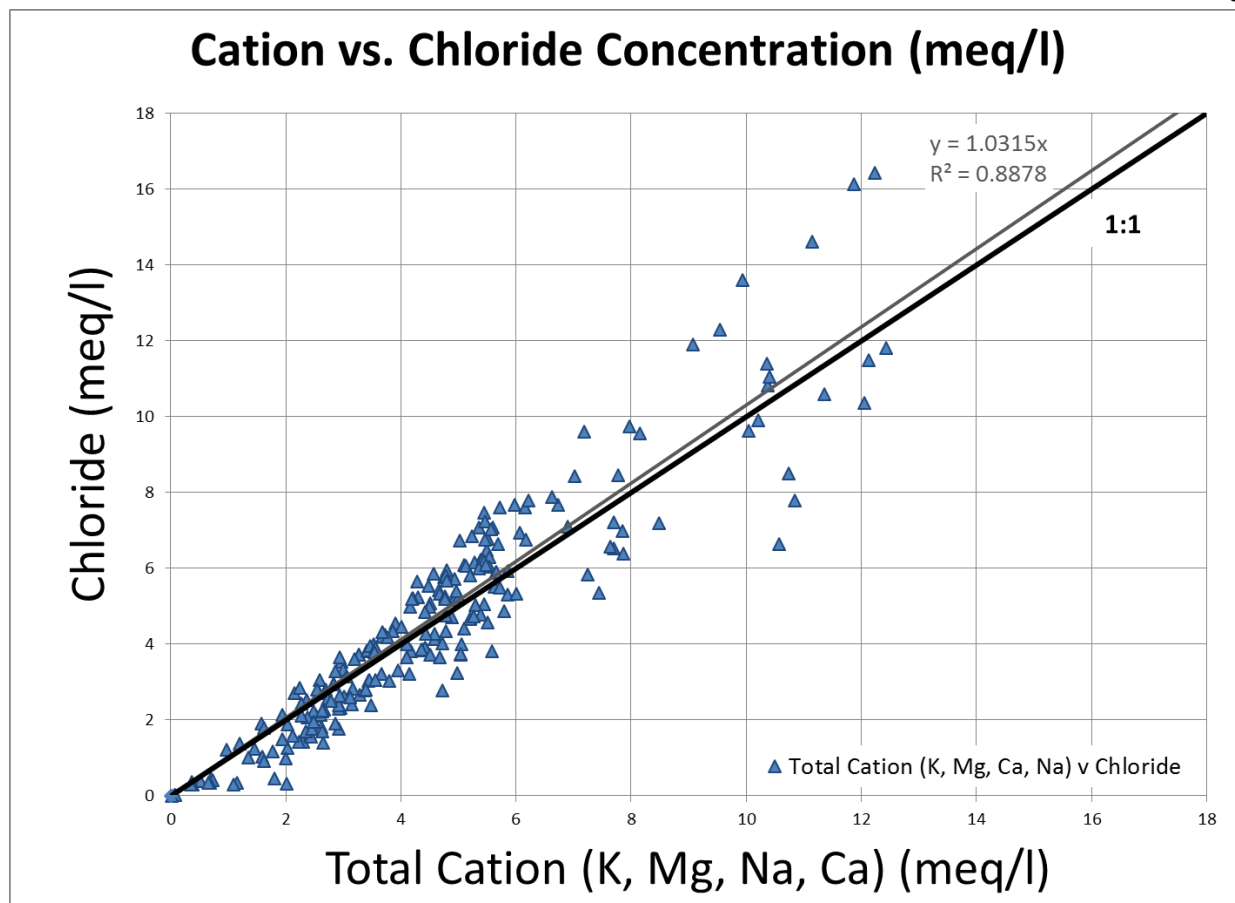


Figure 35: Summation of the concentrations of K^+ , Mg^{+2} , Ca^{+2} , and Na^+ (meq/l) vs. chloride (meq/l) for all samples analyzed with IC.

5.4.b - Grain Size Analysis

In the grain size analysis, the sample from near NOR-1 was more well-sorted and had smaller grains (Fig. 36). Over 90% of the sample by weight was smaller than very coarse sand. In contrast, the NOR-6 sample was more heterogeneous and contained larger grains. For example, approximately 30% of the NOR-6 sample was very fine gravel or fine gravel.

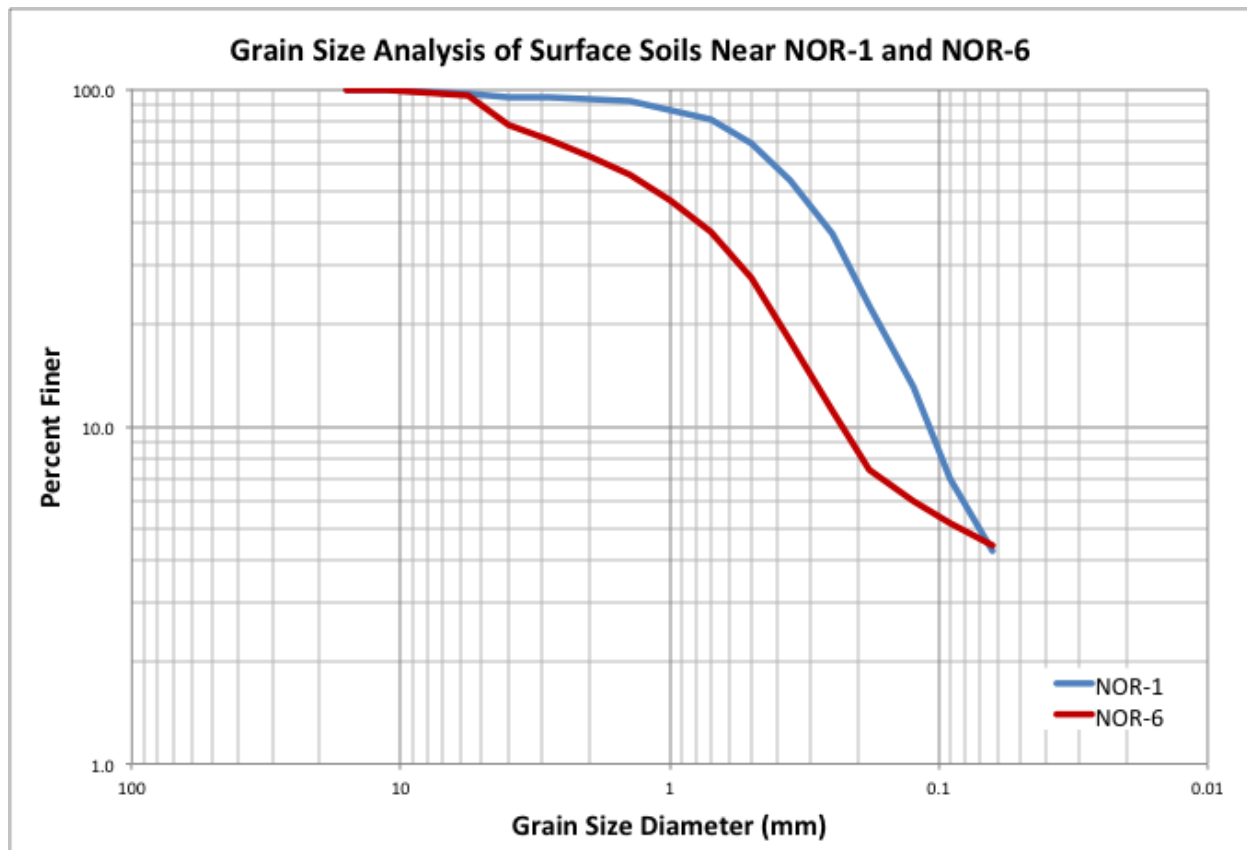


Figure 36: Grain size analysis from soil samples near NOR-1 and NOR-6.

5.5 Overview of Results

- The highest chloride concentrations in near-surface ground water were found in close proximity to roads.
- The highest concentrations of redox sensitive elements such as Fe and Mn were located in the deep aquifer and near wetlands.
- Chloride concentrations at shallow and medium aquifer depths near NOR-1 show seasonal trends. The deep aquifer concentrations at this location were steadily increasing.
- While the sodium to chloride molar ratio showed significant variation, there was a near 1:1 ratio for chloride to major cations.
- There were smaller grains in the O soil horizon near NOR-1 than near NOR-6.
- There was no relationship observed between pH and $\text{Na} / (\text{Ca} + \text{Mg} + \text{K})$.

Section 6. Discussion

6.1 Aquifer Characteristics

The dataset of chloride concentrations organized by the Norwell Water Department over the past twenty years has been augmented with hundreds of water samples and other measurements in this study. Contaminant plumes and transport pathways were interpreted from spatial and temporal trends in solute concentrations. The collected data suggest that sodium and chloride are retained in the aquifer and continue to increase.

The physiographic characteristics of the aquifer have implications for likely solute pathways. The map of aquifer thickness (Fig. 19) showed a bedrock outcrop through the middle of the aquifer. Therefore, ground water flow was limited from the northwest section to the southeast section except through bedrock fractures. However, the THB still transports surface water between these two areas.

In contrast to the relatively thin aquifer thickness in the northern section of the OPM aquifer, the thick aquifer in the southern section relates to lower solute concentrations in ground water (Fig. 19). The high aquifer thickness corresponds to a larger volume of water. Additionally, the Old Pond Meadow wetland was a kettle pond that has an estimated porosity of 70% (Reed, 1999). Consequently, the lower solute concentrations from the historical wells than penetrate this area (Table 6) may result from the dilution of road salt with a large volume of water.

6.2 High Concentrations Near Roads

Data from samples collected in March 2013 generally showed that higher solute concentrations in groundwater were measured near roads. These high values are likely a result of surface runoff that had been contaminated with road salt infiltrating through the vadose zone and into groundwater.

However, highway runoff containing deicers can quickly enter streams by overland flow or interflow without infiltrating into ground water. Between 40% and 90% of highway runoff can directly join surface water bodies depending on infrastructure such as stormwater drainage system and soil properties (Tedder, 2009; Lax and Peterson, 2009).

In contrast to interflow or surface flow, road salt can discharge into streams via baseflow over longer time intervals. It is likely that the unsaturated zone near highways can serve as a chloride reservoir that continually discharges solutes to shallow groundwater (Lax and Peterson, 2009). Chloride is retained in the vadose zone as a result of low vertical water flow in low permeability, compacted soils near roadways (Lax and Peterson, 2009). A numerical simulation of chloride transport in the vadose zone showed chloride retention for the first 10 years of simulation. After 10 years, equilibrium was achieved where the vadose zone continually discharged chloride to groundwater (Lax and Peterson, 2009). Other studies have suggested that approximately one year's worth of salt is stored in the unsaturated zone (Locat and Gelinas, 1989; Toler and Pollock, 1974). Therefore, the chloride measured in March 2012 may have been applied years before the sample collection date.

In addition to salt storage within the vadose zone, cycles of freezing and thawing can delay road salt from entering groundwater. When highway runoff containing NaCl is diluted, the freezing temperature of the solution rises above eutectic point of $-21\text{ }^{\circ}\text{C}$ but below the freezing temperature of pure water ($0\text{ }^{\circ}\text{C}$). If ambient air temperatures fluctuate between -21 and $0\text{ }^{\circ}\text{C}$ throughout the winter, deicer-affected water can remain frozen along roadways or in the unsaturated zone. Since sampling was completed in March, the high concentrations may reflect solutes that were frozen in snow or ice from the previous winter.

6.3 Lateral Sampling

The hydrochemistry from the historical wells suggests that the deep part of the aquifer is hydraulically connected to the Old Pond Meadow wetland, as evidenced by the high levels of dissolved iron and manganese that are only possible in a reducing environment (Fig. 31). Consequently, the amount of dissolved oxygen in this area is likely close to zero. In contrast, the upper part of the aquifer has low concentrations of nearly every solute (Fig. 25). Low concentrations and the surface topography suggest that this area is recharged by precipitation.

The primary well for the Norwell Water Department is NOR-1 even though sodium and chloride concentrations are steadily increasing in this well. While the area near NOR-6 has lower sodium and chloride concentrations, it has water quality problems of its own. The influence of the wetlands causes high dissolved iron and manganese, low dissolved oxygen (Krammer, 2005), and possibly the presence of hydrogen sulfide and methane. From a water quality perspective, this water would need to be aerated to precipitate metals before the water can be delivered to the public. Consequently, wells that pump from the Old Pond Meadow wetland are not a desirable alternative for NOR-1.

6.4 Cross-Sections Near NOR-1

The most likely pathway of deicers to NOR-1 is through highly permeable layers in the esker, as evidenced by the observation that concentrations are higher in the esker than in other areas (Figs. 22, 25, 26, and 27). Road salt from Rt-3 and other impervious surfaces in the northern area of the aquifer infiltrates into the esker's groundwater. De-icer application on South Street could augment these concentrations. Hydraulic head differences as a result of elevation relief (Fig. 18 and 20) and pumping could cause this water to flow from the north of the aquifer towards NOR-1.

In contrast to the esker, the OPM wetland contributes water to NOR-1 with lower solute concentrations, as evidenced by low values at sites one through six (Fig. 28). Even though the wetland may receive significant quantities of de-icers, the large volume of water in this area would dilute the overall concentration.

6.5 Cation Transport and Retention

The ratio of sodium to other cations has implications for road salt pathways near NOR-1. Sodium exchange is concerning because it can mobilize previously sorbed heavy metals (Granato et al., 1995) or leach plant nutrients such as calcium and potassium (Ramakrishna and Viraraghavan, 2005). Additionally, sodium exchange can cause sodium concentrations to increase after road salt application has been terminated (Nimiroski and Waldron, 2002). Molar ratios suggest that some sodium is exchanged for other cations within the OPM aquifer.

Fig. 34 shows that chloride from a large group of samples is enriched relative to the 1:1 molar ratio of pure NaCl. It is likely that some of the original sodium exchanged calcium, magnesium, and potassium. When all major cations are accounted for (Fig. 35), a near 1:1 molar ratio is observed suggesting that potassium, calcium, magnesium, and sodium account for nearly all of cations present.

Cation exchange occurs at negatively charged cation exchange sites that are located on clays and organic matter. Both clay particles and organic matter colloids have a grain size diameter less than 1mm. For this reason, grain size distributions with a large percentage of fine particles suggest the possibility of cation exchange sites. In Norwell, grain size analysis shows that the O horizon soil near NOR-1 has more fine particles than NOR-6 (Fig. 36). As a result, it is likely that cation exchange is occurring in this layer. In the future, sodium that had previously been sorbed in the soil near NOR-1 may be exchanged for another cation and enter Norwell drinking water. This situation occurred at a field site

in Rhode Island where sodium from exchange sites entered groundwater for 12 years after road salt application had been terminated in this area (Nimiroski and Waldron, 2002).

The transect cross-sections of cation ratios show a high value near the surface at sites one and two (Fig. 26). This high value is consistent with direct highway runoff containing road salt since sodium would have little interact with cation exchange sites.

This interpretation is supported by the hydrology of the field site. Pumping at the South Street well field caused water to infiltrate from the THB into groundwater (Dillon, 2012). It is reasonable that solutes originating in the upstream THB stream water are found in shallow ground water in the THB floodplain near NOR-1.

Within the esker, the sodium to other major cation ratio shows more variation when compared to data from the floodplain. The low ratio found near the surface at site five could result from cation exchange of sodium in the O soil horizon (Fig. 28). The low grain size in this area supports this conclusion (Fig. 36). As a caveat, higher amounts of magnesium, calcium, and potassium from the decomposition of organic matter would also cause a low ratio (Watson et al., 2002).

At transect site seven in the esker, high sodium to other major cation ratios may delineate soil layers with high hydraulic conductivity (Fig. 29). There is a high sodium to other major cation ratio at aquifer elevations of 14m, 12m, and 4m. These intervals may correspond to layers of glacial sediments that transport road salt from upstream in the aquifer. Silicate minerals found in many glacial sediments have a low cation exchange capacity and may also have a high hydraulic conductivity.

The mobilization of heavy metals from cation exchange does not appear to be occurring at Norwell. Road deicers have been attributed to higher concentrations of mercury (Ramakrishna and Viraraghavan, 2005), cadmium (Lofgren, 2001; Nelson et al., 2009; Granato et al., 1995), lead (Granato

et al., 1995; Nelson et al., 2009) and zinc (Lofgren, 2001). The recommendations for drinking water criteria were exceeded for cadmium and copper downstream of a salted highway in eastern Massachusetts (Granato et al., 1995). At Norwell, concentrations of these trace elements are extremely low (Tables 9 and 10). Consequently, it is improbable that road salt is mobilizing heavy metals.

6.6 Seasonal Effects

The annual pattern of chloride concentrations in the shallow and medium parts of the aquifer relate to seasonal changes in precipitation and atmospheric temperature (Fig. 32). During the summer months, atmospheric temperatures and plant water use are high, and precipitation is moderate (Fig. 8). Solutes concentrations increase in summer because more water is removed from the aquifer by evapotranspiration (ET) than is replenished. In the fall and winter, precipitation increases and ET decreases. These effects decrease solute concentrations. Solute concentrations reach a minimum in early spring as a result of recharge from snowmelt (Fig. 32).

The deep piezometer data had lower concentrations and minimal seasonal effects (Fig. 32). Deep groundwater is usually older. It has time to mix contaminated water with fresh water leading to a lower concentration. The deep aquifer is below the area influenced by plants and the atmosphere resulting in minimal seasonal effects.

Both NOR-1 and NOR-6 pump water from near the base of the aquifer. The advantage of using deep groundwater as drinking water is that atmospheric and plant effects are avoided and point source contamination is dampened by mixing. At the same time, the fact that solute concentrations are high in deep groundwater near NOR-1 show that contamination has been occurring over a large area for a relatively long period of time. Consequently, changes to salt storage and application procedures may not improve water quality in deep groundwater over a time scale of several years. Unfortunately, the

Norwell Water Department may need to filter out solutes in drinking water or abandon NOR-1 in order to comply with the EPA's contaminant level for chloride.

Section 7. Conclusion

In the 1970's, Voorde et al. (1973) concluded that road salt had temporary effects on the environment. It is now known that deicers threaten flora (Lax and Peterson, 2009; Fay and Shi, 2012), fauna (Turtle, 2000), infrastructure (TRB, 1991; Shi et al., 2009), and human health (Jones, 1992). The chloride concentrations in a municipal groundwater well (NOR-1) in Norwell, MA are increasing towards the EPA's limit for chloride. This study has shown that high solute concentrations are a consequence of application rates, bedrock and surface geology, and pumping.

Measurements from surface, groundwater, and near-surface groundwater show spatial and temporal trends in solute concentrations. Specific conductance data from three piezometers shows seasonal changes in chloride concentrations as a result of evapotranspiration. Additionally, the highest concentrations were measured near roads.

The highest solute concentrations are near NOR-1. The most likely pathways are from Rt-3 through highly permeable layers in an esker. In contrast to NOR-1, well NOR-6 has lower sodium and chloride concentrations but higher values of iron and manganese as a result of its proximity to a reducing environment in the Old Pond Meadow wetland. Finally, the ratios of sodium to other major cations suggest that sodium is exchanged for other cations. However, sodium exchange does not appear to be mobilizing heavy metals.

Alternative deicers and best-management practices (BMP) offer a solution to salt pollution. Alternative deicers, such as..., have a higher direct cost but minimize environmental and human health risks. In a survey in Michigan, residents strongly supported finding an alternative to salt as long as it was

economically feasible (D'Itri, F. M., 1992). In addition to alternatives, structural BMP such as wetland-type environments and vegetation filter strips can remove salt (Fay and Shi, 2012). The future application of these types of options in Norwell may mitigate environmental and human health risks.

References

- Besancon, J. 2012. *Optima 7000 Standard Operating Procedures*. (unpublished).
- Bester, M.L., Frind, E.O., Molson, J.W., Rudolph, D.L. 2006. Numerical Investigation of Road Salt Impact on an Urban Wellfield. *Ground Water*. Vol. **44:2** pp. 165-75.
- Bricker, O.P. 1999. An Overview of the Factors Involved in Evaluating the Geochemical Effects of Highway Runoff on the Environment. *USGS Open-File Report 98-630*.
- Dillon, P. 2012. Personal communication.
- D'Itri, F.M. 1992. *Chemical deicers and the environment*. CRC Press, Boca Raton, Florida.
- Fay, L., Shi, X. 2012. Environmental Impacts of Chemicals for Snow and Ice Control: State of Knowledge. *Water, Air, and Soil Pollution*. Vol. **223** pp. 2751-2770.
- Forman, R.T., Alexander, L.E., 1998. Roads and their major ecological effects. *Annual Review of Ecology and Systematics*. Vol. **29** pp. 207–231.
- Godwin, K.S., Hafner, S.D., Buff, M.F., 2003. Long-term trends in sodium and chloride in the Mohawk River, New York: the effect of fifty years of road-salt application. *Environmental Pollution*. Vol. **124** pp. 263-281.
- Granato, G.E., Church, P.E., Stone, V.J. 1995. Mobilization of Major and Trace Constituents of Highway Runoff in Groundwater Potentially Caused by Deicing Chemical Migration. *Transportation Research Record*. Vol. **1483**.
- Harte, P.T., Trowbridge, P.R. 2010. Mapping of road-salt-contaminated groundwater discharge and estimation of chloride load to a small stream in southern New Hampshire, USA. *Hydrological Processes*. Vol. **24:27** pp. 2349–2368.
- Hoffman, R.W., Goldman, C.R., Paulson, S., Winters, G.R., 1981. Aquatic impacts of deicing salts in the central Sierra Nevada Mountains, California. *Water Resources Bulletin* Vol. **17**, pp. 280–285.
- Howard, K.W.F., Haynes, J. 1993. Groundwater contamination due to road de-icing chemicals- salt balance implications. *Geoscience Canada*. Vol. **20** pp. 1–8.
- Kim, K., Yun, S.T. 2005. Buffering of sodium concentration by cation exchange in the groundwater system of a sandy aquifer. *Geochemical Journal*. Vol. **39** pp. 273-284.

- Kelly, V.R., Lovett, G.M., Weathers, K.C., Findlay, S.E., Strayer, D.L., Burns, D.J., Likens, G.E. 2007. Long-term Sodium Chloride Retention in a Rural Watershed: Legacy Effects of Road Salt on Streamwater Concentration. *Environmental Science & Technology*. Vol. **42:2** pp. 410-415.
- Kelly, W.R., Panno, S.V., Hackley, K.C. 2012. Impacts of Road Salt Runoff on Water Quality of the Chicago, Illinois, Region. *Environmental & Engineering Geoscience*. Vol. **18:1** pp. 65-81.
- Kostick, D.S., 2007. Salt. *USGS Mineral Resources Program*.
<http://minerals.usgs.gov/minerals/pubs/commodity/salt/saltmyb01.pdf>. Last accessed July, 29, 2013.
- Krammer, D., 2005. Hydrogeochemical comparisons of groundwater contaminated by road salt. (unpublished).
- Jones, P. H., Jeffrey, B. A., Watler, P. K., Hutchon, H. 1992. Environmental impact of road salting. *IN: Chemical Deicers and the Environment*. Lewis Publishers, Boca Raton, Florida. pp. 1-116.
- Lax S., Peterson, E. 2009. Characterization of chloride transport in the unsaturated zone near salted road. *Environmental Geology*. Vol. **58(5)** pp. 1041-1049.
- Locat, J., Gelin, P. 1989. Infiltration of De-icing Road Salts in Aquifers: The Trois-Riveriere-Ouest Case, Quebec, Canada. *Canadian Journal of Earth Science*. Vol. **2193** pp. 2186.
- Lofgren, S. 2001. The Chemical Effects of Deicing Salt on Soil and Stream Water of Five Catchments in Southeast Sweden. *Water, Air, and Soil Pollution*. Vol. **130:1-4** pp. 863-868.
- Ma, C., Eggleton, R.A. 1999. Cation exchange capacity of kaolinite. *Clays and Clay Minerals*. Vol. **47:2** pp. 174-180.
- Manning, T.J., Grow, W.R. 1997. Inductively Coupled Plasma – *Atomic Emission Spectrometry*. *The Chemical Educator*. Vol. **2:1** pp. 1-19.
- Marion, G.M. 1995. Freeze-Thaw Processes and Soil Chemistry. US Army Corps of Engineers – Cold Regions Research and Engineering Laboratory Special Report 95-12.
http://www.crrel.usace.army.mil/library/specialreports/SR95_12.pdf. Last accessed July, 29, 2013.
- Mason, C.F., Norton, S.A., Fernandez, I.J., Katz, L.E. 1999. Deconstruction of the Chemical Effects of Road Salt on Stream Water Chemistry. *Journal of Environmental Quality*. Vol. **28:1** pp. 82-91.
- MassGIS. 2012. MassGIS Data – Digital Terrain Model (DTM) Files. <http://www.mass.gov/anf/research-and-tech/it-serv-and-support/application-serv/office-of-geographic-information-massgis/datalayers/dtm.html>. Last accessed May 7, 2013.
- MassGIS, 2005. MassGIS Datalayers. <http://www.mass.gov/anf/research-and-tech/it-serv-and-support/application-serv/office-of-geographic-information-massgis/datalayers/layerlist.html>. Last accessed July 29, 2013.
- MHD. 2008. Commonwealth of Massachusetts – Massachusetts Highway Department Standard Operating Procedures. <http://www.massdot.state.ma.us/Portals/8/docs/utilities/CSD-23-16-1-000.pdf>. Last accessed July 29, 2013.

- MHD. 2012. MassDOT Snow and Ice Control Program. http://www.mhd.state.ma.us/downloads/projDev/ESPR_2012/EnvironStatus_PlanningRpt_0212.pdf. Last accessed July 29, 2013.
- Nimiroski, M.T., Waldron, M.C. 2002. Sources of Sodium and Chloride in the Scituate Reservoir Drainage Basin, Rhode Island. *USGS Water Resources Investigation Report* Vol. **02-4149**.
- Nelson, S.S., Yonge, D.R., Barber, M.E. 2009. Effects of Road Salts on Heavy Metal Mobility in Two Eastern Washington Soils. *Journal of Environmental Engineering*. Vol. **135:7** pp. 505-510.
- NOAA. 2013. *Past Weather Data*. <http://www.noaa.gov/pastweather.html>. Last accessed April 26, 2013.
- Norwell Water Department, 2012. *Virtual Town Hall*. http://norwellma.virtualtownhall.net/Public_Documents/NorwellMA_Water/water. Last access April, 25, 2013.
- Ohon, T. 1990. Levels of total cyanide and NaCl in surface waters adjacent to road salt storage facilities. *Environmental Pollution*. Vol. **67:2** pp. 123-132.
- Ostendorf, D.W., Hinlein, E.S. Rotaru, C., DeGroot, D.J. 2006. Contamination of Groundwater by Outdoor Highway Deicing Agent Storage. *Journal of Hydrology*. Vol. **326:1-4** pp. 109-121.
- Panno, S.V., Nuzzo, V.A., Cartwright, K., Hensel, B.R., Krapac, I.G. 1999. Impact of Urban Development on the Chemical Composition of Ground Water in a Fen-Wetland Complex. *Wetlands*. Vol. **19:1** pp. 236-245.
- Pugh, A.L., Norton, S.A., Schauffler, M., Jacobson, G.L., Kahl, J.S., Brutsaert, W.F., Mason, C.F. 1996. Interactions between peat and salt-contaminated runoff in Alton Bog, Maine, USA. *Journal of Hydrology*. Vol. **182:1-4** pp. 83-104.
- Ramakrishna, D.M., Viraraghavan, T. 2005. Environmental Impact of Chemical Deivers – A Review. *Water, Air, and Soil Pollution*. Vol. **166** pp. 49-63.
- Reed, D. 1995. Zone II Delineation Old Pond Meadows Aquifer Towns of Hanover and Norwell. (unpublished) *Internal Report to the Board of Public Works, Hanover, MA*.
- Sarojam, P. 2010. Analysis of Wastewater for Metals Using ICP-OES. *PerkinElmer internal report*. http://www.perkinelmer.com/CMSResources/Images/44-74211APP_MetalsinWastewater.pdf. Last accessed July 29, 2013.
- Shanley, J.B. 1994. Effects of Ion Exchange on Stream Solute Fluxes in a Basin Receiving Highway Deicing Salts. *Journal of Environmental Quality*. Vol. **23:5** pp. 977-986.
- Shi, X., Akin, M., Pan, T., Fay, L., Liu, Y., Yang, Z. 2009. Deicer Impacts on Pavement Materials: Introduction and Recent Developments. *Open Civil Engineering Journal*. Vol. **3** pp. 16-27.
- Sun, H., Lucarino, K., Huffine., M., Husch, J.M. 2010. Retention of Sodium in a Watershed due to the Application of Winter Deicing Salt. *Proceedings of the 10th Internatinoal Symposium on Stochastic Hydraulics and 5th Conference on Water Resources and Environmental Research*.
- Tedder, N.W. 2009. Dissolved Road Salt Transport in Urban and Rural Watershed in Massachusetts. (unpublished).

- Toler, L.G., Pollok, S.J. 1974. Retention of Chloride in the Unsaturated Zone. *Journal of Research of the U.S. Geological Survey*. Vol. **2:1** pp. 119-123.
- TRB, 1991. Highway deicing, comparing salt and calcium magnesium acetate, Special Report 235, *Transportation Research Board, National Research Council, Washington, DC*
- Turtle, S.L., 2000. Embryonic Survivorship of the Spotted Salamander (*Ambystoma maculatum*) in Roadside and Woodland Vernal Pools in Southeastern New Hampshire. *Journal of Herpetology*. Vol. **34:1** pp. 60-67.
- USEPA. 2006. Secondary drinking water regulations: guidance for nuisance chemicals. U.S. Environmental Protection Agency. <http://www.epa.gov/safewater/consumer/2ndstandards.html>. Last accessed April 11, 2013.
- USEPA. 2010. Low Stress (low flow) Purging and Sampling Procedure for the Collection of Groundwater Samples from Monitoring Wells. U.S. Environmental Protection Agency <http://www.epa.gov/region1/lab/qa/pdfs/EQASOP-GW001.pdf>. Last accessed April 11, 2013.
- USEPA. 2012. Road Salt Application and Storage. U.S. Environmental Protection Agency. http://cfpub.epa.gov/npdes/stormwater/menuofbmps/index.cfm?action=factsheet_results&view=specific&bmp=106. Last accessed April 11, 2013.
- Voorde, H., Nijs, M., Duck, P.J. 1973. Effects of road salt in winter. *Environmental Pollution*. Vol **5:3** pp. 213-218.
- Watson, L.R., Bayless, E.R., Buszka, P.M., Wilson, J.T. 2002. Effects of Highway-Deicer Application on Ground-water Quality in a Part of the Calumet Aquifer, Northwestern Indiana. *U.S. Geological Survey Water-Resources Investigations Report* Vol. **01-4260**.
- Wilcox, D.A. 1986. The effects of deicing salts on water chemistry in Pinhook Bog, Indiana. *Journal of American Water Resources*. Vol. **22:1** pp. 57-65.
- Wegner, W. Yaggi M. 2001. Environmental impacts of road salt and alternatives in the New York City Watershed. *Stormwater*. Vol. **2:5** pp. 1-15.
- Zimmerman, M.J., Massey, A.J., Campo, K.W. 2005. Pushpoint Sampling for Defining Spatial and Temporal Variations in Contaminant Concentration in Sediment Pore Water near the Ground-Water/Surface-Water Interface. *USGS Scientific Investigations Report* Vol. **5036**.